AN IMPROVED LEAST SQUARES VOLTAGE PHASOR ESTIMATION TECHNIQUE TO MINIMIZE THE IMPACT OF CCVT TRANSIENTS IN PROTECTIVE RELAYING

A Thesis

Submitted to the College of Graduate Studies and Research

in Partial Fulfillment of the Requirements of the

Degree of Master of Science

in the

Department of Electrical Engineering

University of Saskatchewan

Saskatoon, Saskatchewan

Canada

By

ELI PAJUELO

PERMISSION TO USE

In presenting this thesis in partial fulfillment of the requirements for a Master's degree from the University of Saskatchewan, I agree that the Libraries of this University may make it freely available for inspection. I further agree that permission for copying of this thesis in any manner, in whole or in part, for scholarly purposes may be granted by the professor or professors who supervised my thesis work or, in their absence, by the Head of the Department or the Dean of the College in which my thesis work was done. It is understood that any copying, publication, or use of this thesis or parts thereof for financial gain shall not be allowed without my written permission. It is also understood that due recognition shall be given to me and to the University of Saskatchewan in any scholarly use which may be made of any material in my thesis.

Requests for permission to copy or to make other use of material in this thesis in whole or part should be addressed to:

Head of the Department of Electrical Engineering,
University of Saskatchewan,
Saskatoon, Saskatchewan, Canada S7N 5A9

ABSTRACT

Power systems are protected by numerical relays that detect and isolate faults that may occur on power systems. The correct operation of the relay is very important to maintain the security of the power system.

Numerical relays that use voltage measurements from the power system provided by coupling capacitor voltage transformers (CCVT) have sometimes difficulty in correctly identifying a fault in the protected area. The fundamental frequency voltage phasor resulting from these CCVT measurements may result in a deviation from the true value and therefore may locate this phasor temporarily in the incorrect operating region. This phasor deviation is due to the CCVT behavior and the CCVT introduces spurious decaying and oscillating transient signal components on top of the original voltage received from the power system in response to sudden voltage changes produced during faults. Most of the existing methods for estimating the voltage phasor do not take advantage of the knowledge of the CCVT behavior that can be obtained from its design parameters.

A new least squares error method for phasor estimation is presented in this thesis, which improves the accuracy and speed of convergence of the phasors obtained, using the knowledge of the CCVT behavior. The characteristics of the transient signal components introduced by the CCVT, such as frequencies and time constants of decay, are included in the description of the curve to be fitted, which is required in a least squares fitting technique. Parameters such as window size and sampling rate for optimum results are discussed.

The method proposed is evaluated using typical power systems, with results that can be compared to the response if an ideal potential transformer (PT) were used instead of a CCVT. The limitations of this method are found in some specific power system scenarios, where the natural frequencies of the power system are close to that of the CCVT, but with longer time constants. The accuracy with which the CCVT

parameters are known is also assessed, with results that show little impact compared to the improvements achievable.

ACKNOWLEDGEMENTS

The author expresses his gratitude and appreciation to Dr. R. Gokaraju and Dr. M. S. Sachdev for their guidance, support and patience throughout this work. Their advice and assistance on the preparation of this thesis are thankfully acknowledged.

The author also would like to thank his beloved wife Erlinda Huamani, for her patience and unconditional support during all this work. Also, the author would like to thank his parents Fortunato Pajuelo and Ricardina Rubina, for their continued moral support and encouragement.

Financial support provided by the Natural Sciences and Engineering Research Council (NSERC) of Canada and the University of Saskatchewan is thankfully acknowledged.

Dedicated

To

My children: Diego, Mara, Andres

TABLE OF CONTENTS

LIST OF TABLES

LIST OF FIGURES

LIST OF ACRONYMS

CCVT	Coupling capacitor voltage transformer
PT	Potential (or voltage) transformer
VT	Voltage (or potential) transformer
CT	Current transformer
DC	1) direct current, or 2) non oscillating component of a signal
AC	Alternating current
EMTP	Electromagnetic transients program, i.e. time domain solution of electrical networks
ATP	Alternative transients program, i.e. a version of EMTP
Fs	Number of samples per second, i.e. sampling frequency
A/D	Analog to digital converter, i.e. sampling device
Δt	Time period between sample measurements, i.e. sampling period
pu	Per unit
IEC	International Electrotechnical Commission
ANSI	American National Standards Institute
$V_{PREFAULT}$	Voltage measured immediately before a fault condition
V_{FAULT}	Voltage measured during a fault after all transients subsided
SIR	Source to line impedance ratio, at fundamental frequency

1. INTRODUCTION

1.1 POWER SYSTEM PROTECTION

1.1.1 Power Systems

Power systems are electrical energy networks that interconnect energy sources with energy users, typically covering large geographical areas. The main functions performed in a power system are: transform the energy from different sources to electrical form, transport the electrical energy to different locations and deliver the electrical energy to the final users.

To perform the different functions, a power system includes several components: 1) generators, that convert energy to electrical form; 2) power lines, that transport the electrical energy to wherever it is needed; 3) power transformers, that reduce or elevate from, or to, the higher voltages used in a power system and the lower voltages required by the final users; and 4) loads, that convert the energy to the required form for usage. The loads are the final users, such as houses, buildings, hospitals, industry, etc.

1.1.2 Prevention and Protection Against Faults

Fault prevention minimizes the possibility of a fault in a power system component by using proper design and construction techniques. Not all faults can be prevented, however, due to cost limitations [30,39].

Fault protection minimizes the consequences of the faults that occur by quickly isolating the affected component. The protection methodologies provide coverage for most faults, including those not preventable. This coverage is limited by the sensitivity of the protection used.

1.1.3 Fault and Isolation

1.1.3.1 Fault: A fault can be defined as an undesired abnormal disturbance in the power system and/or its components [39,43]. Faults may cause a negative impact, such as damage to equipments, instability of the network, etc. One of the most typical faults is the short circuit.

A fault is caused often by a dielectric insulation breakdown, producing a short circuit. In a power line, the dielectric is air typically; therefore, once the fault is cleared, the insulation recovers and the system can be brought back quickly to service. The fault in this case is temporary. On the other side, in an electrical machine, the dielectric is made of other materials that get damaged by a fault condition, needing replacement and keeping the machine out from service. The fault is "permanent", i.e. waiting for repair.

Other fault causes are abnormal operating conditions of equipments. Examples of these are: *overheating* associated with overload or overvoltage or other reasons, *overspeed* in rotating machines, etc.

1.1.3.2 Isolation: Figure 1.1 shows the main elements involved in the process of isolating a fault. Two steps are involved in this process: fault detection and fault isolation.

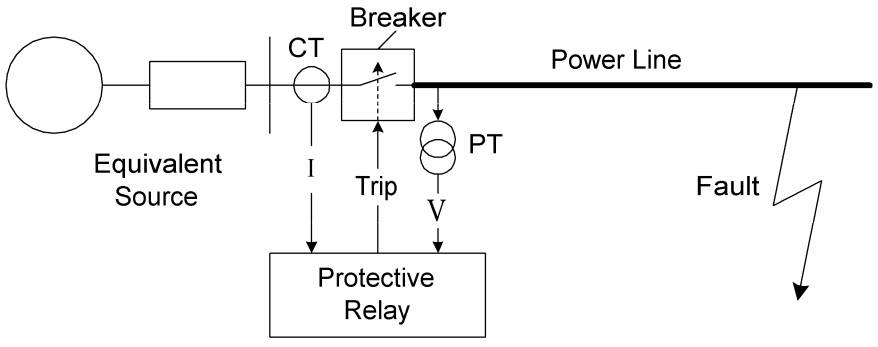

Figure 1.1 Detection and isolation of a fault

The fault detection is the process of identifying the presence of a fault in the protected area. To perform this identification, the currents and voltages during faults and normal conditions should be already known, these quantities that show the power system behavior are obtained from power system studies.

The desired current and voltages are calculated in these power system studies, by solving the network for different fault conditions [35,38,39,44]. The results of these studies define the protective relay *settings*, i.e. the limits, thresholds or boundaries used to identify a fault from a normal condition.

Two elements are involved in the task of fault detection: 1) current transformers (CT) or voltage/potential transformers (VT or PT) and 2) protective relay. The CTs and PTs [39,43,46,47] perform several functions: 1) interface the high *primary* voltage of the power system with the low *secondary* voltage of substation equipments, 2) scale down currents or voltages from the power system before they are measured, 3) electrically isolate the substation equipment from the power system, and 4) normalize the secondary currents and voltages.

The protective relays receive the secondary current and voltage signals from the CTs and PTs and measure them. These relays decide if the current and voltage characteristics correspond to a fault in the protected area, using the relay settings for this purpose. When a decision to operate is made, the command to isolate the fault is issued, via a *trip* contact output.

The fault isolation, performed once a fault is detected, is the process of disconnecting power to the area closest to the fault location. The protection areas in a power system are typically separated by breakers; these areas are sometimes called as zones [30,38,44]. The objective of the fault isolation is to open the minimum number of breakers that achieve this purpose.

The breaker [39,45] is a high voltage device that performs the isolation of a fault, interrupting the desired circuit at the command of the protective relay. This command comes in the form of a contact closure that energizes the trip coil of the

breaker, i.e. operates the breaker to the open position. Sometimes, automatic energization of the faulted power circuit is attempted, because a high percentage of faults in power lines are temporary. This re-energization command is received from the appropriate relay in the close coil of the breaker, and this automatic energization is called “reclose”. The trip and reclose operations are, however, not very frequent; because the breakers are more typically opened or closed as part of normal operations.

A special case of protective device is the fuse. The fuse [39,46] integrates two functions in one: detection and isolation. The detection follows certain desired thermal limit response curve that covers the protected power system component. The isolation occurs when the limit is exceeded and the detection element in the fuse is destroyed, interrupting the circuit protected. In addition to this advantage of integrating two functions, the fuse is typically less expensive than the combination of relay, CT/PT and breaker. The disadvantage is that a fuse needs replacement after a protective operation, and requires the intervention of maintenance personnel before the circuit is re-energized.

1.1.4 Incorrect Operation

1.1.4.1 Implications: Two kinds of undesired incorrect operation [16,45] are known: operate when not required, and not operate when required. The operation of a relay when it is not required causes a circuit to be disconnected unnecessarily, and has several implications: 1) economic and service impact, by removing energy supply to some area or customer; 2) may cause or increase the instability of a system, by removing a needed energy link; and 3) raises concern on the existence of a fault in that area, requiring maintenance personnel intervention for verification.

The non-operation of a relay when required, typically known as a failure to operate, also has several implications: 1) may cause damage to some equipments, 2) increases the area to be disconnected from power supply by requiring that breakers in adjacent zones to open, 3) increases the time to disconnect by activating backup protection (typically time delayed for coordination) from adjacent zones that also cover the affected area; 4) has increased economic impact, because the area disconnected is

larger; and 5) reduce the stability of the system, due to energy imbalance occurring during the faulted condition.

1.1.4.2 Risk: In general, the chances for incorrect operation are much more than for correct operation. Normal disturbances are experienced frequently by the power system, examples of these are: 1) connection or disconnection of lines, loads or generation; 2) energization of equipments such as transformers or motors, the current levels produced sometimes are similar to some faults; 3) switching of reactive compensation such as shunt capacitors or reactors banks; 4) temporary overload; and 5) stable power swings. External faults are also another risk factor to be considered, because they may be more difficult to discriminate than a normal power system operating condition. Another risk factor of incorrect operation is the failure of any of the equipments involved in the protection function: the relay, the breaker or the CTs or PTs.

1.1.5 Protection Requirements

A protection system should satisfy the following general requirements for a correct performance [4,6,30,38,44].

Selectivity: The selectivity is the capability to discriminate between faults inside the protected area and other faults or disturbances. This requirement is important to ensure that the minimum area is isolated for any fault condition.

Sensitivity: The sensitivity is the capability to discriminate between a fault and normal conditions, although the difference between these two conditions is small. This requirement is important to ensure the correct operation for faults under many different power system scenarios which can bring fault and normal conditions closer to each other.

Speed: The speed is the time elapsed from the fault initiation until its detection and isolation. This requirement is important to minimize the impact of a fault in the power system or its equipments.

Reliability: The reliability of a protection system is the degree of certainty that it will work correctly. This requirement depends on two factors: dependability and security. The dependability is the ability of a relay to operate correctly when required. This factor is important because a lack of it means not to operate when required, which is explained in section 1.1.4.1. The security is the ability of a relay of never operating incorrectly. This factor is also important because the lack of it means to operate when not required, which is also explained in section 1.1.4.1.

1.1.6 CT and PT Considerations

The quality of the scaled down currents and voltages depends on several performance characteristics, such as: accuracy, linearity, frequency response and range. The accuracy specifies the amount of deviation from the ideal response at certain desired condition. The linearity measures the deviation from an ideally proportional response. The frequency response indicates the gain or attenuation as well as the angle shift introduced to each individual frequency component of the input when producing the output. The range specifies the maximum and minimum limits where these performance parameters are applicable.

1.1.6.1 CT: The CT is a special power transformer that uses the balance of ampere-turns to achieve the scaling down of currents. This balance implies ideally that $N_P * I_P = N_S * I_S$, where N_P, N_S are number of turns in primary and secondary respectively, and I_P, I_S are primary and secondary currents respectively. In the real implementation this balance is broken by the presence of a small magnetizing current, that produces the magnetic flux required, and is obtained from the primary side. Therefore, the accuracy of a CT is a function of the amount of magnetizing current, which in normal operation is relatively small compared to the current to be measured.

One of the problems that is most concerning with the use of CTs is the saturation of the magnetic core due to the non-linear magnetic characteristic of the core. This saturation occurs when the flux increases beyond the linear range of the magnetic material, and is characterized by a significant increase on the magnetizing current.

The saturation of the CT core can be produced due to the following reasons: a) significant secondary voltage and b) DC component in the current measured. A significant secondary voltage is equivalent to a high magnetic flux that may enter the non-linear region of the magnetic characteristic. This significant voltage is obtained when the product of the current and the burden impedance results in a high value, such as during high current fault conditions. The effect of a DC component of current on a CT can be understood by reviewing the effect of a pure DC signal applied to a power transformer. A DC current produces a magnetic flux constant in time, which does not induce any voltage; therefore no secondary current is produced. The DC current applied becomes completely a magnetizing current, because no balancing ampere-turns are produced in the secondary to compensate. This DC component is of concern in cases where the power system location is very inductive presenting a long time constant of decay for this component. This kind of saturation may be experienced even with low current fault conditions.

1.1.6.2 PT: The PT is a magnetic transformer that uses the ratio of turns between primary and secondary windings to scale down voltages. The magnetic flux that links both windings produces voltages on each that are proportional to the number of turns, which means ideally that $K * N_P * \Phi = V_P$ and $K * N_S * \Phi = V_S$, where K is a design constant, N_P, N_S are primary and secondary turn ratios respectively, V_P, V_S are primary and secondary voltages respectively, Φ is the flux linking both windings. In the real implementation, these voltages are slightly modified by the voltage drop in the leakage inductances of each winding. The accuracy of a PT is then a function of the voltage drop on these inductances, which is relatively low compared to the voltage measured.

No significant problems are experienced with a PT i.e. the quality of the scaled down voltage is good in most cases, even during fault conditions. The only concern is perhaps the cost, which is a function of the level of insulation required with very high voltages.

1.1.6.3 Coupling Capacitor Voltage Transformer (CCVT): The CCVT scales down voltage using a circuit more complex than that of a conventional PT. The CCVT consists basically of a capacitive divider, a series inductance and an intermediate PT. The accuracy in this case is a function of several parameters. The main reason to use a CCVT is the lower cost compared to an equivalent PT, because of the lower insulation level required in the intermediate PT. A more complete description is provided later in Chapter 3.

One of the most severe problems experienced with a CCVT is the response during fault conditions. This response includes transient components not present in the input signal that are introduced by the CCVT. These components are produced by the interaction of the capacitors, series inductance, burden connected and other internal CCVT circuits. This interaction is characterized by natural oscillating frequencies that are obtained by sudden changes in the voltage input signal.

1.2 OBJECTIVE OF THE THESIS

The protective relays that use voltage measurements have difficulties in their operation due to the coupling capacitor kind of voltage transformer (CCVT). The CCVT response under transient conditions may cause the incorrect operation of these relays. These protective relays use typically a fundamental frequency voltage phasor obtained from the CCVT output signal to identify the fault condition. A significant deviation from the true value is produced in the resulting phasor, because of distortions introduced by the CCVT in the voltage signal. This deviation, i.e. phasor error, may locate the phasor outside the correct operating region, thus an incorrect operation decision results.

The purpose of this thesis is to reduce the impact of CCVT transients on protective relaying applications. For that, a method is developed to improve the accuracy and speed of the voltage phasor estimation. The results of the method are then verified to evaluate the advantages and limitations under realistic scenarios.

1.3 OUTLINE OF THE THESIS

Chapter 1 provides a basic background in power system protection. The fault and its isolation process are described. The implications of an incorrect operation of the protection are listed. The main requirements to provide adequate protection are explained. The objective and outline of the thesis are presented.

In Chapter 2, the numerical relays are described. The main functional elements involved in this type of relays, from the measurement inputs to the decision outputs are described. Particular attention is paid to the fault detection components, i.e. the phasor estimation and the protective function. The Discrete Fourier Transform and the Least Squares Error methods applied to phasor estimation are developed in this thesis. The most common protective functions are explained, indicating the basic protection problems they can solve.

Chapter 3 is dedicated to the characteristics of the CCVT. The CCVT response in the frequency and time domain is investigated, indicating the factors that influence these responses. Methods and considerations for modeling the CCVT are described, such as Laplace Transfer Function and Electromagnetic Transients Program (EMTP).

Chapter 4 identifies the impact of CCVT on protective relays. The error introduced in the voltage phasor estimated by the CCVT distortion is identified as magnitude and angle deviations from the true values. The impact of these errors in different protective principles is analyzed, identifying the risks of incorrect operation. Some techniques in use that intend to overcome the CCVT impact are also described.

The method proposed to overcome the CCVT impact is presented in Chapter 5. This method reduces the error introduced in the voltage phasor estimation using a least squares error approach. The basic difficulty of traditional estimation methods to obtain a reliable voltage phasor is stated. The idea of the improvement over traditional methods is presented. The theoretical development of the proposed method is described.

In Chapter 6, the performance of the proposed phasor estimation method is evaluated. Several simulations of faults are performed using realistic models of power systems. Cases that show the improvements achieved are illustrated. Other special cases where the method presents limitations are also illustrated and explained. The sensitivity of the proposed method to the CCVT parameters is also studied.

Chapter 7 provides a summary and conclusions to this thesis, and is followed by a list of references.

1.4 THESIS CONTRIBUTION

The primary contributions of this thesis are:

1) A new phasor estimation method using least error squares technique is proposed that minimizes the error caused by the CCVT (Chapter 5). The method improves the accuracy and speed of the phasor estimated by using the information available of CCVT parameters and characteristics (Chapter 3).
2) The performance of the proposed method is evaluated under real fault scenarios to identify advantages and limitations (Chapter 6). Significant improvements are observed in many cases (Chapter 6). The limitations of the method are also seen in certain cases (Chapter 6).
3) The practicality of the proposed method is validated by doing a sensitivity study on the method due to inaccuracies in CCVT parameters. It is found that the proposed method has a low sensitivity to CCVT parameter inaccuracies (Chapter 6).

1.5 SUMMARY

This chapter provides an overview on power system protection concepts. The role and importance of protection in a power system is explained. The faults and its isolation are described. The implications and risk of incorrect operations are listed. The main requirements to provide adequate protection to the power systems are introduced. The objective of the proposed research and thesis contributions are listed.

2. NUMERICAL RELAYS

2.1 INTRODUCTION

The power system protection requirements and concepts explained in the previous chapter are implemented in the numerical relays. These relays issue a command signal to isolate the protected circuit as soon as a fault in that area is detected. The numerical relays got this name, i.e. numerical, because they perform calculations with numbers for the decision of a protective operation; this is possible by the use of microprocessor based architectures. These relays typically perform many other useful functions in addition to the protective functions.

In this chapter the numerical relay is described. The basic components necessary to perform the protective functions are explained starting from the inputs to the relay received from the power system, down to the outputs from the relay that issue command signals for the protective operations. The two most important functions in the fault detection process are described in detail: the phasor estimation and the protective functions. Two phasor estimation methods are presented: one based on the Discrete Fourier Transform and the other based on the Least Squares Error technique.

2.2 BASIC RELAY COMPONENTS

The numerical relays consist mostly of few basic components [11,21,33,48]:

- Current (CT) / voltage (PT) inputs
- Contact inputs
- Fault detection element
- Contact outputs
- Target or alarm indicator

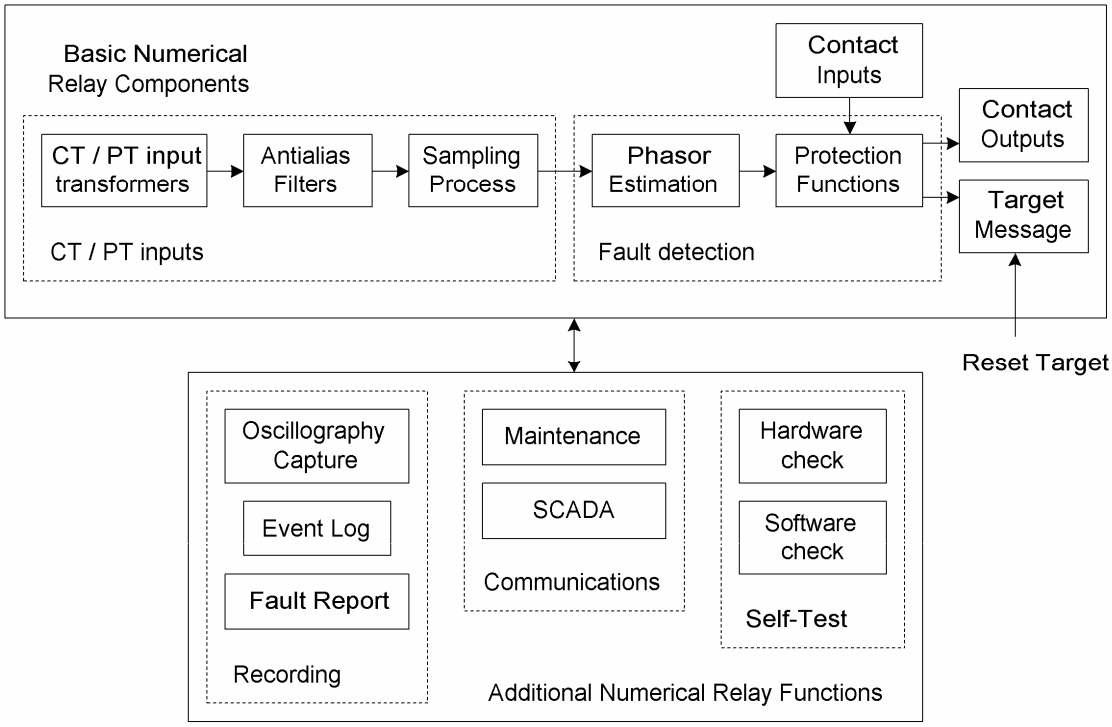

Figure 2.1 Numerical Relay Components and Functions

An overall picture of the different components of a numerical protective relay and the relationships between them is given in Figure 2.1. Each of the components and functions of this figure are described in this chapter.

2.2.1 CT / PT Inputs

These inputs receive the currents and voltages from the CTs and PTs, respectively. The CT and PT types of input are important because they allow the instantaneous measurement of the currents and voltages required by the fault detection functions. The number and type of these inputs depend on the kind of relay application being considered.

The CT and PT inputs need to satisfy certain performance requirements to ensure a quality on the measurement. The basic requirements are linearity, accuracy and frequency response bandwidth. These requirements should be below the desired tolerances in the current or voltage range selected.

Three main stages can be recognized in the CT/PT inputs: CT/PT input transformers, anti-aliasing filter and sampling process.

The CT input transformer performs three main functions: scales down the current received, provides electrical isolation to internal circuits and converts the current to an internal voltage signal. The main characteristics of this type of input are: 1) rated AC input of 5A or 1A rms, and 2) range of around 40 times the peak of the rated, this peak corresponds to the maximum internal voltage range. A typical implementation consists of a small transformer that scales down the current with a burden resistor connected that converts the current output to a voltage signal.

The PT input transformer performs two main functions: scales down the voltage received to an internal voltage signal and provides electrical isolation to internal circuits. The main characteristics of this type of input are: 1) rated AC input of 100/1.732 V to 120/1.732 V rms for phase to ground or 100 V to 120 V rms for phase to phase, and 2) range of around 3 times the peak of the rated, this peak corresponds to the maximum internal voltage range used. A typical implementation consists of a small transformer that scales down the voltage received.

The anti-aliasing is an analog filter [11,20,21,32,33] that conditions the voltage signals received from the CT and PT input transformers before these signals are measured by the sampling process. This conditioning overcomes a limitation in the sampling due to the misinterpretation of the frequency components, contained in the signal, that are above half of the sampling frequency. This step is necessary because these voltage signals received contain a wide range of frequencies. The method used to resolve this problem is the removal of frequencies above half of the sampling frequency using one anti-aliasing analog filter on each signal before the sampling is performed.

The sampling process receives the conditioned voltage signals from the anti-aliasing filter and delivers periodically samples in numerical form to the fault detection function. The sampling is the process of taking instantaneous measurements of each of the signals received at discrete points in time; these measurements are the samples. The

sampling frequency F_S defines the time period Δt between samples, by the following relationship $F_S = 1/\Delta t$. The sampling frequency is fixed or variable depending on the requirements of the application. A typical implementation of the sampling process requires an analog to digital (A/D) converter and commonly also sample and hold with multiplexing circuits to handle multiple analog channels. Before the samples can be used by the fault detection functions, they need to be properly scaled and corrected. The scaling takes into account all previous scaling applied to the signal since it was originally received in the CT or PT inputs. The correction takes into account the calibration needed to obtain the desired accuracy and to compensate for component tolerances.

2.2.2 Contact Inputs

These inputs receive the status of external contacts and deliver that information periodically in the form of digital bits to the fault detection function. The update period for this status information depends on the time resolution desired; this is typically of the order of one millisecond. Examples of these inputs are: 1) breaker position, open or closed, 2) permission from a remote substation, active or inactive, and 3) others.

2.2.3 Fault Detection Function

The fault detection function receives the samples from the sampling process and the status of contact inputs; and decides the appropriate protective operation. This function consists of two main components: phasor estimation and protection function. The phasor estimation uses the most recent time window of samples to calculate the fundamental frequency component of each analog channel, i.e. CTs and PTs, in the form of phasors. The protection function takes the phasors estimated and contact input status to identify the presence of a fault in the protected area. If a fault is identified, a trip decision is made so that the high voltage breaker interrupts the fault currents and isolates the faulted circuit. The fault detection function is typically implemented in a software program that runs on a microprocessor platform.

2.2.4 Contact Outputs

These outputs receive commands from the fault detection function and execute them by closing or opening the required contacts. A trip command is executed by closing the contact that energizes the trip coil of the breaker, so that interruption of the protected circuit is initiated. Once the breaker opens the fault is isolated. The implementation of the contact outputs is typically with small relays that open or close their contacts at the command of the microprocessor that runs the protection functions.

2.2.5 Relay Target

Traditionally, protective relays have given a visual indication that there has been a tripping operation. This indicative or *flag*, also called “target message”, remains active until a resetting command is received; this command can be the pushing of a button or a remote reset received via communications. A typical implementation of the target uses LEDs or an alphanumeric display for this purpose.

2.3 ADDITIONAL FUNCTIONS

The use of microprocessors has the advantage of including different elements that are part of this architecture [25], such as memory storage, communication capability, and programmability among others. The most noticeable additional functions available in numerical relays are: recording, communication and self-test.

2.3.1 Recording

Recording is, in protective relaying, the automatic storage in memory of certain important information. The information saved is available for posterior analysis of fault operations or other kind of disturbances of interest. The most important types of information recorded in a numerical relay are: events, oscillographies and fault reports.

The events are changes in the state of variables. These variables have typically two states, active or inactive, but in some cases few more states are used. Examples of these variables are: status of contact inputs or outputs, internal “flag” bits generated by the protection functions, and others. A change of state is recorded with a time stamp

that locates the event in time with respect to others. The resolution of the time stamp in relaying applications is typically of the order of one or two milliseconds.

The oscillographies are a way to record a time window of analog samples as well as digital flags. The recording of pre-fault and fault time windows during a protective operation is the most important use of oscillographies. The time zero in this kind of recording is defined by the trigger signal, the pre-fault is located before and the fault is located after this trigger time.

A fault report is generated typically after every protective operation of the relay. This report contains important information, such as: prefault currents and voltages, fault currents and voltages, operating time, protective function that operated, and others.

2.3.2 Communication

The numerical relays offer the possibility of communicating with other devices. One of the most important uses of communication in relaying has been the relay maintenance. The sending or retrieval of configuration settings, retrieval of recordings, upgrading of firmware, are among the most important relay maintenance procedures. Another important use of communication is to integrate the numerical relays as part of a supervisory control and data acquisition (SCADA) system. The sending of alarms, events and analog measurements are among the most typical information needed in SCADA applications.

2.3.3 Self-Test

The self-test, also called auto-diagnostic, intends to identify a failure in the relay before it is required to operate. There are basically two kinds of self-test: hardware and software.

The hardware self-test, checks the integrity of the relay from the point of view of component failure. Every relay design is distinct and no generic rule of what to be checked is available, so common sense should be exercised. Examples of hardware

self-test are: check of the redundancy in the dual paths that link the contact inputs and/or outputs with the microprocessor, check that the level of analog reference voltage remains constant, check that the power supply is working, and others.

The software self-test, checks the integrity of the relay from the point of view of a software failure, i.e. a “bug” for instance. Examples of software self-test are: check that the software is “alive” using a hardware watchdog timer, check for memory corruption of certain key areas, check for stack memory overflow, and others.

A contact output is typically designated as the critical alarm contact. This contact notifies an external alarm system about the failure of the numerical relay.

2.4 PHASOR ESTIMATION

In the phasor estimation process, the desired frequency component of the signal received is converted to a representative phasor. This process is called estimation because the true value of the desired component is not known upfront; the quality of the phasor estimated depends on the method used.

Typically, the phasor estimation processes a time window of data to obtain the desired phasor using the method selected. The data window is continuously updated including newer samples and discarding older samples, the phasor estimation is performed for every new data window to obtain updated phasors [20].

Two phasor estimation methods are presented here: Discrete Fourier Transform (DFT) and Least Squares Error. The angle normalization applied sometimes to the resulting phasors estimated is also presented.

An example for a fixed data window size of $N = 8$ samples is shown in Figure 2.2. The distance between samples in the time scale is the sampling period Δt. The sampling frequency is $F_S = 1/\Delta t$.

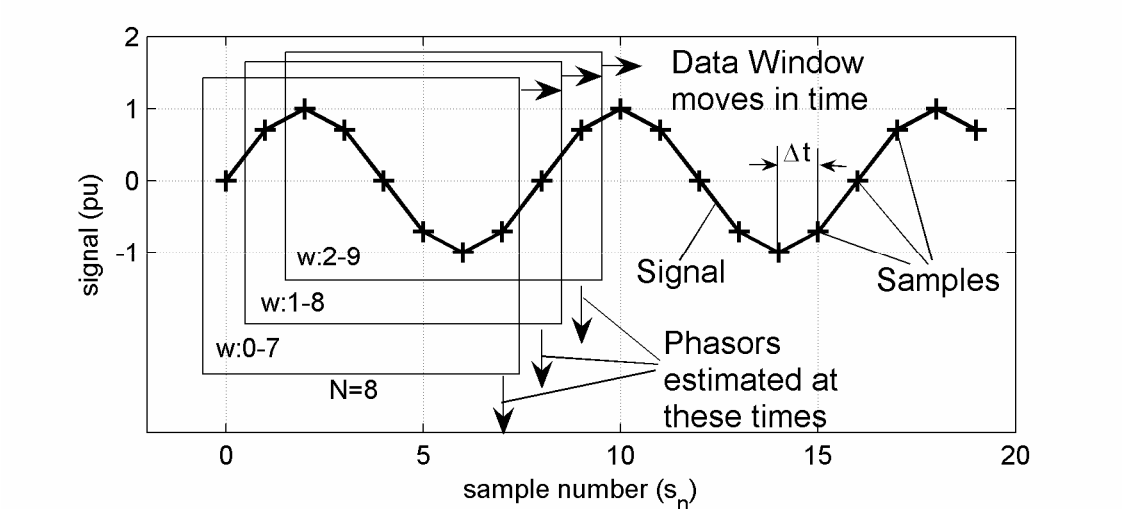

Figure 2.2 Phasor estimation process

2.4.1 Discrete Fourier Transform (DFT) Method

Two concepts are required to understand the physical meaning of this method: the Discrete Fourier Series and the Discrete Fourier Transform. This method uses the capability of the Discrete Fourier Series to represent a given set of sample measurements. The cosine and sine coefficients for the desired harmonic component of this Fourier series are calculated, using some properties of the DFT. The result of the phasor estimation applied to a typical signal, i.e. the time response of the method, is illustrated. The frequency response characteristic of the DFT method presented is also discussed.

2.4.1.1 The Discrete Fourier Transform (DFT): The DFT is a transform that converts a sequence of time samples to another sequence of frequency samples. The sampling period Δt in the time domain is the inverse of the sampling rate $F_S = 1 / \Delta t$. F_S corresponds to the length of the sequence of frequency samples, i.e. $F_S = N\Delta f$, where the sampling period Δf in the frequency domain is the fundamental frequency of the DFT, defined by the length of the set of time samples $T = N\Delta t$, i.e. $\Delta f = 1 / T$.

The DFT of a given set of real number time samples $x(n)$, $n = 0,1,\ldots,N\text{-}1$; with N even; is defined as [32]:

$$X(k) = \sum_{n=0}^{N-1} x(n) e^{-j\frac{2\pi}{N}kn} \qquad k = 0,1,\ldots,N\text{-}1 \tag{2.1}$$

The number of frequency samples $X(k)$ is the same as the time samples $x(n)$, however only half of the frequency samples are relevant. The index k indicates the multiple of fundamental frequency, also called harmonic number, from zero up to $N / 2$, the remaining index values above $N / 2$ have the following relationship,

$$X(N-k) = \sum_{n=0}^{N-1} x(n) e^{-j\frac{2\pi}{N}(N-k)n} = \sum_{n=0}^{N-1} x(n) e^{-j2\pi n} e^{+j\frac{2\pi}{N}kn} = \sum_{n=0}^{N-1} x(n)(1) e^{+j\frac{2\pi}{N}kn}$$

$$= \sum_{n=0}^{N-1} x(n) e^{+j\frac{2\pi}{N}kn} = X(k)^{*} \tag{2.2}$$

Where $X(k)^{*}$ is the conjugate of $X(k)$. The Inverse DFT (IDFT) of a given set of frequency samples $X(k)$, $k = 0,1,\ldots,N\text{-}1$; is defined [32] as:

$$x(n) = \frac{1}{N} \sum_{k=0}^{N-1} X(k) e^{+j\frac{2\pi}{N}nk} \qquad n = 0,1,\ldots,N\text{-}1 \tag{2.3}$$

The IDFT performs the conversion from a sequence of frequency samples to a sequence of time samples. If the DFT of certain time sequence is known, the original time sequence can be obtained using the reverse conversion provided by the IDFT.

2.4.1.2 The Discrete Fourier Series: The Discrete Fourier Series [32] can be obtained by rewriting the IDFT from Equation 2.3 as follows:

$$x(n) = \frac{1}{N} \left(\sum_{k=0}^{\frac{N}{2}-1} X(k) e^{+j\frac{2\pi}{N}nk} + \sum_{k=\frac{N}{2}}^{N-1} X(k) e^{+j\frac{2\pi}{N}nk} \right) \tag{2.4}$$

Substituting $(N\text{-}k)$ instead of k in the second sum of the Equation 2.4, gives,

$$x(n) = \frac{1}{N}\left(\sum_{k=0}^{\frac{N}{2}-1} X(k) e^{+j\frac{2\pi}{N}nk} + \sum_{k=1}^{\frac{N}{2}} X(N-k) e^{+j\frac{2\pi}{N}n(N-k)} \right) \tag{2.5}$$

Rearranging the Equation 2.5, gives,

$$x(n) = \frac{1}{N}\left(X(0) + \sum_{k=1}^{\frac{N}{2}-1} \left\{ X(k) e^{+j\frac{2\pi}{N}nk} + X(N-k) e^{+j\frac{2\pi}{N}n(N-k)} \right\} + X(\frac{N}{2}) e^{+j\frac{2\pi}{N}n\frac{N}{2}} \right) \tag{2.6}$$

Simplifying and using the property that $X(k) = X(N\text{-}k)^*$ from Equation 2.2 gives,

$$x(n) = \frac{1}{N} X(0) + \frac{1}{N} \sum_{k=1}^{\frac{N}{2}-1} \left\{ X(k) e^{+j\frac{2\pi}{N}nk} + X(k)^* e^{-j\frac{2\pi}{N}nk} \right\} + \frac{1}{N} X(\frac{N}{2}) e^{+j\pi n} \tag{2.7}$$

Equation 2.7 indicates that the time samples $x(n)$ can be represented as the sum of $(N / 2 + 1)$ components: a) the DC component $X(0)$, b) the $(N / 2 - 1)$ harmonics, and c) the $X(N / 2)$ harmonic corresponding to half of the sampling rate, with all of the components affected by the factor $(1 / N)$. The second term in the right hand of the Equation 2.7 can be rewritten as,

$$\frac{1}{N} \sum_{k=1}^{\frac{N}{2}-1} \left\{ \left(X(k) + X(k)^* \right) \cos\left(\frac{2\pi}{N} nk \right) + \left(X(k) - X(k)^* \right) j \sin\left(\frac{2\pi}{N} nk \right) \right\} \tag{2.8}$$

The cosine coefficient for any harmonic k (= 1,..., N/2-1) of interest can be obtained from Equation 2.8 using the definition of the DFT elements, as follows

$$\frac{1}{N}\left(X(k) + X(k)^* \right) = \frac{1}{N} \sum_{n=0}^{N-1} x(n) \left(e^{-j\frac{2\pi}{N}kn} + e^{+j\frac{2\pi}{N}kn} \right)$$

$$\frac{2}{N} \mathrm{Re}\{X(k)\} = \frac{2}{N} \sum_{n=0}^{N-1} x(n) \cos\left(\frac{2\pi}{N} kn \right) \tag{2.9}$$

and the sine coefficient is,

$$\frac{1}{N} j\left(X(k) - X(k)^*\right) = \frac{1}{N}\sum_{n=0}^{N-1} x(n) j\left(e^{-j\frac{2\pi}{N}kn} - e^{+j\frac{2\pi}{N}kn}\right)$$

$$-\frac{2}{N}\mathrm{Im}\{X(k)\} = \frac{2}{N}\sum_{n=0}^{N-1} x(n)\sin\left(\frac{2\pi}{N}kn\right) \qquad (2.10)$$

2.4.1.3 Phasor Estimation Based on DFT: The estimation of the fundamental frequency phasor consists of calculating the first DFT component with Equation 2.1 over a data window of N samples, and scaling it by (2 / N). The real and imaginary components can be calculated separately using Equations 2.9 and 2.10 [20,21]. The magnitude of this phasor is equal to the peak amplitude of the fundamental frequency component of the given signal. The time window of T=1/60 seconds (or 1/50 seconds in 50 Hz systems) corresponds to the fundamental frequency of 60 Hz. A sampling rate of 64 samples per cycle, i.e. F_S = 3840 Hz [2] at 60 Hz, is a representative value available at the present technology. For the sampling rate to be the integer number of N samples per cycle, a sampling synchronization process is required, which keeps track of changes in the power system frequency and adjust the sampling rate accordingly [5]. For instance, to keep the rate of 64 samples per cycle, if the power system frequency changes from 60 to 61 Hz then the sampling rate should change from 3840 to 3904 Hz.

2.4.1.4 Time Response of Phasor Estimation Based on DFT: The time response obtained applying this method to the signal of Figure 2.2 is shown in Figure 2.3 (a) and (b).

The phasor estimation requires a window full of data, N = 8 in this case, to produce a reliable estimate. For this reason, in Figure 2.3, the phasor output is only shown from sample s_n = 7 although the signal starts from sample s_n = 0. The resulting phasor magnitude is constant because the input signal corresponds to a steady state condition, with no disturbance present. The resulting angle is continuously changing, however, at a steady rate of 45^o every sample. A technique to overcome this variation is described later in section 2.4.3.

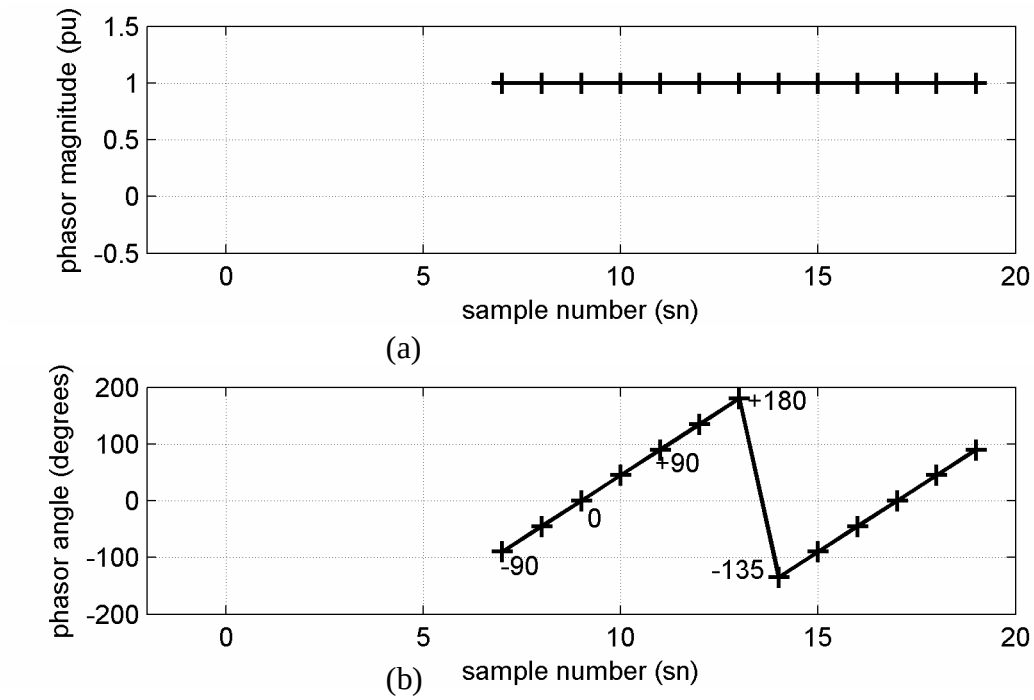

Figure 2.3 Magnitude and angle of phasor estimated with DFT method

2.4.1.5 Frequency Response of Phasor Estimation: The frequency response of this type of method can be calculated using the concept of convolution [32] and filter response. Given a signal $x(n)$ and a filter specified by its impulse response $h(m)$, $m = 0,\ldots,N\text{-}1$; the response $y(n)$ by applying the filter $h(m)$ to the signal $x(n)$ is,

$$y(n) = \sum_{m=0}^{N-1} h(m)x(n-m) = \sum_{m=n-N+1}^{n} h(n-m)x(m) \tag{2.11}$$

The frequency response of the filter $h(m)$ is obtained applying a signal $x(n) = e^{j\omega n}$, which is a phasor rotating at a frequency of ω radians every sample.

$$y(n) = \sum_{m=0}^{N-1} h(m)e^{j\omega(n-m)} = \left\{ \sum_{m=0}^{N-1} h(m)e^{-j\omega m} \right\} x(n) \tag{2.12}$$

The maximum frequency is $\omega = \pi$, that means one rotation every two samples, i.e. half of the sampling rate. The frequency response of the filter $h(m)$ is then,

$$H(j\omega) = \sum_{m=0}^{N-1} h(m) e^{-j\omega m} \qquad 0 < \omega < \pi,\ \omega \text{ is real} \tag{2.13}$$

2.4.1.6 Frequency Response of Phasor Estimation Based on DFT: Before applying Equation 2.13 to calculate the frequency response for the fundamental frequency real and imaginary components (k=1) of the phasor estimation based on DFT, Equations 2.9 and 2.10 need to be rearranged in convolution form, with the $h(m)$ elements and the $x(n)$ elements in opposite order. For the real component, this is done as follows,

$$\frac{2}{N}\sum_{n=0}^{N-1} x(n)\cos\left(\frac{2\pi}{N}(1)n\right) = \frac{2}{N}\sum_{n=0}^{N-1} x(N-1-n)\cos\left(\frac{2\pi}{N}[N-1-n]\right)$$

$$= \frac{2}{N}\sum_{n=0}^{N-1} x(N-1-n)\cos\left(\frac{2\pi}{N}[n+1]\right) \tag{2.14}$$

$$h_{REAL}(m) = \frac{2}{N}\cos\left(\frac{2\pi}{N}[m+1]\right) \qquad m = 0,\ldots,N\text{-}1 \tag{2.15}$$

For the imaginary component, the rearrangement is done as follows,

$$-\frac{2}{N}\sum_{n=0}^{N-1} x(n)\sin\left(\frac{2\pi}{N}(1)n\right) = -\frac{2}{N}\sum_{n=0}^{N-1} x(N-1-n)\sin\left(\frac{2\pi}{N}[N-1-n]\right)$$

$$= \frac{2}{N}\sum_{n=0}^{N-1} x(N-1-n)\sin\left(\frac{2\pi}{N}[n+1]\right) \tag{2.16}$$

$$h_{IMAG}(m) = \frac{2}{N}\sin\left(\frac{2\pi}{N}[m+1]\right) \qquad m = 0,\ldots,N\text{-}1 \tag{2.17}$$

Figures 2.4-2.7 show the frequency responses calculated for N = 64 and 60 Hz system. The magnitude response in both real and imaginary components shows a unity gain (= 0 dB) at the fundamental frequency of 60 Hz, as seen in Figures 2.4 and 2.6. A significant attenuation of more than 50 dB is observed for the harmonic frequencies, i.e. multiples of the fundamental. However the frequencies in between harmonics are less attenuated, for instance in the real component, the attenuation is only of 10 dB between 120 and 180 Hz, as shown in Figure 2.4.

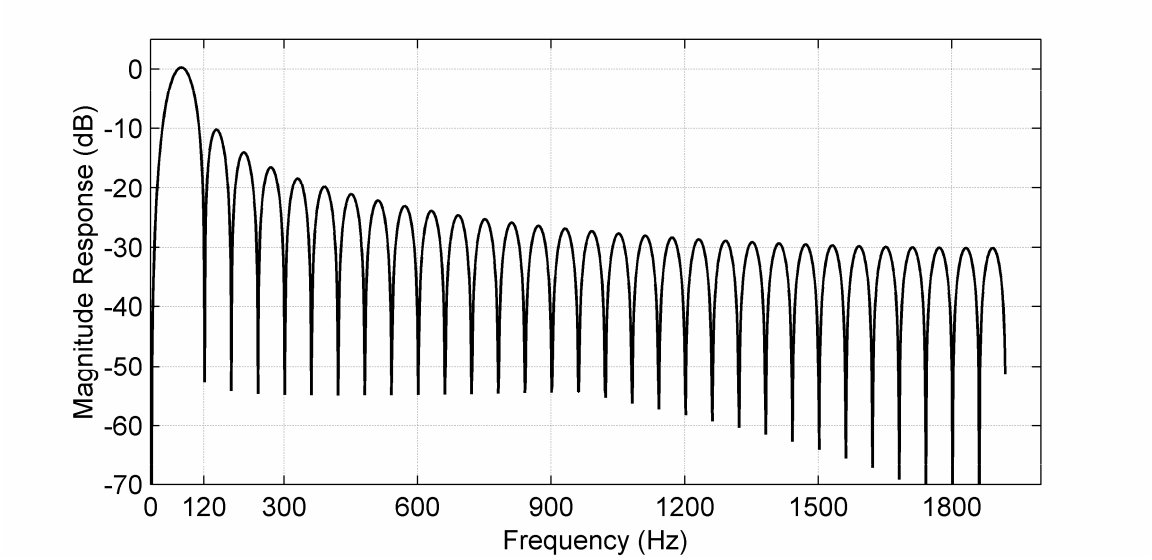

Figure 2.4 Magnitude response of real component estimator (cosine)

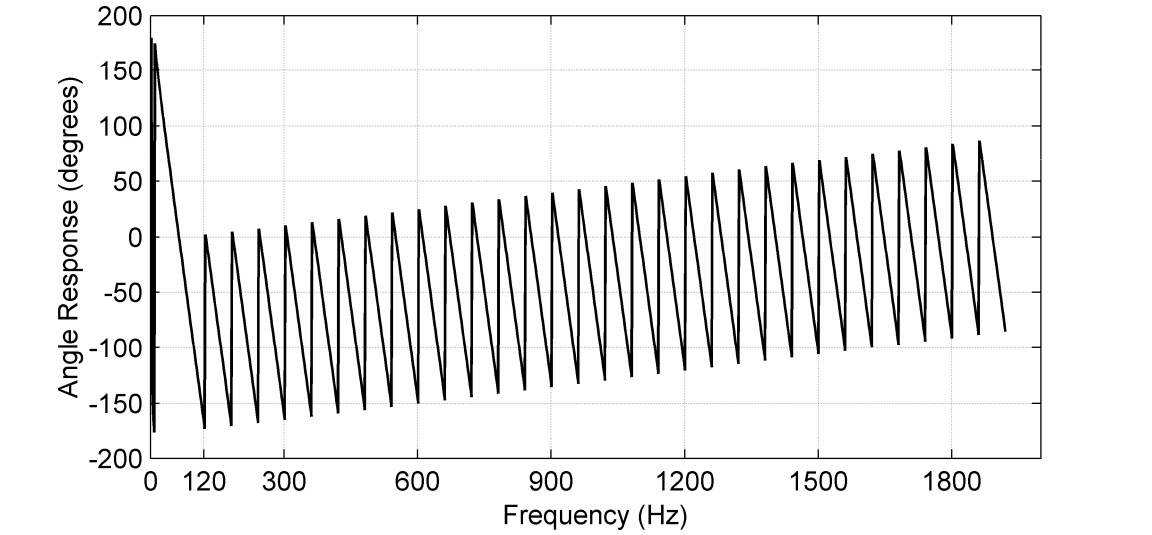

Figure 2.5 Angle response of real component estimator (cosine)

The angle response shows a zero degree response for the real component and 90° degrees lagging response for the imaginary component, both at the fundamental frequency of 60 Hz.

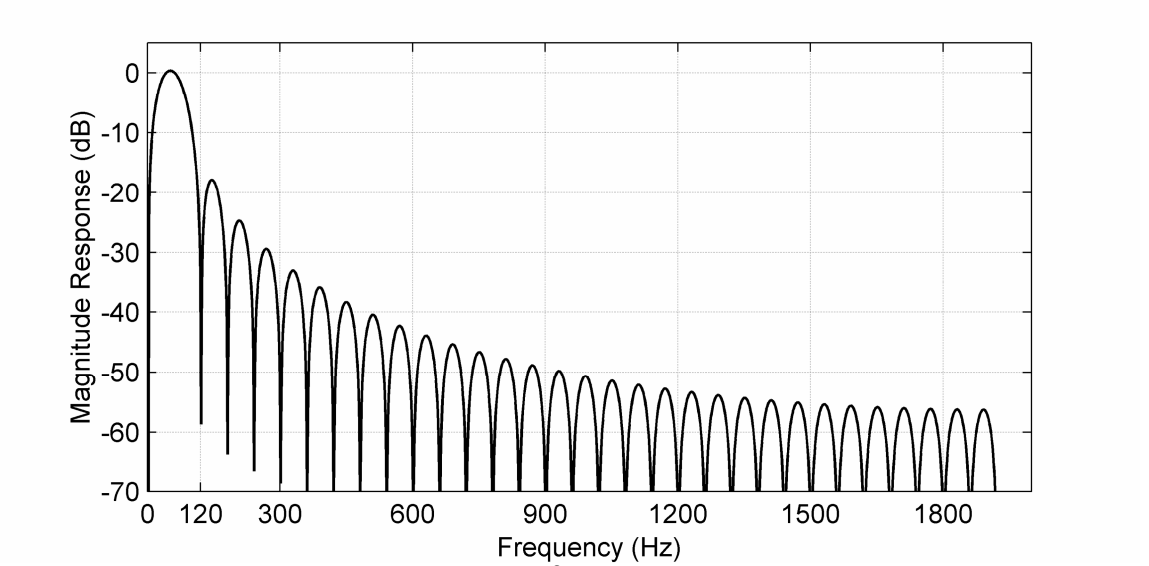

Figure 2.6 Magnitude response of imaginary component estimator (sine)

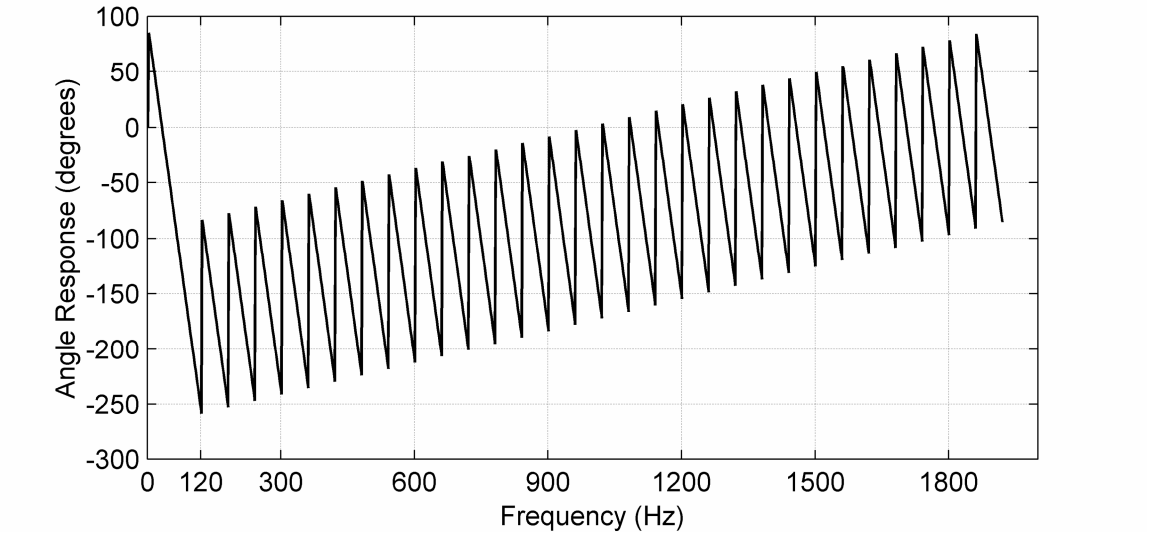

Figure 2.7 Angle response of imaginary component estimator (sine)

2.4.2 Least Squares Method

This method is based on the fitting of a curve to a set of measurements as close as possible. The measurements are samples of a signal taken at evenly distributed points in time over certain time window. The time between samples is the sampling period Δt, the number samples in the time window is the window size N, and the total time window is $N\Delta t$.

The curve to be fitted is pre-selected based on the expected characteristics of the signal measured. The description of this curve is dependent on parameters that are the unknowns. The fitting process consists of finding the value of the curve parameters that minimize the sum of squares of the differences between the measurements and the pre-selected curve. The application of the least squares method to obtain the desired phasors has been described by Sachdev [34]. The basic least squares method is described briefly in the following sections 2.4.2.1 and 2.4.2.2.

2.4.2.1 Curve Fitting Applied to Phasor Estimation: The curve selected for this method is a sine function of the fundamental frequency of the power system, i.e. typically 60 Hz or 50 Hz. The amplitude Y and phase angle θ of this sine function are unknown. This curve is decomposed in two orthogonal sine and cosine functions of unknown amplitudes, Y_R and Y_I. The parameters, Y_R and Y_I also represent the real and imaginary respectively of the desired phasor estimated [34]. The difference between the curve selected and the measurements is assumed to be the noise ε.

$$\begin{aligned} y(t) &= Y\sin(\omega_O t+\theta)+\varepsilon(t) \\ &= Y\cos(\theta)\sin(\omega_O t)+Y\sin(\theta)\cos(\omega_O t)+\varepsilon(t) \\ &= Y_R\sin(\omega_O t)+Y_I\cos(\omega_O t)+\varepsilon(t) \end{aligned} \tag{2.18}$$

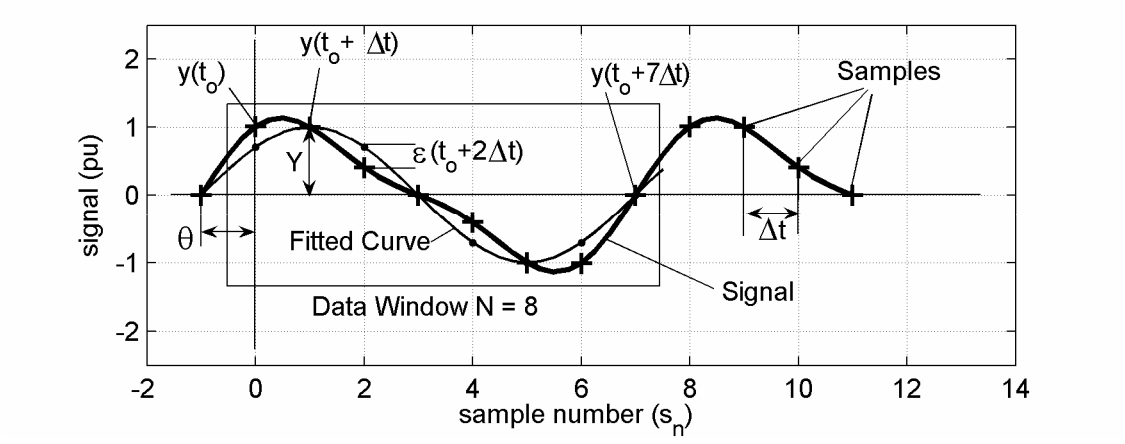

Figure 2.8 Curve fitting concept

Figure 2.8 illustrates the different variables used in the process of fitting a curve to a power system signal measured. In this example, the signal contains a distortion caused by a second harmonic component.

2.4.2.2 Finding the Least Squares Solution: In order to find the least squares solution, Equation 2.18 is applied to each of the *N* samples measured, resulting in an overdefined set of linear equations [34]. The system of linear equations is arranged in matrix form. In one side is the vector of *N* measurements as a function of the sampling time $t = t_O + k\Delta t$, $k = 0,\ldots,N\text{-}1$. On the other side there are two terms: one is the matrix with the sine and cosine coefficients, also a function of the sampling time; this matrix multiplies the vector of unknowns with Y_R and Y_I. The other term is the vector of errors, which also is a function of the sampling time.

$$\begin{bmatrix} y(t_O + 0\Delta t) \\ y(t_O + 1\Delta t) \\ \vdots \\ y(t_O + [N-1]\Delta t) \end{bmatrix} = \begin{bmatrix} \sin(\omega_O 0\Delta t) & \cos(\omega_O 0\Delta t) \\ \sin(\omega_O 1\Delta t) & \cos(\omega_O 1\Delta t) \\ \vdots & \vdots \\ \sin(\omega_O [N-1]\Delta t) & \cos(\omega_O [N-1]\Delta t) \end{bmatrix} \begin{bmatrix} Y_R \\ Y_I \end{bmatrix} + \begin{bmatrix} \varepsilon(t_O + 0\Delta t) \\ \varepsilon(t_O + 1\Delta t) \\ \vdots \\ \varepsilon(t_O + [N-1]\Delta t) \end{bmatrix} \tag{2.19}$$

In matrix notation this is,

$$[b] = [A][x] + [\varepsilon] \tag{2.20}$$

The least squares solution for this system, which minimizes the sum $[[\varepsilon]^T[\varepsilon]]$, is obtained using the left pseudo-inverse of $[A]$ as follows:

$$[x] = \left[[A]^T[A]\right]^{-1}[A]^T[b] \tag{2.21}$$

One of the advantages of the least squares method over the DFT based method is that the sampling rate does not need to be an integer number of samples per cycle. However, the sampling rate needs to be proportionally adjusted when the power system frequency changes, to minimize the magnitude and angle errors introduced by this change. Another advantage of the least squares method is that the description of the

curve to be fitted does not need to be a sine function, in this sense the least squares method is more general.

If the sampling rate is selected to have an integer number of samples per power system cycle, so that $\omega_O N\Delta t = 2\pi$, using a sine curve as previously described, then a relationship similar to the DFT based method is obtained, the following identity is satisfied,

$$\left[[A]^T[A]\right]^{-1} = \begin{bmatrix} 2/N & 0 \\ 0 & 2/N \end{bmatrix} \tag{2.22}$$

and the pseudo inverse becomes,

$$\left[[A]^T[A]\right]^{-1}[A]^T = \frac{2}{N}\begin{bmatrix} \sin(\omega_O 0\Delta t) & \sin(\omega_O 1\Delta t) & \cdots & \sin(\omega_O[N-1]\Delta t) \\ \cos(\omega_O 0\Delta t) & \cos(\omega_O 1\Delta t) & \cdots & \cos(\omega_O[N-1]\Delta t) \end{bmatrix} \tag{2.23}$$

2.4.3 Angle Normalization

The angle of the phasor estimated with any of the two methods previously presented is not constant in time. In steady state conditions, without any disturbance, the angle estimated changes steadily completing one rotation every power system cycle.

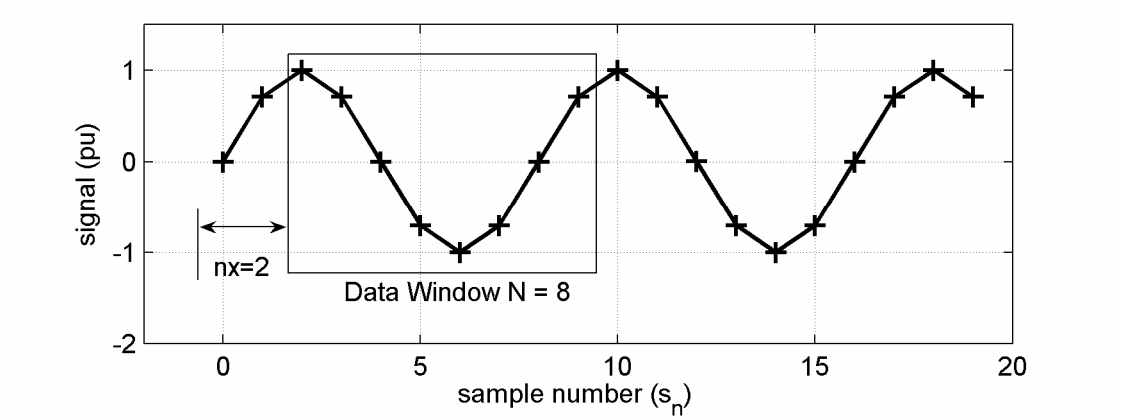

Figure 2.9 Signal used for the angle normalization example

An example is used to clarify this behavior of the phasor estimation methods presented. Suppose that the signal to be processed is a sine function with amplitude of 1.0, as shown in Figure 2.9 that satisfies Equation 2.24,

$$y(s_n) = \sin\left(\frac{2\pi}{N} s_n\right) \qquad N = 8,\ s_n = \text{sample number} \tag{2.24}$$

The DFT based method with a data window $N = 8$ is used here for the estimation. This window is currently processing samples $s_n = 2,\ldots,9$; the next time the window will process samples $s_n = 3,\ldots,10$. Before applying Equations 2.9 and 2.10, the signal should be arranged so that the first sample in the window corresponds to the index $n = 0$, this is done using the auxiliary variable nx as follows,

$$y(n) = \sin\left(\frac{2\pi}{N}[n + nx]\right) \tag{2.25}$$

Expanding Equation 2.25,

$$y(n) = \sin\left(\frac{2\pi}{N} n\right)\cos\left(\frac{2\pi}{N} nx\right) + \sin\left(\frac{2\pi}{N} nx\right)\cos\left(\frac{2\pi}{N} n\right) \tag{2.26}$$

The real and imaginary component, applying Equations 2.9 and 2.10, results in,

$$\begin{aligned} Y_{RE} &= \frac{2}{N}\sum_{n=0}^{N-1}\left\{\sin\left(\frac{2\pi}{N} n\right)\cos\left(\frac{2\pi}{N} nx\right) + \sin\left(\frac{2\pi}{N} nx\right)\cos\left(\frac{2\pi}{N} n\right)\right\}\cos\left(\frac{2\pi}{N} n\right) \\ &= \frac{2}{N}\left\{(0)\cos\left(\frac{2\pi}{N} nx\right) + \frac{N}{2}\sin\left(\frac{2\pi}{N} nx\right)\right\} \\ &= \sin\left(\frac{2\pi}{N} nx\right) \end{aligned} \tag{2.27}$$

$$\begin{aligned} Y_{IM} &= -\frac{2}{N}\sum_{n=0}^{N-1}\left\{\sin\left(\frac{2\pi}{N} n\right)\cos\left(\frac{2\pi}{N} nx\right) + \sin\left(\frac{2\pi}{N} nx\right)\cos\left(\frac{2\pi}{N} n\right)\right\}\sin\left(\frac{2\pi}{N} n\right) \\ &= -\frac{2}{N}\left\{\frac{N}{2}\cos\left(\frac{2\pi}{N} nx\right) + (0)\sin\left(\frac{2\pi}{N} nx\right)\right\} \end{aligned}$$

$$= -\cos\left(\frac{2\pi}{N} nx\right) \tag{2.28}$$

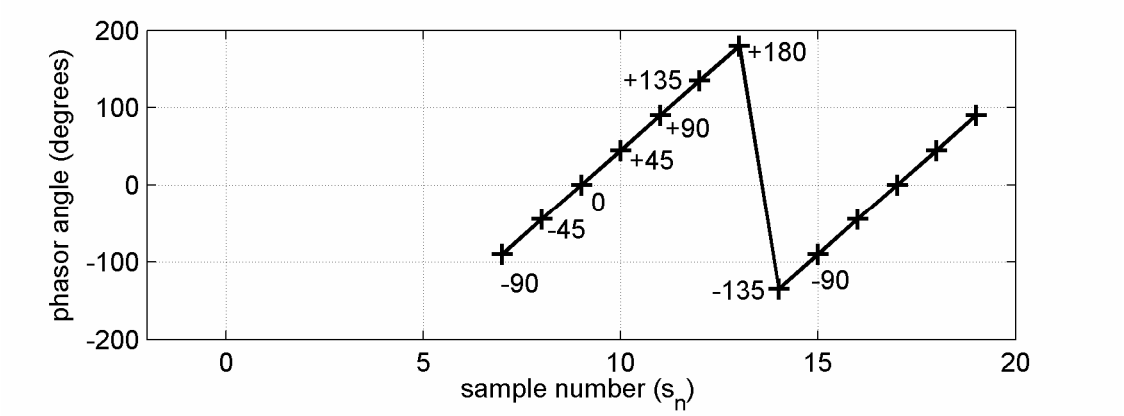

Figure 2.10 Angle estimated using DFT method

Figure 2.10 shows the angle of the phasor estimated as a function of time. The phasor angle increases in time, i.e. 45° degrees (= 2π / *N* radians) every sample. For instance for s_n = 7 (nx = 0) the estimation, using Equations 2.27 and 2.28, gives Y_{RE} = 0 and Y_{IM} = -1, with an angle of -90° degrees, and for the next sample s_n = 8 (nx = 1), the estimation gives Y_{RE} = 0.7071 and Y_{IM} = -0.7071, with an angle of -45° degrees.

It is useful for analysis purposes or for some relay functions, to normalize the angle using some reference, so that the normalized angle remains constant in time during steady state conditions, instead of changing continuously. An angle change in time caused by a disturbance is more noticeable and easier to detect, once the angle is normalized. The same reference should be used for all phasors estimated; to keep the relative angle between all of them at any specific point in time unchanged.

The phasor $e^{-j\omega sn}$ provides a good angle reference. The angle of this phasor decreases ω radians per sample, with every increment of the integer sample index s_n. This phasor also makes one rotation every power system cycle, but in the opposite direction as the phasor estimated, a value of ω = 2π / *N* is used for that. The phasors estimated are multiplied by this reference phasor every sample, the result is a normalized phasor.

2.4.4 Phasor Estimation Method Using Single Component

The real and imaginary components of a rotating phasor, when plotted against time, are sine functions oscillating at the fundamental frequency with amplitudes equal to the magnitude of that phasor. This concept is illustrated in Figure 2.11. The real component signal leads the imaginary component by ninety electrical degrees, for a counterclockwise rotation. These two orthogonal sine functions may be produced by time shifting one of them; a method for phasor estimation using this idea is described in this section.

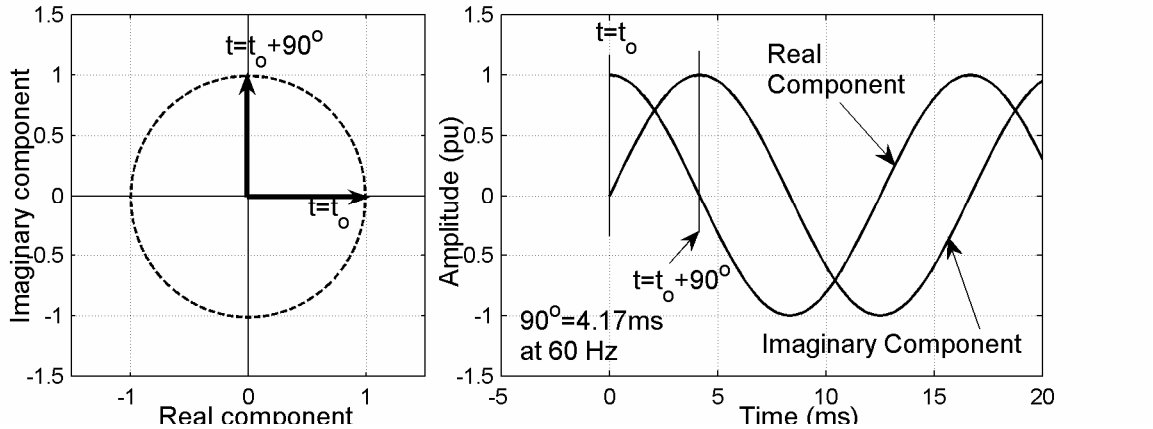

Figure 2.11 Rotating phasor concept

Assume that an ideal fundamental frequency signal $v(t)$ is measured. The real component of the phasor is $V_{RE}(t) = v(t)$. The imaginary component of this phasor is $V_{IM}(t) = v(t\text{-}90^o)$. The ninety electrical degrees in time units is a quarter of a fundamental frequency period, i.e. $90^o = (1/4)*(1/60) = 4.17$ ms. The expression $(t\text{-}90^o)$ indicates that a measurement of the $v(t)$ signal taken 90^o before is needed.

This method has an inherent delay of one quarter of a cycle to obtain a phasor. An advantage of this method is that it requires a single component signal oscillating at the desired frequency. For the case of an ideal sine function illustrated in Figure 2.11, the magnitude of the phasor is constant, but the angle of this phasor increases continuously at a rate of 360^o every power system cycle. The disadvantage is that the presence of other frequencies may introduce an error in the estimation results.

In a practical implementation using this method, the frequencies other than the fundamental should be removed first. One such example is the Cosine Filter described by Schweitzer in [49], which is equivalent to the use of Equation 2.9, i.e. the real component of the DFT method. Other filters with desired response characteristics may be used instead.

2.5 BASIC RELAY TYPES

The phasors estimated are used to decide if there is a fault in the protected circuit. The protective relays are classified mainly based on the principle used to make this decision. The basic protective relay principles that are discussed here are:

- Overcurrent
- Over/under voltage
- Directional
- Distance
- Current differential

2.5.1 Overcurrent Relay

The overcurrent relay [30,43,44] solves the fault detection problem by using two types of discrimination: current level and time, these are illustrated in Figure 2.12. The discrimination by current level recognizes two conditions: fault current, which should be detected; and load current which should be ignored. The difference between these two levels of current should be enough to clearly identify any one from the other; and care should be taken because these levels vary, i.e. they are not constant.

The time discrimination is used as a complement because the current level method detects internal and external fault conditions; i.e. there is an overlap of current level coverage with downstream relays. The time discrimination ensures that the relay closer to a fault trips faster; to obtain this discrimination other relays should delay their operation in order of closeness.

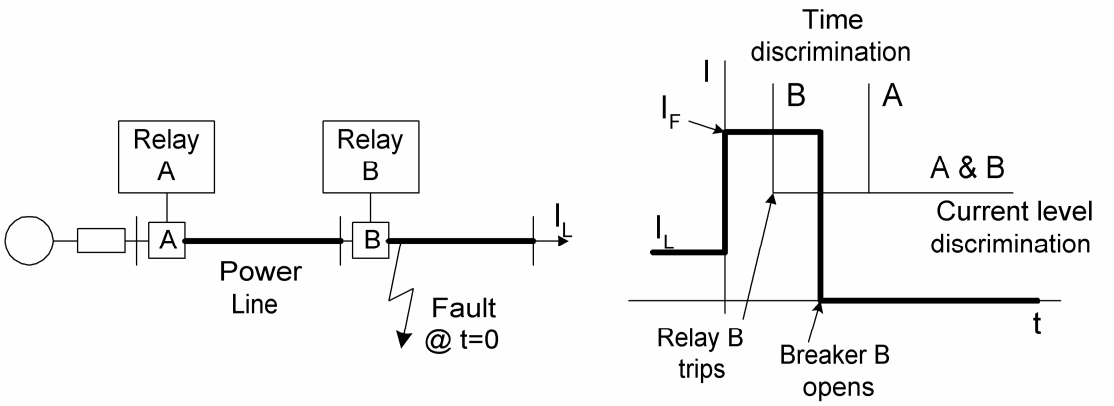

Figure 2.12 Current level and time discrimination

The overcurrent protective function consists of a current level detector combined with a time delay. The current level detector is activated, or "picks up", when the current measured | I | exceeds a pickup threshold I_{PICKUP}, i.e. when | I | > I_{PICKUP}. The time delay measures the time t since the current detector picked up; when this time exceeds an operating time limit ($t > T_{OP}$), the trip operation is decided.

The overcurrent relays can be classified in two main types: instantaneous and time delayed. The instantaneous overcurrent operates without any intentional time delay, as soon as the current level detector picks up. The term "instantaneous" is not exact, because there is an inherent time delay in the process of measuring the current | I |. In numerical relays, the phasor estimation method requires that the data window is inside the fault, i.e. contains no pre-fault samples, to provide a reliable estimate.

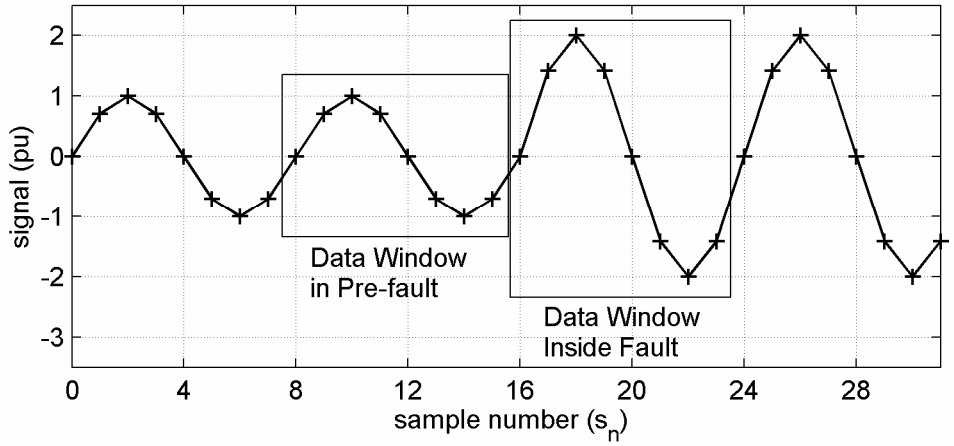

Figure 2.13 Signal current increasing from 1.0 to 2.0 pu

Figures 2.13 and 2.14 illustrate the concept of “instantaneous” operation. The data window is moving in time, from pre-fault to fault. The magnitude | *I* | of the pre-fault current is 1.0 pu and the fault current is 2.0 pu. During the transition from pre-fault to fault, the data window contains information from both pre-fault and fault, producing a phasor with a magnitude in between 1.0 and 2.0 pu. The threshold I_{PICKUP} shown in Figure 2.14 is only exceeded when the data window is completely inside the fault. The one cycle time window becomes here an inherent time delay in the operation of this instantaneous overcurrent relay.

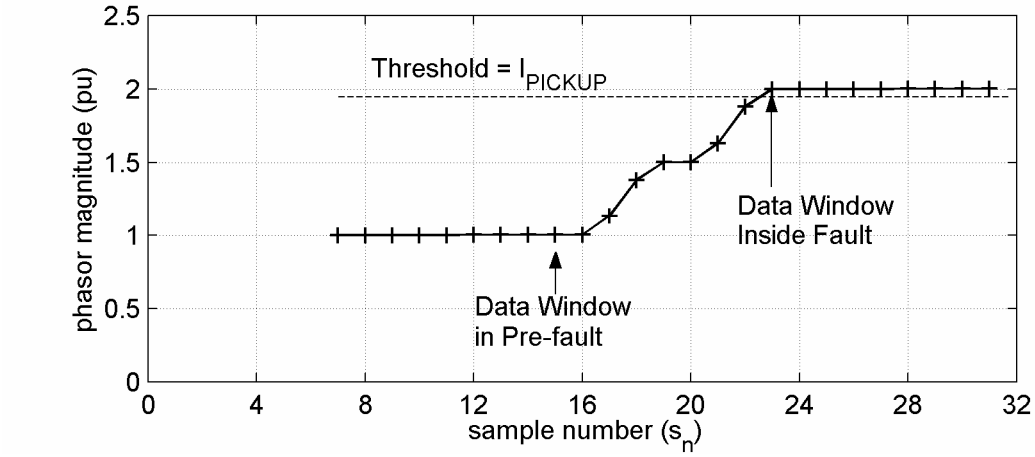

Figure 2.14 Phasor magnitude response in time for Figure 2.13 signal

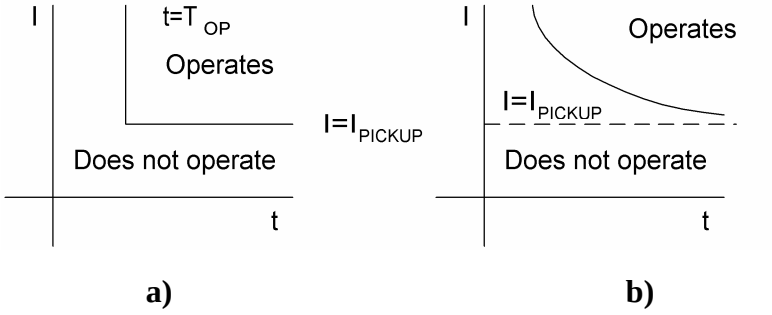

Figure 2.15 Time overcurrent curves: a) definite time, b) inverse time

The time overcurrent operates using both current level and time delay discrimination combined. Typically, a relationship is defined between current and time, so that the operating time is shorter for higher current levels; the relationship is called time curve. In general, two kinds of time curve are commonly used: definite time and

inverse time, they are shown in Figure 2.15. The definite time curve is defined completely by one point in the current-time plane: the pickup current I_{PICKUP} and the operating time T_{OP}. The operation occurs when $| I | > I_{PICKUP}$ and $t > T_{OP}$ simultaneously. The inverse time curve is actually a functional relationship between current and time. The inverse time has the following characteristics: 1) Higher currents correspond to a shorter operating time, 2) Lower currents correspond to a longer operating time and 3) With currents below a pickup value, I_{PICKUP}, the operating time is infinite, i.e. there is no operation.

2.5.2 Over/under Voltage Relay

The voltage relay is responsible for protecting power system components that are sensitive to changes in voltage magnitude [30,43,44]. An overvoltage condition stresses the dielectric insulation and increases the magnetic flux beyond normal limits in electrical machines. An undervoltage condition may produce an abnormal increase in current for loads with constant power behavior such as electrical motors supplying a constant torque.

The voltage protective function consists of a voltage level detector combined with a time delay. There are two kinds of voltage level detectors depending on how the threshold, V_{TH}, is compared to produce a pick up: 1) overvoltage is when the voltage measured needs to exceed the threshold, i.e. $| V | > V_{TH}$ and 2) undervoltage is when $| V | < V_{TH}$. The time delay measures the time t since the level detector picked up; when the time exceeds a time limit ($t > T_{LIM}$), the trip operation is decided.

2.5.3 Directional Relay

The directional relay [30,43,44] solves a problem with the overcurrent relay in non radial power system networks. The main difference between radial and a non radial system that affects the overcurrent relay is the level of fault current for reverse faults, i.e. faults behind the relay and outside the protected area; this problem is illustrated in Figure 2.16. In radial systems, reverse faults do not show fault current at all in downstream overcurrent relays, i.e. relays that are beyond the fault location in the

direction of the load. Non radial systems, on the other side, show a significant reverse fault current making it difficult to discriminate forward and reverse fault conditions based on current level alone. The directional relay solves this discrimination problem identifying the fault direction: forward or reverse; and combines this with the regular overcurrent function to produce a correct operation; this is called the directional overcurrent relay.

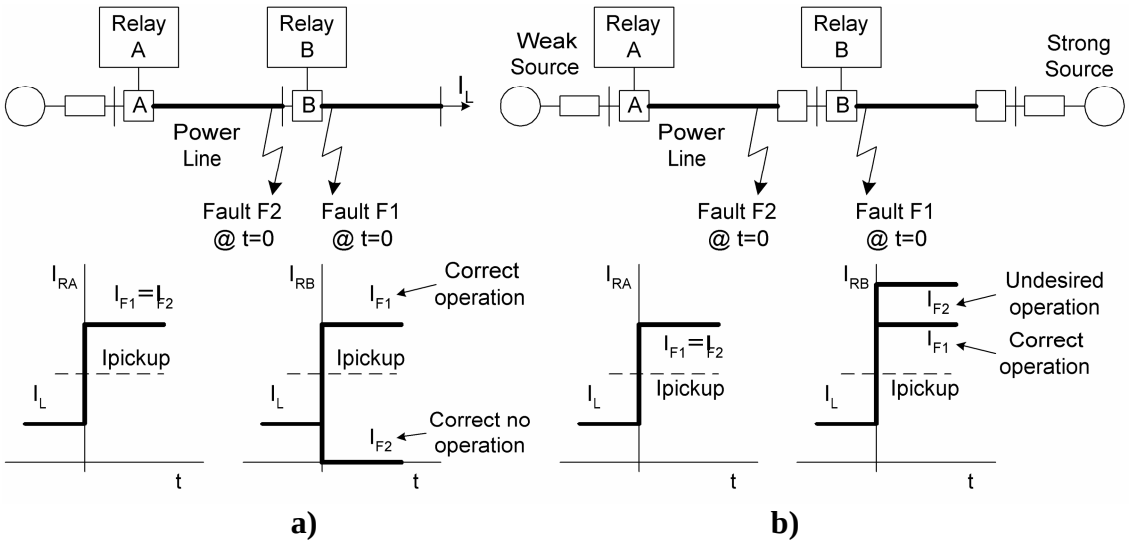

Figure 2.16 : Problem with overcurrent protection: a) radial network, b) non-radial network

The directional protective function consists of an angle comparison between two phasors: operating and polarizing phasors. The operating phasor is commonly the current phasor, whose angles for forward and reverse fault conditions are typically 180^o apart, i.e. this angle is function of the fault direction. The polarizing phasor is typically a voltage phasor, whose angle is not much dependent on the fault direction and therefore is used as a reference. The exact angle relationship between operating and polarizing phasors is obtained from power system analysis or studies.

2.5.4 Distance Relay

The distance relay [30,43,44] solves a problem with directional overcurent relays, whose reach coverage vary with the level of fault current. The fault current level depends on the strength of the equivalent source that feeds the fault; a stronger source produces higher fault current than a weaker source. The strength of the equivalent source varies with the amount of generation; a maximum generating condition is stronger than a minimum generating condition, and these conditions vary with the load demand during the day. The reach coverage of an overcurrent relay is reduced in weak source conditions, and is extended in strong source conditions.

The reach of a distance relay is independent from the fault current. The reach limit is defined by the distance of the power line covered in the specified direction. A fault inside the reach is an internal fault and should be detected, and a fault beyond the reach is an external fault and should be ignored. A distance relay, like the overcurrent relay, typically requires the use of a directional element to ensure selectivity against reverse faults.

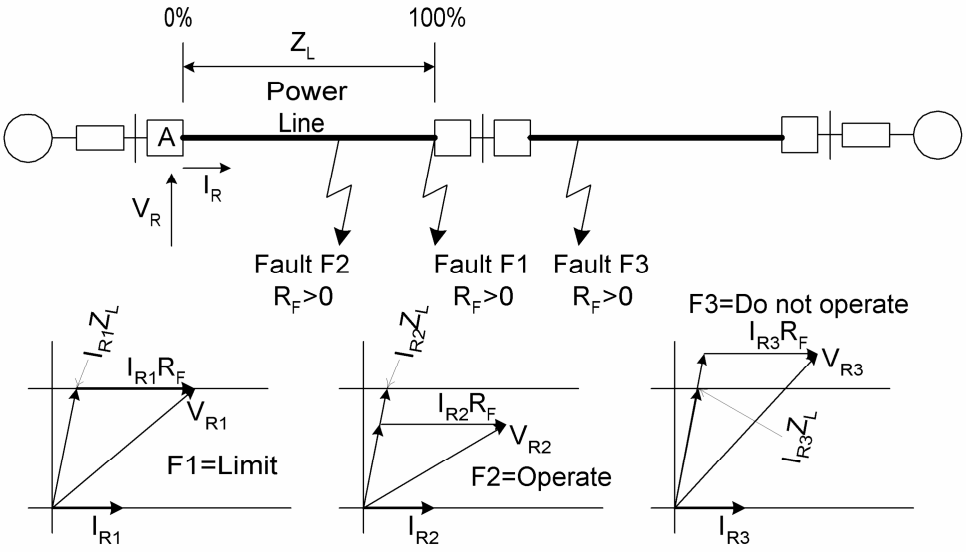

Figure 2.17 : Distance protective function principle

The distance protective function consists of a comparison of the impedance of the power line Z_L and the impedance measured Z_R during fault conditions. For faults with no resistance the magnitude of the impedance measured is proportional to the

distance to the fault, considering the total power line impedance as 100%, the fault detection here becomes a simple comparison of impedance magnitudes. In a general case, where faults have some resistance, the voltage measured V_R is compared to the estimated voltage drop across the line impedance $I_R Z_L$ using a region in the complex plane of voltages, this principle is illustrated in Figure 2.17. This plane uses the current measured I_R as the reference with zero degrees, the reach limit is defined by a horizontal line passing by the end of the phasor $I_R Z_L$, faults with voltage measured V_R below this line are internal and faults above are external, i.e. beyond the reach. The line that defines the reach limit represents the hypothetical voltage drop, in phase with I_R, across the fault resistance for faults at the end of the line.

2.5.5 Current Differential Relay

The current differential relay solves a number of difficulties that the distance relay has to overcome to ensure the required level of selectivity. Among the difficulties that a distance relay has to solve are: 1) voltage transients at the fault inception [11,14,38,43], which are more severe in CCVT applications, 2) faults with zero voltage [11,14], may cause wrong directional decision, 3) effect of load flow [43], affect the percent coverage for resistive faults, 4) mutual coupling [38,43], induces voltage in the non faulted parallel line and 5) others.

The current differential relay makes use of the Kirchoff's Law of electricity to achieve selectivity. This relay is immune to most of the conditions that affect a distance or other relays; the number of design issues to consider is lower in this aspect. A current differential relay requires the measurement of all currents entering the protected circuit. For a power line this requirement implies the use and dependence of communication to share this information between both ends of the line.

The current differential protective function [30,43], as shown in Figure 2.18, consists basically of a direct application of Kirchoff's Law, the sum of all currents entering a protected circuit should add to zero. A non-zero differential current indicates therefore the presence of a fault in the protected area. In a real application, however, there are some conditions that produce a differential current that are not faults and

should be ignored: 1) CT errors, 2) shunt currents, i.e. currents to ground, inherent to the protected circuit and 3) others. The CT error is present for two reasons: one is the accuracy error that has a non-zero finite value and the other is the saturation error which is present for high currents entering the non-linear region of the CT. The inherent shunt currents depend on the type of protected component: in power transformers the inrush current experienced during energization is one example, another is the capacitive shunt currents in power lines. Other reason for a differential current is the change of transformation ratio in a power transformer, typically known as "tap change".

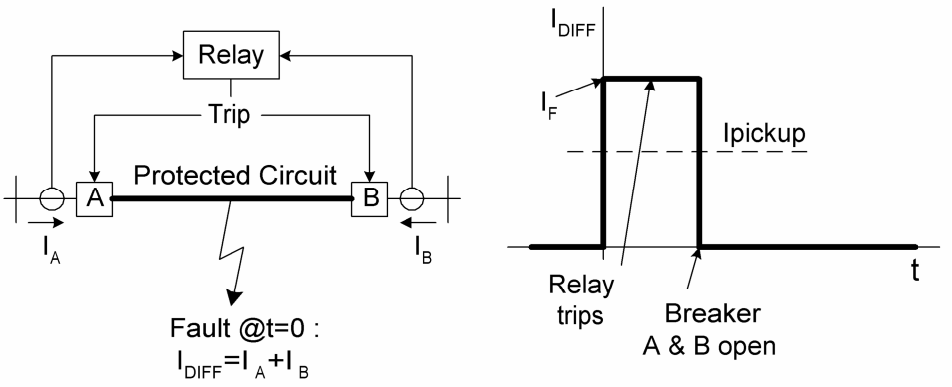

Figure 2.18 : Current differential protective function principle

2.6 SUMMARY

The numerical relays are described in this Chapter. The main functional components of these relays are listed indicating their importance in the overall operation. Particular attention is dedicated to the fault detection components: phasor estimation and protection function. Two common methods for phasor estimation are described: the Discrete Fourier Transform and the Least Squares Error methods. The basic protection functions and the protection problems they can solve are explained.

3. COUPLING CAPACITOR VOLTAGE TRANSFORMER (CCVT) CHARACTERISTICS

3.1 INTRODUCTION

The CCVTs scale down the high voltage received from the power system to a voltage level that can be directly applied to protection, measurement and control equipments on a substation; the protection equipments are typically the numerical relays described in the previous chapter. Also, the CCVTs provide electrical isolation and protection to these low voltage substation equipments from the high voltage circuit. The lower voltage level, also known as secondary voltage, is typically normalized to 100V, 110V, 115V or 120V depending on the standards [3] of the country being considered.

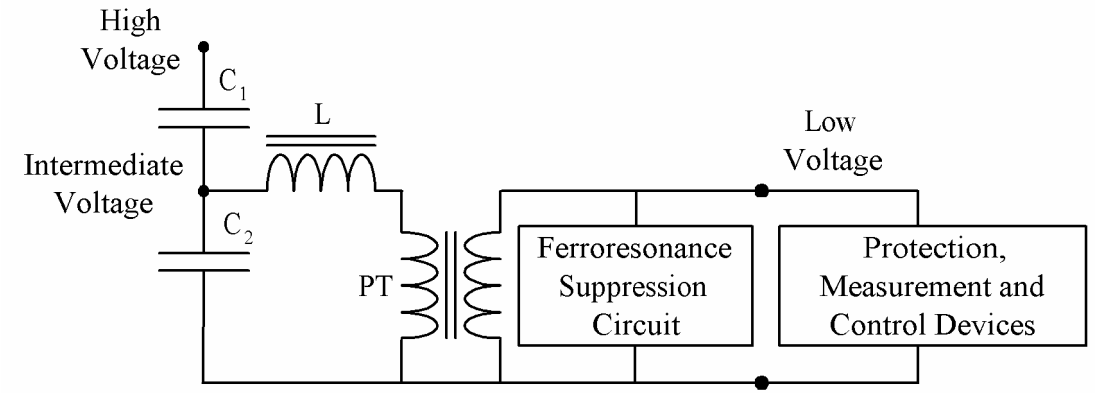

Figure 3.1 Basic CCVT elements

3.1.1 Description

A CCVT, as shown in Figure 3.1, consists of three main elements: a capacitive divider C_1 and C_2 , a series inductance L and an intermediate potential transformer PT. The capacitive divider scales down the high voltage, also known as primary voltage, to

some intermediate voltage level in the range of 5kV to 20kV. The series inductance compensates the equivalent capacitive reactance of the divider; its inductance value is selected to obtain a reactance very close, but of the opposite sign, to that of the divider at the rated fundamental frequency. The intermediate PT scales down the intermediate voltage to the normalized secondary voltage level required by the protection, measurement and control equipments connected to the CCVT output. These equipments are also referred to as the CCVT burden.

The CCVT is protected against ferroresonance by a special circuit included: the ferroresonance suppression circuit. A condition of ferroresonance produces overheating and possibly damage to the intermediate PT, due to the high currents associated with ferroresonance that brings the magnetic flux in the core of this transformer into the non-linear region. The risk of ferroresonance is present whenever a non-linear inductance, i.e. the PT, and capacitances are in the same circuit.

3.1.2 Justification

The CCVT design is more complex than that of a simple PT to perform the same function of scaling down voltage. However, CCVTs are commonly the preferred choice, for the following reasons:

1. CCVTs are significantly less expensive than PTs, especially at higher voltage levels [36]. The main cost variable is the dielectric insulation required for the PT.
2. The steady state accuracy of CCVTs is acceptable even for the most demanding applications. Typical accuracies of 0.2% IEC or 0.3% ANSI are available nowadays [8].
3. Additional functionality, such as power line carrier (PLC) communication [19], is possible with the CCVT. The CCVT capacitors provide the coupling required to apply the carrier signals into the power line.

3.1.3 Problems Associated with the CCVT

The CCVT response is far from ideal, power system voltage transients are not reproduced with good accuracy on the CCVT output, because significant distortion may

be introduced by the CCVT [12,15,17,18,22-24,37,40]. The acceptable accuracy previously mentioned (section 3.1.2) corresponds to steady state conditions, not transient. In the following section 3.2, the CCVT response characteristics as well as the factors that affect this response will be discussed in more detail.

3.2 CCVT RESPONSE

A review of the CCVT response will explain the reasons behind the inaccuracies that are present during transient conditions. Two kinds of response are considered for this review: frequency response and transient response. The model used to obtain these responses is described later in section 3.3.2.1.

3.2.1 CCVT Frequency Response

The frequency response consists of two parameters plotted against frequency: the magnitude gain and the angle shift, these plots are known as the magnitude response and the angle response respectively. A magnitude gain of unity (1.0) and angle shift of zero (0°) degrees for the whole range of frequencies applied is considered as an ideal frequency response. The scale used for the magnitude gain is the Decibel (dB), and satisfies the following relationship: $gain_{dB} = 20*\log_{10}(gain)$, for instance a unity $gain = 1.0$ is equivalent to a zero $gain_{dB} = 0.0$.

3.2.1.1 Characteristics of the CCVT Frequency Response: Figure 3.2 shows a typical CCVT magnitude response [12,13,17,22,26-28,40-42]. This figure shows that the magnitude response is not ideal, the main characteristics of this response are:

1. Unity gain (in per unit) at the rated fundamental frequency, i.e. steady state.
2. Amplification of some undesired frequencies, slightly above and below the fundamental.
3. Attenuation of higher frequencies and the DC (0 Hz).

The magnitude response of the CCVT varies with the frequency, i.e. the gain is not always unity. This is not a problem in steady state, because it is a single frequency point in the plot with unity gain. The transient response, however, is affected because it

is a combination of several frequencies. The end result during transient conditions is that the output signal is different from the input signal, because the relative composition of frequencies is varied by the CCVT.

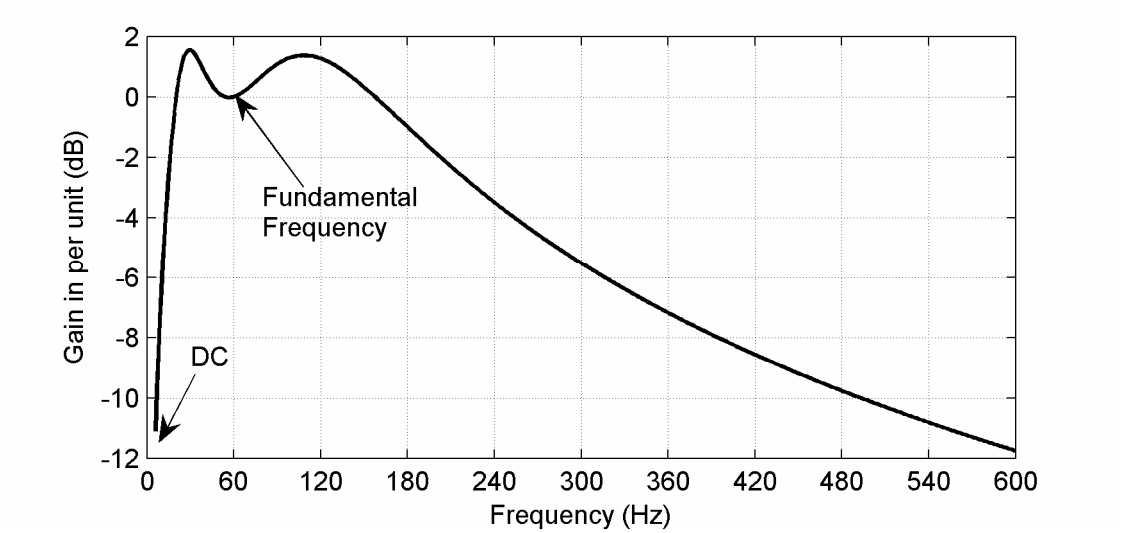

Figure 3.2 Typical CCVT magnitude response

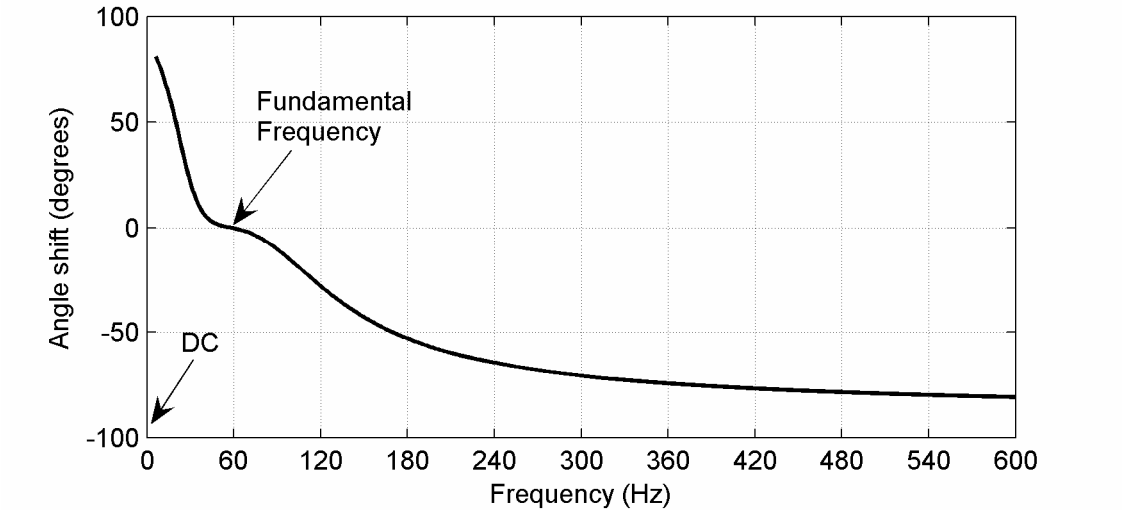

Figure 3.3 Typical CCVT angle response

Figure 3.3 illustrates a typical CCVT angle response [12,13,27]. This figure shows that the angle response is not ideal, the main characteristics of this response are:

1. Zero (0°) degree angle shift at the rated fundamental frequency.
2. Leading angle shift from DC (0 Hz) to the fundamental frequency.
3. Lagging angle shift for higher frequencies.

The angle response of the CCVT varies with the frequency. The steady state is not affected, because the angle shift for this point in the plot is zero degrees. The transient response is affected because it is composed of several frequencies, and every frequency is shifted by a different angle in a non linear way, i.e. the relative position in time of each frequency component is different when comparing the input signal with the output signal. Therefore, the output is different from the input.

3.2.1.2 Factors Influencing the CCVT Frequency Response: There are three factors that influence the CCVT frequency response: the type of ferroresonance suppression circuit, the overall CCVT design parameters and the external burden.

The most significant factor that affects the CCVT response is the type of ferroresonance suppression circuit. Two kinds of design for this circuit are known: active and passive [17,26,36,41]. The active design affects the frequency response more significantly [17,26], and was chosen for this work. This design incorporates a narrow filter composed of inductance, capacitance and loading resistor, tuned to the fundamental frequency, and permanently connected to the CCVT. In contrast, the passive design of CCVT produces a response very close to the ideal [17,26]. This almost ideal response is explained by the fact that the suppression circuit remains inactive, i.e. “passive”, until a ferroresonance condition is detected by the presence of an instantaneous overvoltage.

Another factor that affects the frequency response is the overall CCVT design parameters [15,22,26,37,41], which basically is the combination of capacitive divider and series inductance.

The burden connected, although is external to the CCVT, is also an important factor, because it is necessary to precisely define the frequency response of the CCVT [15,22,26,37]. Figures 3.4 and 3.5 show the dependence of the CCVT frequency response on the burden.

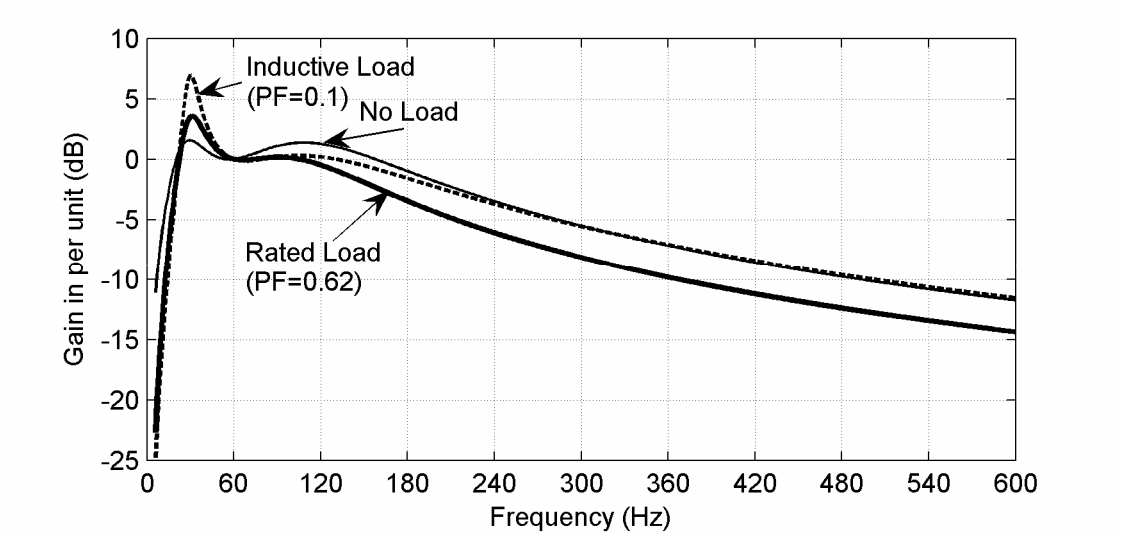

Figure 3.4 CCVT magnitude response dependence on the load

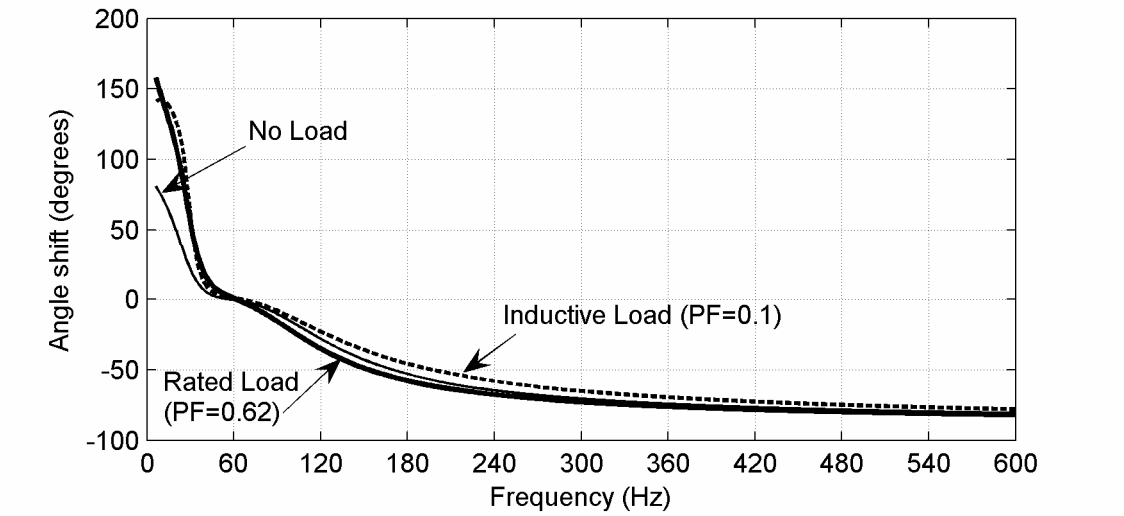

Figure 3.5 CCVT angle response dependence on the load

The impact of the burden, also called load here, can be classified qualitatively as follows:

1. Higher power factor, i.e. larger resistive load, cause larger attenuation of higher frequencies.
2. Lower power factor, i.e. larger inductive load, cause amplification of frequencies slightly below the fundamental.

3. A no load condition results in higher amplification of frequencies slightly above and lesser amplification of frequencies slightly below the fundamental frequency.
4. The angle response is less affected than the magnitude response.

3.2.2 CCVT Transient Response

The transient response considered here is the time domain response to a change in the stationary conditions originally applied to a CCVT. A transient response that is an exact scaled down replica of the voltage input with no time delay is considered as an ideal response.

3.2.2.1 Characteristics of the CCVT Transient Response: The transient response can be separated in two basic components [22,40]: a new steady state voltage, and a decaying oscillatory transient. These two components are shown in Figure 3.6.

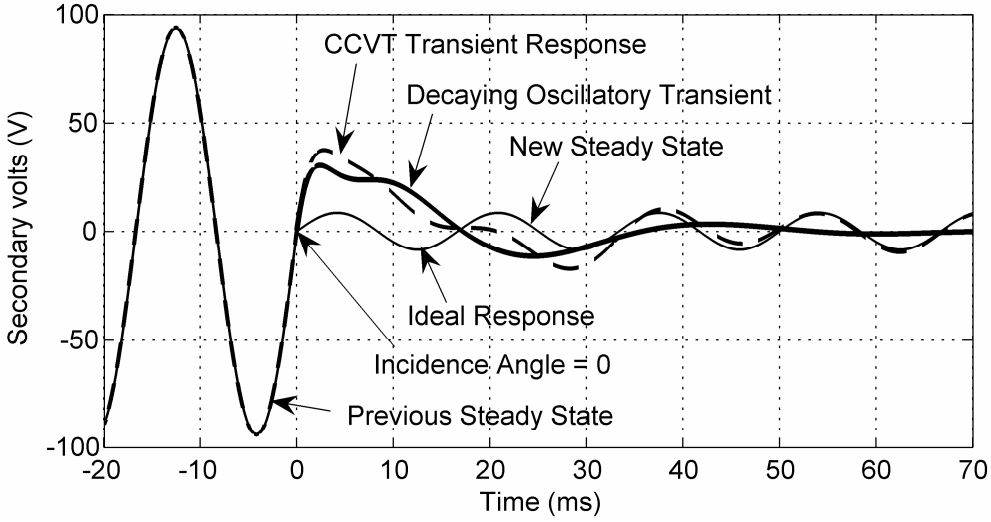

Figure 3.6 CCVT transient response (0 degree incidence angle)

The new steady state voltage is representative of a fault condition that has not been cleared yet. For clarity, the transition of the power system to this new voltage is assumed here to be instantaneous. In a realistic scenario the transition to a fault also includes a transient component.

As shown in Figure 3.7, the decaying oscillatory transient can be further separated into the following three basic components: a high frequency component, a

low frequency component and a DC decaying component. The high and low frequency components can be described each by a frequency and a time constant. The DC component can be described with just a time constant. One of the objectives of this thesis is to obtain these characterizing frequencies and time constants.

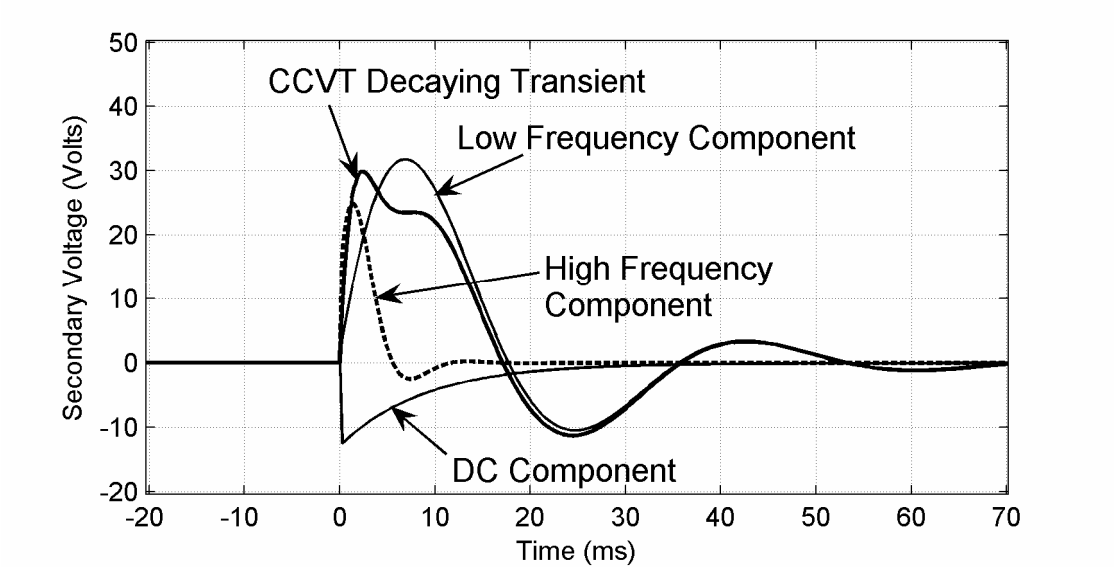

Figure 3.7 CCVT transient response decomposition

3.2.2.2 Factors that Affect the CCVT Transient Response: The transient response is affected by the same factors that affect the frequency response, which are described in the previous section 3.2.1.2. Additionally, there are two other factors that affect the CCVT transient response [17,24,37,40]: fault incidence angle and magnitude of voltage change.

The incidence angle is measured from the last zero crossing, either +/- or -/+, of the power system voltage sinewave to the time the fault occurs. One half period of this voltage sinewave is equivalent to an angle of 180° degrees, which according to the definition just given above should be the maximum incidence angle limit. Considering the incidence angle as the only variable parameter, a zero (0°) degree incidence causes the largest distortion in the CCVT transient response. On the other hand, an incidence angle of ninety (90°) degrees produces the smallest amount of distortion, this is shown in Figure 3.8. In this figure, the distortion introduced is small compared to that of Figure 3.6 for zero degrees incidence angle.

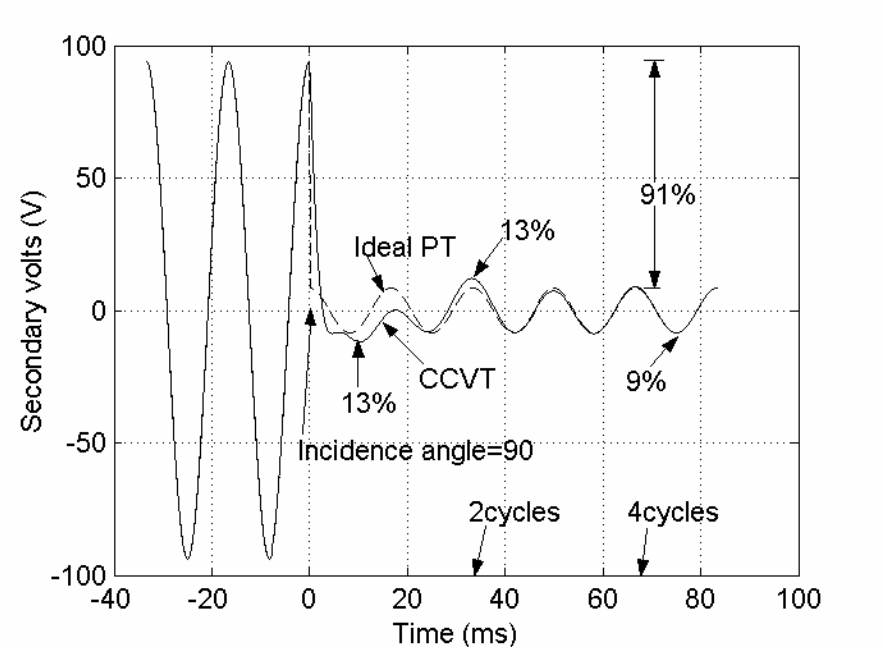

Figure 3.8 CCVT transient response (90 degree incidence angle)

The magnitude of voltage change is defined here as the difference of two signals: 1) the previous steady state voltage sinewave extrapolated in time and 2) the new steady state voltage sinewave. The dependence of the CCVT transient distortion on the magnitude of voltage change is proportional: for a larger change, a larger distortion is introduced.

A relatively small voltage change, smaller than that of Figure 3.6, is illustrated in Figure 3.9. In this figure, the CCVT response for this small change is not much different with the ideal, even for the worst case of zero degrees incidence angle.

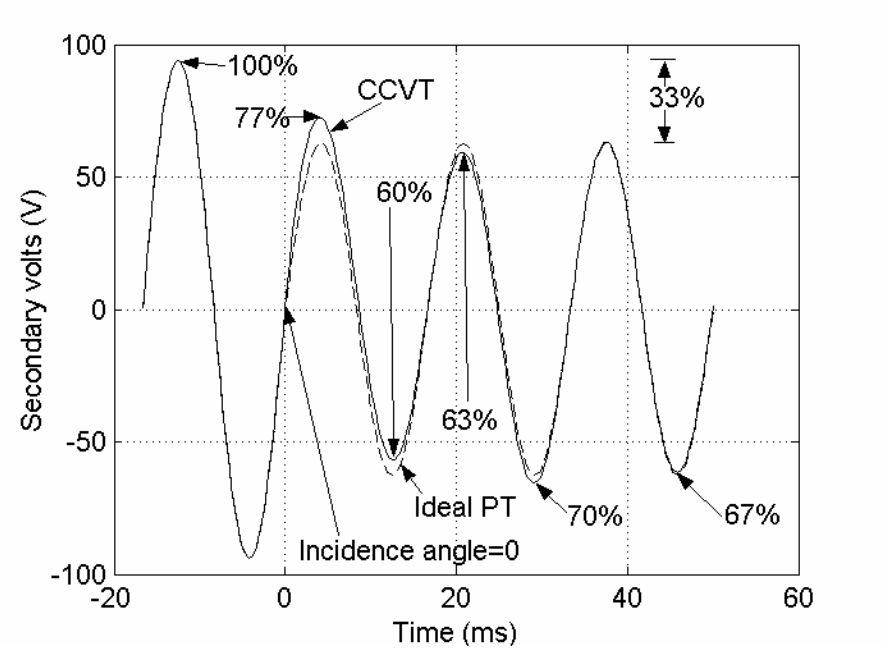

Figure 3.9 CCVT transient response for a small voltage change

3.3 CCVT MODELING

The CCVT response, discussed in the previous section 3.2, can be obtained either by simulation or real tests on a CCVT device. Modeling allows the simulation of the CCVT response without stressing a physical device. The quality of the model used is important to ensure accurate simulation results.

3.3.1 CCVT Components

The values of each CCVT component can be obtained from the corresponding manufacturer or from measurements [12,13,22-24,26-28,41,42]. In both cases it is important to know the accuracy or degree of certainty of those values. Another important consideration is the frequency range of validity for such values [29,31]. In this work each component was considered to be linear, the justification for each is provided where appropriate in sections 3.3.1.1 to 3.3.1.6.

3.3.1.1 Capacitive Divider: With reference to Figure 3.10, the capacitive divider consists of two capacitors C_1 and C_2 in series. Each one of these includes a

resistance, R_1 and R_2 respectively, in series to represent the losses. Typically the lower voltage capacitor output is protected by an air gap against instantaneous overvoltage conditions. This type of overvoltage typically lasts a short time in the range of hundreds of microseconds; therefore it was not included in the model.

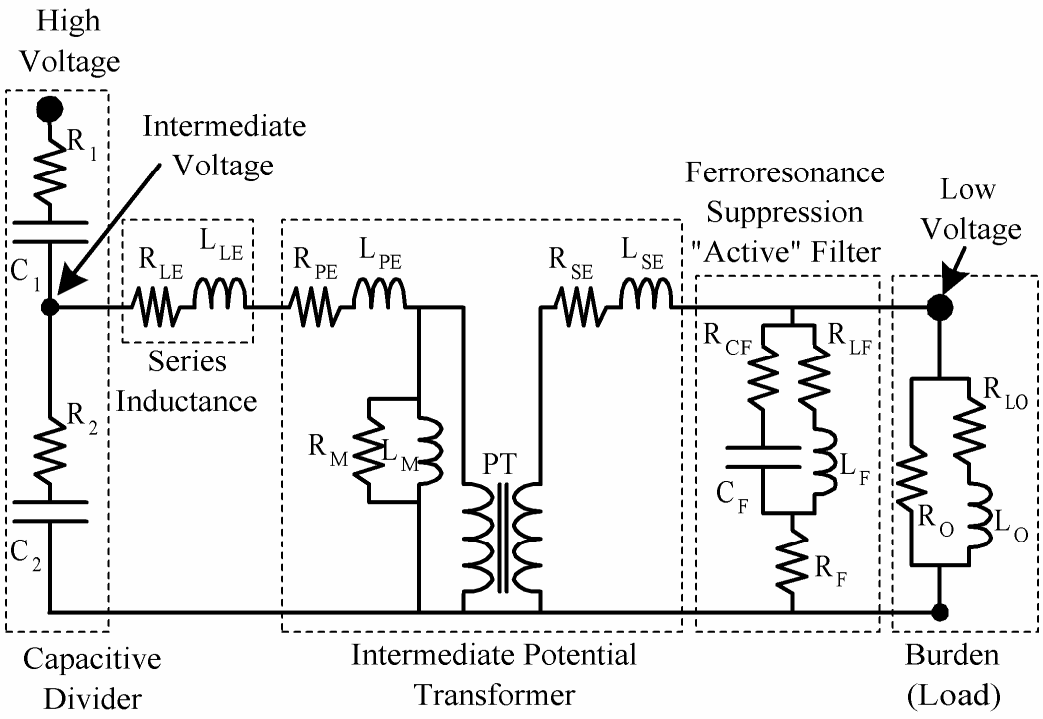

Figure 3.10 CCVT model and components detail

3.3.1.2 Series Inductance: The series inductance L_{LE} includes a resistance R_{LE}, also in series, to represent the losses. This inductance is typically protected against short circuit by an air gap that triggers at a predefined instantaneous overvoltage condition. The air gap was not included in the model, because this condition is not a power system fault. Stray capacitance in the inductance model need to be considered for higher frequencies in the range of 2 kHz [12,22,26,27,41,42], far from the frequencies of interest in this work, therefore stray capacitance was not included.

3.3.1.3 Intermediate PT: The intermediate PT is modeled using an inductance in each winding, L_{PE} and L_{SE}, to represent the leakage flux. The losses in the winding conductors are modeled including one resistance in series, R_{PE} and R_{SE}, with each inductance. The magnetizing current is represented by a shunt inductance L_M in the

primary side of the PT. The losses in the magnetic core are modeled as one shunt resistance R_M, also in the primary side of the PT. These two shunt elements can be represented linearly because the fault conditions to be studied are typically voltage drops [18,23,24], these conditions remain within the linear region of the magnetic core of the PT. Moreover, the risk of ferroresonance, from the possible interaction of the capacitors with the non-linear magnetizing inductance, is non-existent due to the suppression circuit included. Stray capacitances are important in this model only at high frequencies [12,22,26,27,41,42], therefore they were not included.

3.3.1.4 Ferroresonance Suppression Circuit: The ferroresonance suppression circuit can be designed, as mentioned earlier, in two ways: passive and active. The active design was selected for this work, because it causes a bigger distortion in the CCVT response. This design has two main components: a narrow resonant L/C filter and a loading resistor. The filter is tuned to present high impedance to the fundamental frequency and low impedance to all others, thus keeping the resistor from loading the CCVT in steady state conditions. The inductance L_F and the capacitance C_F on the filter, connected in parallel, include each a series resistance, R_{LF} and R_{CF} respectively, to represent the corresponding losses.

3.3.1.5 Burden: The burden was modeled as two shunt elements: one resistance R_O and one inductance L_O. The inductance includes in series a resistor R_{LO} to represent the losses.

3.3.1.6 Others: One component not included in the model is the drain coil. This coil is required for PLC applications [3,19]. Other components not included are certain air gaps used for instantaneous overvoltage protection at different points inside the CCVT.

3.3.2 Modeling Methods

The knowledge of the values of the different components allows the construction of the CCVT model. Two modeling methods were used in this work: Laplace and Electromagnetic Transient (EMTP/ATP).

3.3.2.1 Laplace Equations. This method was used to obtain the CCVT linear transfer function. Some simplifications were made to develop this model:

- The magnetizing branch of the intermediate PT is neglected, because typically the current flowing in this branch is small [15,23,24,37].
- All components are referred to the primary side of the intermediate PT. The PT ratio was included as a gain factor.
- The components are consolidated into groups.

The simplified circuit that was used in this development is shown in Figure 3.11.

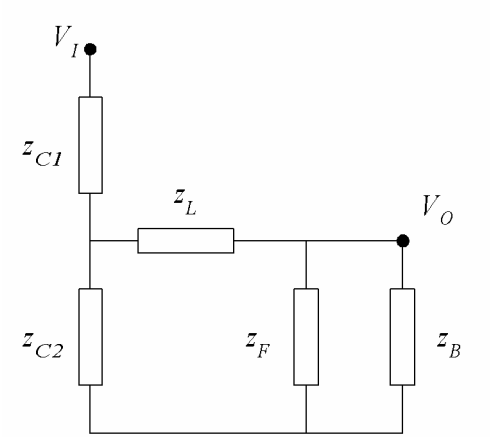

Figure 3.11 CCVT simplified model

In Figure 3.11:

z_{C1}, z_{C2} is the capacitive divider

z_L includes series inductance and resistance, primary and secondary leakage inductance and resistance

z_F is the ferroresonance suppression circuit

z_B is the burden

The input voltage, V_I, and the capacitive divider were simplified using the Thevenin Theorem, as show in Figure 3.12:

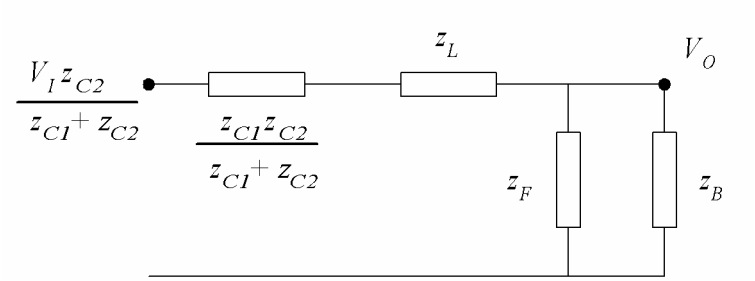

Figure 3.12 CCVT model with capacitor divider simplified

From this circuit, the output voltage V_O can be expressed as a function of the input voltage V_I , using the voltage divider technique, thus obtaining:

$$V_O = \frac{V_I z_{C2}}{z_{C1} + z_{C2}} \frac{\frac{z_F z_B}{z_F + z_B}}{\frac{z_{C1} z_{C2}}{z_{C1} + z_{C2}} + z_L + \frac{z_F z_B}{z_F + z_B}} \tag{3.1}$$

$$\frac{V_O}{V_I} = \frac{z_{C2}}{z_{C1} + z_{C2}} \frac{z_F z_B}{\left[\frac{z_{C1} z_{C2}}{z_{C1} + z_{C2}} + z_L\right](z_F + z_B) + z_F z_B} \tag{3.2}$$

A change of variables is used to simplify Equation 3.2:

$$\frac{r}{s} = z_F \tag{3.3}$$

$$\frac{t}{u} = z_B \tag{3.4}$$

$$\frac{v}{w} = \frac{z_{C1} z_{C2}}{z_{C1} + z_{C2}} \tag{3.5}$$

$$\frac{x}{y} = \frac{z_{C2}}{z_{C1} + z_{C2}} \tag{3.6}$$

Substituting Equations 3.3-3.6 into Equation 3.2 gives

$$\frac{V_O}{V_I} = \frac{x}{y} \frac{\frac{r}{s}\frac{t}{u}}{\left[\frac{v}{w} + z_L\right]\left(\frac{r}{s} + \frac{t}{u}\right) + \frac{r}{s}\frac{t}{u}} \tag{3.7}$$

Simplifying the right hand side of this equation gives

$$\frac{V_O}{V_I} = \frac{xrtw}{y[vru + vst + z_L wru + z_L wst + wrt]} \tag{3.8}$$

For this method to be effective, each individual variable is arranged to be a polynomial of the Laplace variable, *s*. The polynomials are obtained from the detailed model of Figure 3.10, as follows:

$$\frac{r}{s} = R_F + \frac{\left(R_{CF} + \frac{1}{sC_F}\right)\left(R_{LF} + sL_F\right)}{R_{CF} + \frac{1}{sC_F} + R_{LF} + sL_F} \tag{3.9}$$

$$\frac{r}{s} = \frac{s^2 C_F L_F \left(R_{CF} + R_F\right) + s\left[C_F\left(R_F R_{CF} + R_F R_{LF} + R_{CF} R_{LF}\right) + L_F\right] + \left(R_F + R_{LF}\right)}{s^2 C_F L_F + sC_F\left(R_{CF} + R_{LF}\right) + 1} \tag{3.10}$$

$$\frac{t}{u} = \frac{\left(R_O\right)\left(R_{LO} + sL_O\right)}{R_O + R_{LO} + sL_O} = \frac{sR_O L_O + R_O R_{LO}}{sL_O + \left(R_O + R_{LO}\right)} \tag{3.11}$$

$$\frac{v}{w} = \frac{\left(R_1 + \frac{1}{sC_1}\right)\left(R_2 + \frac{1}{sC_2}\right)}{R_1 + \frac{1}{sC_1} + R_2 + \frac{1}{sC_2}} = \frac{s^2 R_1 R_2 C_1 C_2 + s\left(R_1 C_1 + R_2 C_2\right) + 1}{s^2 C_1 C_2\left(R_1 + R_2\right) + s\left(C_1 + C_2\right)} \tag{3.12}$$

$$\frac{x}{y} = \frac{\left(R_2 + \frac{1}{sC_2}\right)}{R_1 + \frac{1}{sC_1} + R_2 + \frac{1}{sC_2}} = \frac{sR_2C_2 + 1}{sC_2(R_1 + R_2) + \left(1 + \frac{C_2}{C_1}\right)} \tag{3.13}$$

$$z_L = R_{LE} + sL_{LE} + R_{PE} + sL_{PE} + R_{SE} + sL_{SE} \tag{3.14}$$

$$z_L = s(L_{LE} + L_{PE} + L_{SE}) + (R_{LE} + R_{PE} + R_{SE}) \tag{3.15}$$

To obtain the overall transfer function, the variables in Equations 3.9 - 3.15 are substituted, in the numerator and denominator of Equation 3.8, by the corresponding polynomials in 's' that use the values of the appropriate CCVT parameters. A fifth order transfer function is obtained for a typical CCVT, after removing couple of repeated zeros and poles found during the simplifications, and is shown in the following equation.

$$G(s) = \frac{K_{CCVT}(s - z_1)(s - z_1^*)(s - z_2)(s - z_3)}{(s - p_1)(s - p_1^*)(s - p_2)(s - p_2^*)(s - p_3)} \tag{3.16}$$

where:

$p_1 = \sigma_1 + j \cdot \omega_1$; *high frequency poles*
$p_2 = \sigma_2 + j \cdot \omega_2$; *low frequency poles*
$p_3 = \sigma_3$; *dc pole*

3.3.2.2 Electromagnetic Transient (EMTP/ATP). The solution of the network is performed using the method proposed by Dommel [9,10]. No simplifications are required for this modeling method, because of the capabilities available in the electromagnetic transient program used: EMTP/ATP. The CCVT model is included as a library component inside a more detailed power system model to be studied and is located at each terminal of that power system where the relays need to be evaluated. The Figure 3.13 shows the model used. The construction of this model requires the use of components and nodes.

Two kinds of components are used in the construction of the CCVT model: the RLC branch [7] and the ideal transformer. The RLC branch is a linear component that represents a series resistance, inductance and capacitance. In Figure 3.13 some elements are shown as resistance or inductance only, but are in reality simplified versions of the RLC branch. The ideal transformer component [7] is completely defined by a transformation ratio.

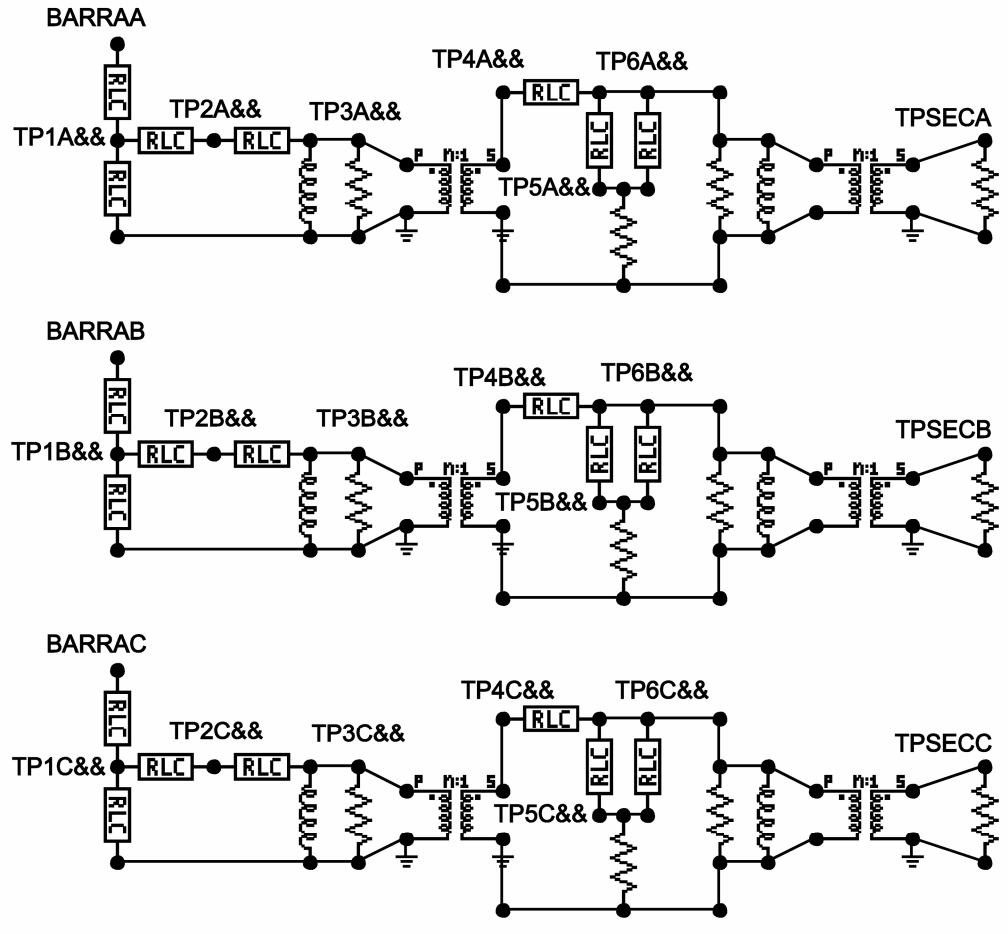

Figure 3.13 CCVT electromagnetic transients model

The nodes used in the model are of two types: internal and external. The internal nodes are considered as dummy nodes [7]; the ATP program assigns in run-time the actual name to be used. This consideration is required when using multiples copies of the same model in a larger system, because the internal node names for each instance of the model should be unique. The external nodes are the interface of the CCVT model with the rest of the network, in Figure 3.13, i.e. the nodes BARRAA/B/C

are the primary side connection point and the nodes TPSECA/B/C are the secondary side connection point. These nodes, however, are considered argument nodes [7], because their names are substituted with the user given node names when the CCVT is located at the desired point in the network.

3.4 SUMMARY

This chapter analyzes the characteristics of the CCVT. The characteristics of the response in the frequency and time domain are described and explained. The factors that affect this response are listed. Two techniques for modeling the response of the CCVT are presented: Laplace transfer function and EMTP. Using the Laplace method the transfer function is developed and obtained. The considerations and advantages of the EMTP method are also indicated.

4. CCVT IMPACT ON PROTECTIVE RELAYING

4.1 INTRODUCTION

The CCVT distorts the voltage input signal received from the power system, since transients are produced on a voltage change condition (CCVT response and its characteristics were studied in the previous chapter). The voltage output from the CCVTs is needed by the protective relays to decide an operation. These relays typically need the amplitude and angle of the fundamental frequency component of the signal, which are extracted with the phasor estimation methods in numerical phasor form.

In this chapter, the errors caused by the CCVT distortion in voltage phasor estimation are studied. The Discrete Fourier Transform (DFT) phasor estimation method from section 2.4 is used for this purpose. Also, the protective functions affected by these errors are analyzed to identify the risks involved in their operation. Then, some methods in use that overcome the impact from the CCVT distortion are described.

4.2 IMPACT ON VOLTAGE PHASOR ESTIMATION

The impact on the voltage phasor estimation is evaluated using a representative CCVT time response signal, as shown in Figure 4.1. This signal corresponds to a significant voltage change at the CCVT input. From this CCVT time response, the fundamental frequency phasor is estimated, obtaining the resulting phasors as a function of time, as shown in Figure 4.2 and 4.3. The estimation is performed using the DFT method that is applied to the CCVT time response signal using a one cycle data window length. The CCVT input time signal is also processed to be used as a reference for comparison; this signal is shown as the ideal PT plot in Figure 4.1.

The error in the phasor estimation is identified as a deviation from the true value in both magnitude and angle responses, i.e. magnitude and angle error. The true value is

assumed to be the phasor estimated from the input signal applied to the CCVT, i.e. before the distortion is introduced. Another perception of the error is given in the complex plane plot of the results, as shown in Figure 4.4. The error in the phasor estimation presents two main characteristics: time duration and amount of error.

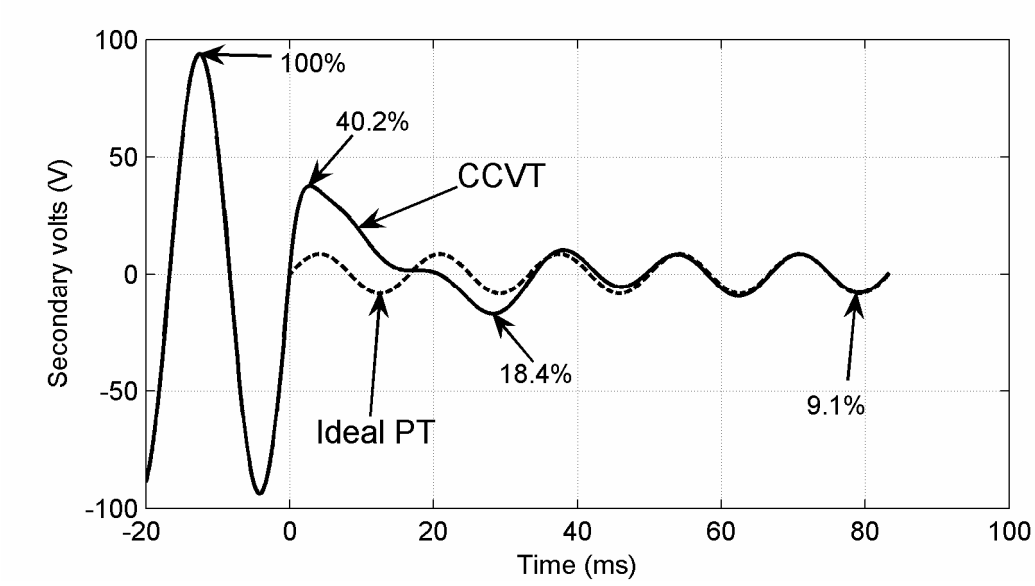

Figure 4.1 CCVT transient response to a fault with 90.9% of voltage change and 0° incidence angle

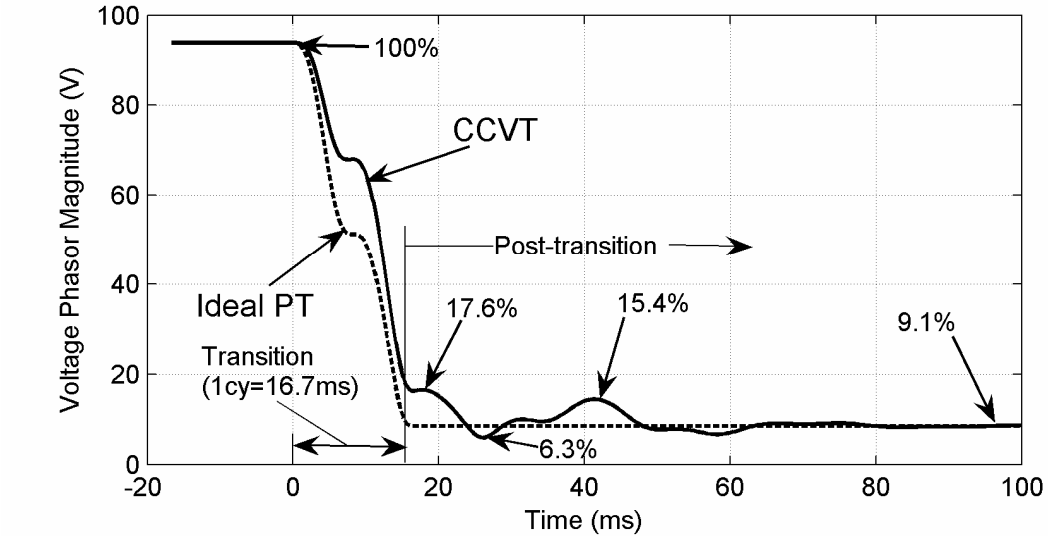

Figure 4.2 Phasor magnitude obtained with once cycle DFT for the signals of Fig. 4.1

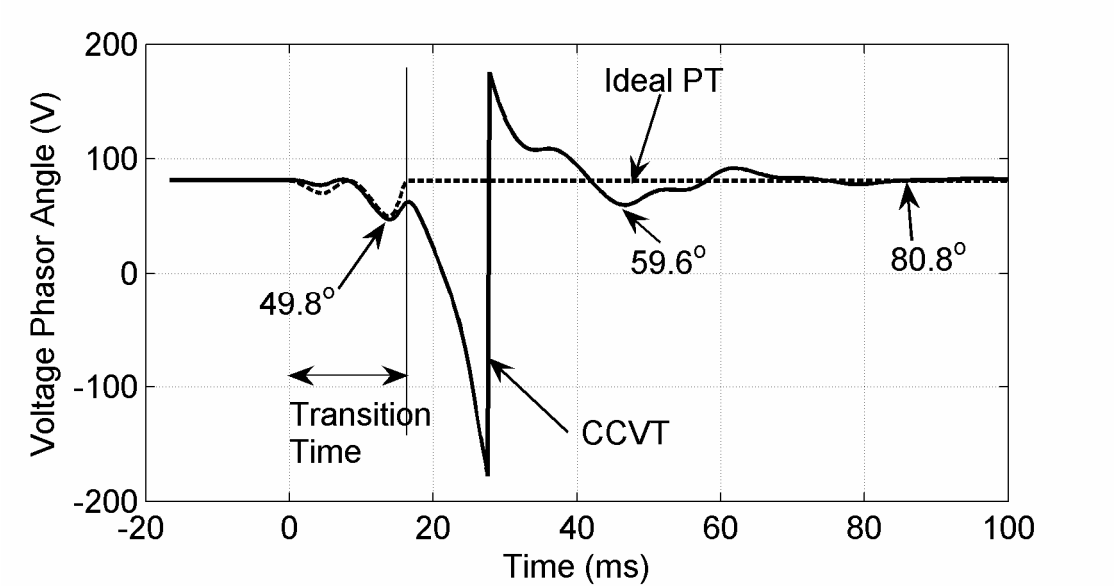

Figure 4.3 Phasor angle obtained with once cycle DFT for the signals of Fig. 4.1

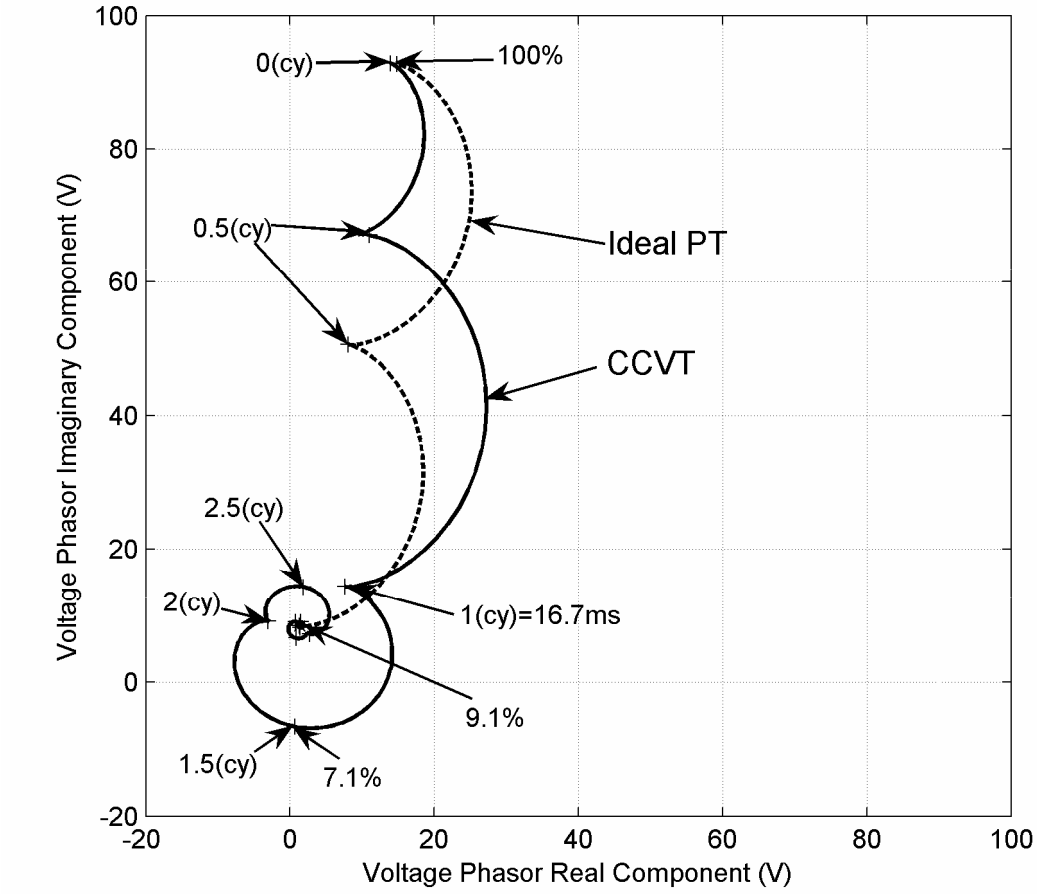

Figure 4.4 Voltage phasor plot in the complex plane for the signals of Fig.4.1

4.2.1 Duration of Error

The duration of the error in the phasor magnitude or angle is limited, because the distortion introduced by the CCVT is also limited in time. The duration of this error depends on the CCVT response characteristics, being typically of 3 to 5 power system frequency cycles. Figure 4.1 shows the response of a CCVT with about 4 cycles of transient duration.

4.2.2 Amount of Error

The amount of error in the phasor estimated depends on three factors: the amount of CCVT distortion, the time since the start of the transient, and the phasor estimation method itself.

The amount of CCVT distortion depends on several factors that are explained in the CCVT characteristics (Section 3.2), such as: a) CCVT design, b) burden characteristics, c) fault incidence angle and d) magnitude of voltage change. The dependence of the error on the amount of distortion is direct: for a larger CCVT distortion, a larger phasor estimation error is obtained.

The time since the start of the transient is divided in two intervals: a) transition and 2) post-transition, these are shown in Figures 4.2 and 4.3. During the transition time, the data window of the phasor estimator contains pre-fault and fault information, therefore the resulting phasors estimated are not very useful, and the corresponding errors found in this interval are not a good measure of the quality of the estimator. In the post-transition time, the data window of the phasor estimator contains only fault information; the errors found in this interval are decaying and oscillating in time, i.e. the maximum error is around the beginning of the post-transition interval.

The error in the phasor estimation depends obviously on the quality of the method used. The capability of the method to distinguish between the desired fundamental frequency and all the other frequencies present in the signal processed is therefore an important requirement to determine the quality of the phasor estimation technique.

Figures 4.2 and 4.3 show the significant amount of error that the CCVT may introduce in the phasor estimation, with an angle phase error that goes beyond 180° degrees and completes one full turn before stabilizing at about 4 to 5 cycles.

4.3 RELAYS AFFECTED

The error caused by the CCVT in the phasor estimation produces an impact that depends on the particular type of protective relay considered. This error may affect the basic protective requirements in several aspects:

- Loss of selectivity, when the relay operates for external faults
- Loss of security, when the relay operates incorrectly

The relays with higher speeds are affected the most, because the CCVT distortion is maximum in the short time window in which these fast relays operate. The impact of the CCVT on two types of relays is discussed in this section: the distance relay and the directional relay.

4.3.1 Distance Relays

This type of relay has been typically used in the most important power lines, where an incorrect operation can produce a bigger impact in the power system. The problem introduced here by the error in the phasor estimated is the risk of incorrect operation for an external fault in the adjacent power line. This problem means a loss of selectivity, which is an important protection requirement. The direct impact of this loss of selectivity is the isolation of a portion of the power system network larger than the minimum required to clear that fault.

A distance relay, in its basic application shown in Figure 4.5, is configured to protect a certain percentage of a power line. Ideally, the desired coverage, also called reach, is 100% of that line, but the accuracy of CT, PT/CCVT and the relay itself limit this percentage to a lower value, typically from 80% to 90%. This reach limit is required to avoid an incorrect operation for a fault beyond 100% of the line, i.e. an

external fault. Physically, this incorrect operation means an effective and undesired increase of reach, also called “overereach” [6,11,14,17,18], from the original, say, 80% of the line to 100% or more. In Figure 4.5, the relay in A may incorrectly overreach to a point where only the relay in B is supposed to operate.

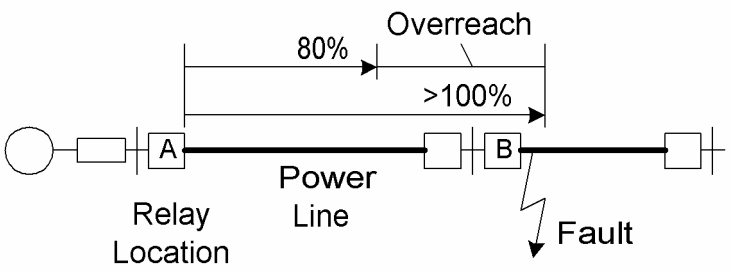

Figure 4.5 Overreach on a distance relay, physical concept

Both magnitude and angle errors in the phasor estimation can affect the correct performance of a distance relay.

4.3.1.1 Impact on Distance Equation: The basic concept of a distance relay is a direct application of the Ohm’s Law for alternating current: $V_R = I_R Z_L$. This condition in a power line is satisfied only for a short circuit with no fault resistance located at the limit of the protected zone; this limit is defined by the impedance Z_L, i.e. the desired reach of the relay. Figure 4.6 illustrates the distance equation concept.

A short circuit of the same fault resistance in another location of the power line breaks the balance represented by the distance equation. If the magnitude of the voltage measured V_R is lower than that of the calculated voltage drop $I_R Z_L$ then the fault is located inside the protected zone, because this unbalance means that the actual impedance V_R / I_R is lower than the desired reach Z_L and the relay should operate. The opposite scenario is obtained for a magnitude voltage V_R bigger than that of the voltage drop $I_R Z_L$, the fault is now beyond the desired reach and no operation should occur. Both ‘operate’ and ‘does not operate’ conditions are also shown in Figure 4.6.

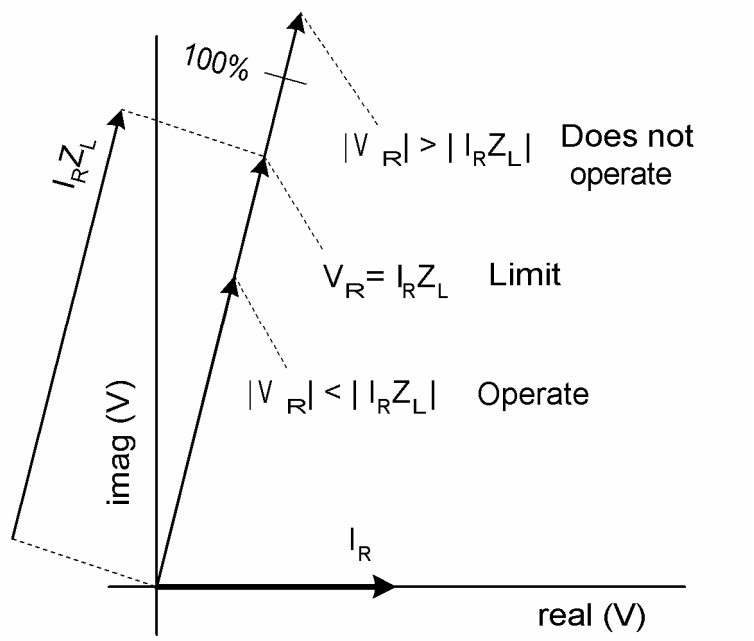

Figure 4.6 Distance equation, 'operate' and 'no operation' conditions

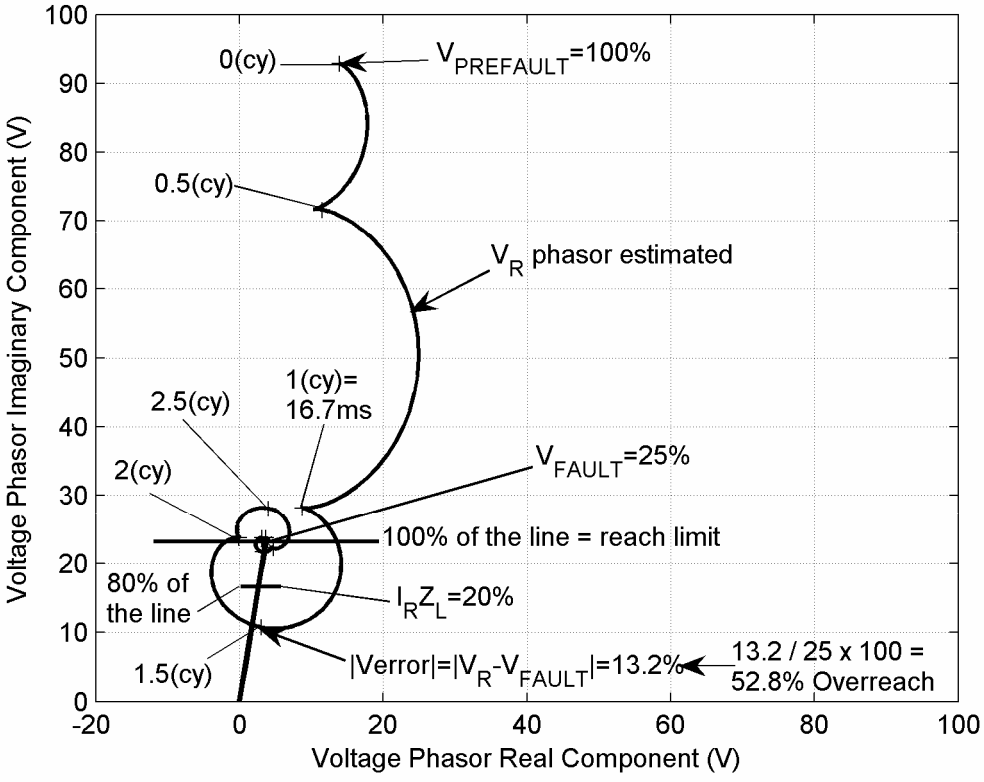

Figure 4.7 Transient overreach caused by CCVT with one cycle DFT phasor estimation

The estimation error in the phasor voltage V_R, assuming that there is no error in the current phasor I_R, may also alter the balance of the distance equation. If the error causes the magnitude of the phasor voltage V_R to become lower than that of the voltage drop $I_R Z_L$ for an external fault condition beyond 100% of the line then an incorrect overreach operation results. This overreach condition is illustrated in Figure 4.7 for an actual CCVT transient affecting the phasor estimated using a one cycle DFT method. In this overreach condition, the true voltage phasor V_{FAULT} is larger than the voltage drop $I_R Z_L$ and this is larger than the estimated voltage phasor V_R at the time of 1.5 cycles from the fault inception, i.e. $| V_{FAULT} | > |I_R Z_L| > |V_R|$.

The overreach may be interpreted as how far the impedance measured is inside the protected zone. The transient overreach is calculated as a percentage difference from the true, say V_T, and estimated, say V_E, voltage phasors in true voltage units, i.e. transient overreach = $(|V_T| - |V_E|)/ |V_T|*100\%$. This is only valid for zero ohm faults because V_E and V_T are expected to be in phase in these cases. These two phasors are different only during the transient period, otherwise they are equal. For the case of Figure 4.7, $|V_T| = 25\%$, $|V_E| = 11.8\%$ resulting an overreach of 52.8%.

4.3.1.2 Impact Characteristics: For distance relays in general, the transient overreach has been typically evaluated with faults located at the remote bus, i.e. 100% of the line, and with low or zero ohm fault resistance only. However, the transient overreach may be caused by the error in the magnitude or the angle of the phasor estimated, therefore the evaluation of these two causes for overreach requires the use of two types of faults, i.e. low and high resistance faults both at 100% of the line.

The error in the estimated magnitude of the voltage phasor affects the distance relay mostly for a short circuit with low or zero ohm fault resistance. The impact of the magnitude error on such a fault condition is illustrated in Figure 4.8, this figure shows that this error may cause overreach or underreach, the overreach is of most concern here. The amount of overreach represents the error in the distance measurement; this error is the ratio of two factors: the absolute magnitude error and the final fault voltage.

Referring to our previous overreach definition the absolute magnitude error is ($|V_E| - |V_T|$) and the final fault voltage is $|V_T|$. These two factors are interrelated; a larger magnitude of voltage change produces: 1) a larger error in magnitude and 2) a lower magnitude of final fault voltage. The end result is that the overreach is amplified and is larger in value than the absolute magnitude error observed. Figure 4.7 confirms this assertion, with an overreach of 52.8% greater than the absolute error of 13.2% (=25% - 11.8%).

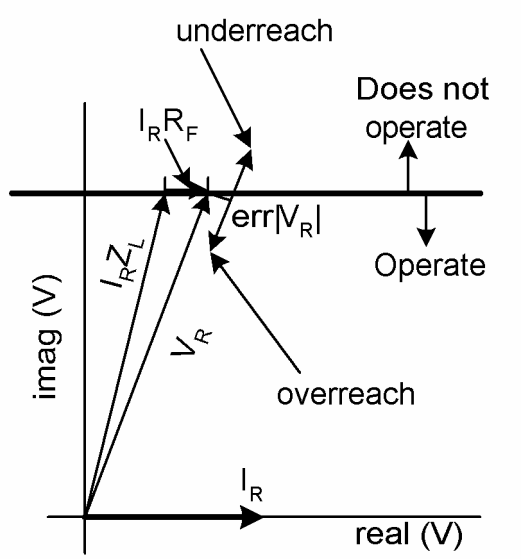

Figure 4.8 Magnitude error impact on a low fault resistance condition

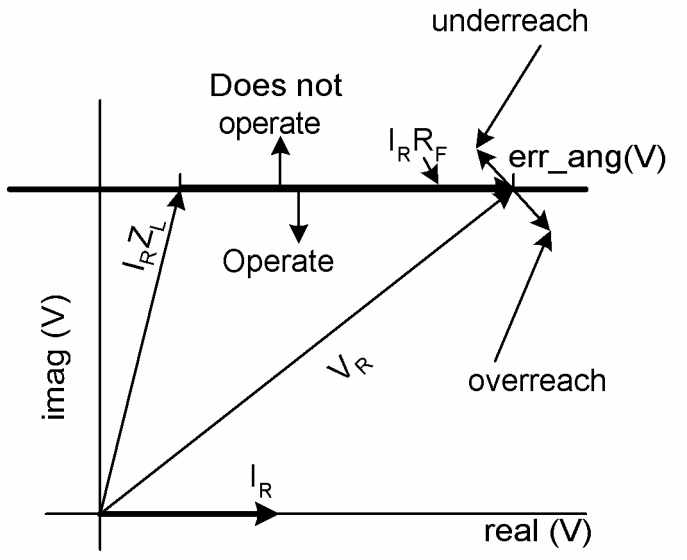

Figure 4.9 Angle error impact on a high fault resistance condition

The error in the estimated angle of the voltage phasor affects the distance relay mostly for a short circuit with a higher resistance value. The impact of the angle error on a high resistance fault is shown in Figure 4.9, the error may cause overreach and underreach. To quantify the overreach in high resistance faults, the true voltage phasor V_T and the estimated voltage phasor V_E should be projected into the $I_R Z_L$ line using the direction of the fault resistance line $I_R R_F$. Then, the overreach is calculated using the projected vectors V_E' and V_T', and the relationship previously defined, i.e. transient overreach = ($|V_T'| - |V_E'|$)/ $|V_T'|$*100%.

4.3.2 Directional Relays

The directional relaying function is an important part of other relays, such as the distance or the directional overcurrent. The directionality adds the required selectivity to these other relays against faults behind them. The problem introduced by the error in the phasor estimation is the risk of incorrect operation for an external fault behind, i.e. a reverse fault. This problem means a loss of selectivity, which is an important protection requirement.

A directional relay is typically set to detect a fault condition in the forward direction. This condition alone does not cause an operation, but needs to be combined with another relay function that defines how far the protection should cover. If the fault is in the reverse direction the relay should block the operation, regardless of any other condition; a failure to identify the fault direction is known as "loss of directionality" [6,11,14,21]. A directional relay subjected to a reverse fault condition is shown in Figure 4.10, the relay in A may loose directionality and operate incorrectly when only the relay in B should operate.

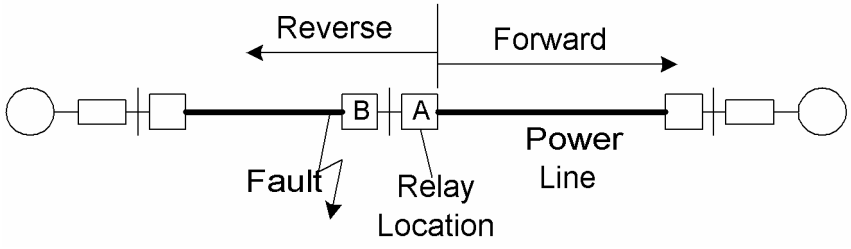

Figure 4.10 Reverse fault condition, physical concept

4.3.2.1 Impact on Directional Equation: The basic directional concept is a variation of the Ohm's Law for alternating current: $\angle(V_R / I_R) = \angle(Z_L)$. This equation is satisfied only for a forward zero ohm fault anywhere in the power line. The only parameter required to define this equation is the angle of the line impedance Z_L. The directional equation concept is illustrated in Figure 4.11.

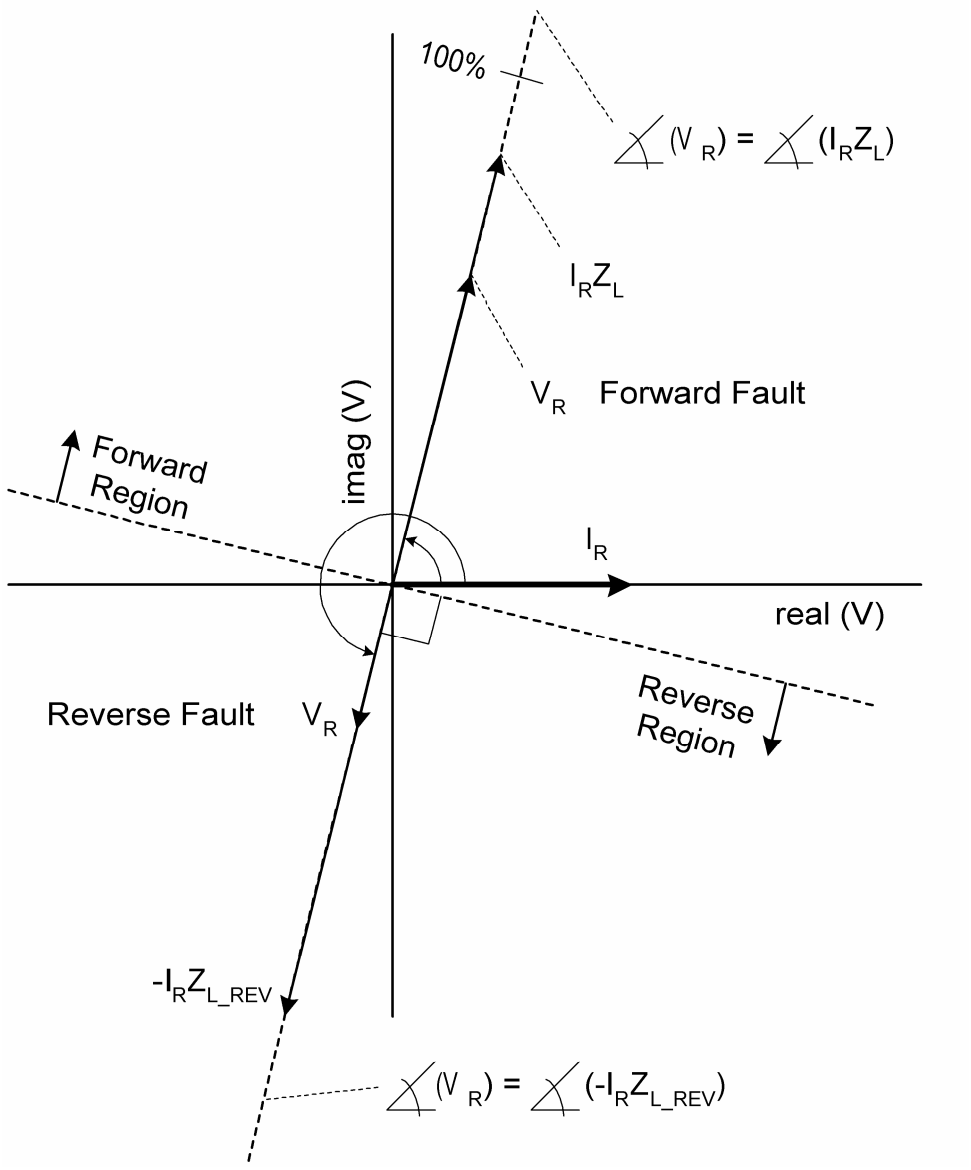

Figure 4.11 Directional equation, forward and reverse operating conditions

Assuming that all impedance angles are equal in the power system network, a reverse fault is identified because the equation to be satisfied is different:

$\angle(V_R/(-I_R)) = \angle(Z_{L\_REV})$. If the angle of the current phasor I_R is considered the 0^o degrees reference then the angle of the voltage V_R for a forward fault and that for a reverse fault are 180^o degrees apart. Because of this significant angle difference typically the plane is split in two regions that define the forward and reverse zones of operation. Each of these regions covers an angle of 90^o degrees leading and lagging from the corresponding impedance Z_L angle. The forward and reverse operating angles and the corresponding regions are also shown in Figure 4.11.

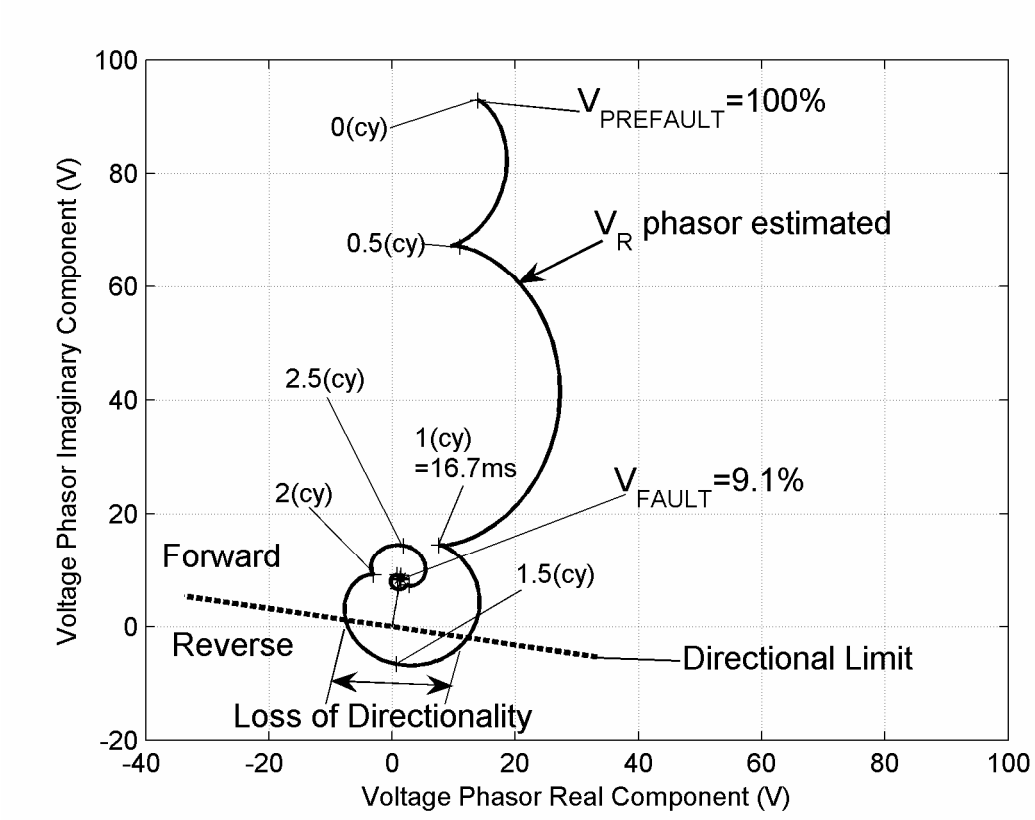

Figure 4.12 Loss of directionality caused by CCVT transient with one cycle DFT phasor estimation

The angle error in the voltage phasor estimated, assuming that there is no error in the estimated angle of the current phasor I_R, may cause the estimated voltage phasor angle to fall in the region corresponding to an incorrect fault directional decision. This incorrect directional decision is obtained when the voltage angle error is greater than 90 degree either leading or lagging the true voltage phasor angle. This loss of

directionality condition is illustrated in Figure 4.12 for an actual CCVT transient affecting the response of a one cycle DFT phasor estimator.

4.4 RELAYS NOT AFFECTED

Obviously, the relays that do not use the voltage inputs are not affected by the CCVT distortion. The current only relays satisfy this requirement, some of these are:

- Overcurrent
- Transformer current differential
- Line current differential
- Bus current different

Slow relays are not affected, at least not significantly, by the CCVT caused error. Some of these relays are:

- Many electromechanical relays
- Time delayed distance
- Time delayed overcurrent directional

Relays that use higher frequency components of the voltage are also less affected by the CCVT distortion, a relay that satisfies this is:

- Traveling wave relay

4.5 TECHNIQUES USED TO MINIMIZE THE CCVT IMPACT

Several methods have been utilized to overcome the difficulty imposed by the presence of the CCVT distortion. These methods can be classified in three groups: avoiding the use of CCVT transient, waiting for the transient to subside and using the transient values.

4.5.1 Avoiding the Use of CCVT Transient

One technique is the use of a memory voltage angle [11,14,18,21]. In this technique, the voltage angle is continuously recorded in some memory for later usage. During steady state conditions, the memorized and the actual angle are the same. But when a disturbance occurs and the voltage angle becomes affected by the CCVT transient, the memorized voltage is used instead until the transient disappears. This memory voltage technique is typically used in directional relays.

4.5.2 Waiting for the Transient to Subside

Adding a time delay is a technique that can be used to avoid the impact of a CCVT transient in the operation of a relay. Two techniques have been used: 1) Fixed delay and 2) Adaptive delay.

4.5.2.1 Fixed Delay: This technique [17,18] delays the operation of the relay for a fixed amount of time. The time delay required is based on the necessary time for the CCVT transient to disappear. Care should be taken on not exceeding the critical clearing times of the power system, in the order of 100ms. The total fault isolation time has to be considered, which includes the typical 3 to 5 cycles of breaker operating time added to the relay operating time. The use of a fixed delay is not always possible.

4.5.2.2 Adaptive Delay: One method that may be used is to delay the operation based on the observed stability of the phasor estimated. In this method, the relative deviation of the magnitude and the angle, either one or both, of the phasor estimated over the time is monitored. A time window is selected to perform this stability evaluation, based on the expected phasor variation in time. If the relative deviation of the magnitude or the angle is lower than a predefined threshold over the selected time window, the phasor is considered stable and no more delay is necessary. On the other hand, if the relative deviation is higher than this threshold, more delay is dynamically introduced in the operation.

4.5.3 Using the CCVT Transient Voltage

When the use of the CCVT transient is necessary, other techniques have to be used. These techniques can be classified in three groups: 1) compensate for the error, 2) identify and reduce the error and 3) use other power system parameters or conditions.

4.5.3.1 Compensate for the Error: This method requires the knowledge of the maximum expected error in the voltage phasor estimated for an external fault condition. The voltage phasor corresponding to this fault is translated into the corresponding protective equation. The limit of the protective relay function under consideration is then adjusted to avoid enclosing this fault condition inside the operating region [1,17,24].

For instance, the impedance reach can be reduced in a distance relay to avoid enclosing the transient overreach caused by the CCVT. The reach reduction method can be applied only if the maximum transient overreach is below 100%, otherwise the distance element has to use another alternative method to prevent an incorrect operation.

4.5.3.2 Identify and Reduce the Error: This method attempts to identify the CCVT distortion in the voltage signal and minimize its effect. Special filters have been proposed to process the signal before the phasor estimation. These filters are based on the parameters of a CCVT for their construction. The problem here is that filters introduce an inherent delay, which has to be added to the phasor estimation transition time. Therefore, the total response time for this pre-filter and phasor estimation is increased [23,24].

4.5.3.3 Use of Other Power System Parameters and Conditions: In this method, additional characteristics of the power system are included in the protection function to decide when a delay is required [14,17]. One method is based on the source to line impedance ratio ($SIR = Z_S / Z_L$) and the stability of the phasors used. In this

method, a delay is added if a higher *SIR* is detected based on the current and voltage measurements, if the phasors are stabilizing faster then this delay is overridden.

4.6 SUMMARY

In this chapter, the impact of the CCVT in protective relaying is explained. This impact is identified as an error in the voltage phasor estimated caused by the distortion introduced by the CCVT. The phasor error is separated in magnitude and angle errors for analysis. The impact of these errors in some different protective functions is evaluated, indicating the risks of incorrect operation. Some techniques in use that intend to overcome the CCVT impact are also described.

The next chapter describes an improved least squares approach that can minimize the impact of CCVT transient voltage in protective relays.

5. PROPOSED PHASOR ESTIMATION ALGORITHM

5.1 INTRODUCTION

The CCVT behavior may cause negative impact on protective relays, in particular on those that require fast operation, as discussed in the previous chapter. This is caused by the transient error introduced in the estimated voltage phasor. In order to reduce this impact, the accuracy and speed of the phasor estimated need to be improved. Present estimation methods do not take full advantage of the available CCVT design information. This thesis proposes a new least squares method that improves the quality of the voltage phasor estimated by including the CCVT design parameters.

5.1.1 Basic Least Squares Method

The basic least squares phasor estimation method is described in a previous section 2.4.2. This method performs two functions: prefiltering and phasor estimation. The prefiltering function allows the attenuation of undesired frequencies present in the voltage signal. The phasor estimation function identifies the desired fundamental frequency and obtains its characterizing parameters: the real and imaginary components.

The least squares method is based on the fitting of a selected curve to a set of measurements. The power system frequency is dominant in the voltage signal; therefore a sine function of that frequency is selected as the curve for this fitting. This sine function is represented as the sum of other two orthogonal sine functions. The amplitudes of these functions become the parameters that completely define the curve for the fitting. With these two degrees of freedom the curve selected is fitted to the measurements as closely as possible.

The amplitudes of these two orthogonal sine functions also represent the real and imaginary components of the desired fundamental frequency phasor.

5.1.2 Problem with the Basic Least Squares Method

The CCVT distortion in the voltage signal affects the basic least squares method. The curve fitted does not correspond to the true fundamental frequency component of the voltage signal. Figure 5.1 shows the errors obtained when fitting this curve to the CCVT transient response. The amplitude and phase angle of the curve fitted show an error compared to the true fundamental component represented as the ideal PT plot in Figure 5.1. As a consequence of this, the phasor estimated is not the true voltage phasor expected, thus a phasor estimation error is produced.

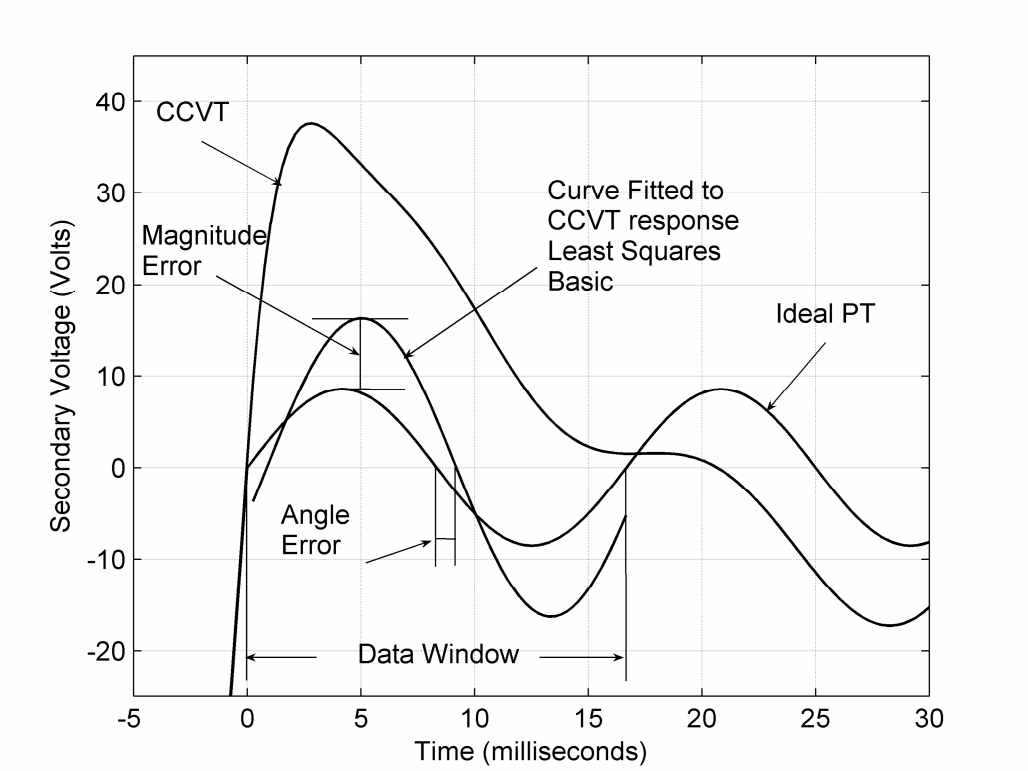

Figure 5.1 Curve fitting error of basic least squares for a CCVT transient.

5.2 IMPROVED LEAST SQUARES

5.2.1 Improving the Description of the Curve to be Fitted

The curve to be fitted can be improved by including a description of the CCVT distortion in addition to the fundamental frequency component [50-52]. To achieve this objective, the transient response of the CCVT was studied in section 3.2.2. The CCVT response includes three different decaying components: a high frequency component, a low frequency component, and a dc component.

The oscillatory decaying components, such as the high and low frequency, are represented as the product of a sine function multiplied by a decaying exponential function. Four parameters are required to completely define this decaying component. Two of these parameters are known: the frequency of the sine function and the decaying rate of the exponential. These parameters were obtained from the CCVT transfer function (Equation 3.16). The sine function is described as the sum of two orthogonal sine functions; their amplitudes are two unknown parameters. Two degrees of freedom, these two unknowns, are available for each frequency, high or low, when performing the fitting process.

The dc decaying component requires two parameters to be defined completely: a constant that multiplies the exponential function and the decaying rate of the exponential. The first parameter is an unknown. The second parameter is also obtained from the CCVT transfer function (Equation 3.16). Only one degree of freedom, the single unknown parameter, is available when performing the fitting to the signal measured.

The equation that describes the curve to be fitted becomes:

$$\begin{aligned} v(t) &= V_R \sin(\omega_O t) + V_I \cos(\omega_O t) \\ &+ V_{R1} e^{(\sigma 1)t} \sin(\omega_1 t) + V_{I1} e^{(\sigma 1)t} \cos(\omega_1 t) \\ &+ V_{R2} e^{(\sigma 2)t} \sin(\omega_2 t) + V_{I2} e^{(\sigma 2)t} \cos(\omega_2 t) \\ &+ V_3 e^{(\sigma 3)t} + \varepsilon(t) \end{aligned} \tag{5.1}$$

where:

ω_0 is the fundamental frequency

ω_1 is the high frequency

ω_2 is the low frequency

σ_1 is the decaying rate for high frequency component

σ_2 is the decaying rate for low frequency component

σ_3 is the decaying rate for dc component

are known parameters, and the unknowns are:

V_R is the real component of fundamental frequency

V_I is the imaginary component of fundamental frequency

V_{R1} is the real component of high frequency component

V_{I1} is the imaginary component of high frequency component

V_{R2} is the real component of low frequency component

V_{I2} is the imaginary component of low frequency component

V_3 is the constant multiplier for dc decaying component

and the following variables are:

v is the voltage measurement

ε. is the noise

t is the time

5.2.2 Finding the Least Squares Solution

Equation 5.1 is applied to a set of measurements, or samples, corresponding to a pre-selected time window. This time window $N\Delta t$ is a function of two parameters: the number of samples N and the sampling period Δt. The resulting set of equations is overdefined, hence the unknowns can be obtained. Note that the number of unknowns including the noise is 8. This system of equations is linear and can be written as:

$$\begin{bmatrix} A_0 & A_1 & A_2 & A_3 \\ Nx2 & Nx2 & Nx2 & Nx1 \end{bmatrix} \begin{bmatrix} V_R \\ V_I \\ V_{R1} \\ V_{I1} \\ V_{R2} \\ V_{I2} \\ V_3 \end{bmatrix} + \begin{bmatrix} \varepsilon(t_O + \Delta t) \\ \varepsilon(t_O + 2\Delta t) \\ \vdots \\ \varepsilon(t_O + N\Delta t) \end{bmatrix} = \begin{bmatrix} v(t_O + \Delta t) \\ v(t_O + 2\Delta t) \\ \vdots \\ v(t_O + N\Delta t) \end{bmatrix} \tag{5.2}$$

where the partial coefficient matrices [A_0], [A_1], [A_2] and [A_3] are defined by:

$$\begin{bmatrix} A_0 \\ Nx2 \end{bmatrix} = \begin{bmatrix} \sin(\omega_O \Delta t) & \cos(\omega_O \Delta t) \\ \sin(\omega_O 2\Delta t) & \cos(\omega_O 2\Delta t) \\ \vdots & \vdots \\ \sin(\omega_O N\Delta t) & \cos(\omega_O N\Delta t) \end{bmatrix} \tag{5.3}$$

$$\begin{bmatrix} A_1 \\ Nx2 \end{bmatrix} = \begin{bmatrix} e^{\Delta t \cdot \sigma 1} \sin(\omega_1 \Delta t) & e^{\Delta t \cdot \sigma 1} \cos(\omega_1 \Delta t) \\ e^{2\Delta t \cdot \sigma 1} \sin(\omega_1 2\Delta t) & e^{2\Delta t \cdot \sigma 1} \cos(\omega_1 2\Delta t) \\ \vdots & \vdots \\ e^{N\Delta t \cdot \sigma 1} \sin(\omega_1 N\Delta t) & e^{N\Delta t \cdot \sigma 1} \cos(\omega_1 N\Delta t) \end{bmatrix} \tag{5.4}$$

$$\begin{bmatrix} A_2 \\ Nx2 \end{bmatrix} = \begin{bmatrix} e^{\Delta t \cdot \sigma 2} \sin(\omega_2 \Delta t) & e^{\Delta t \cdot \sigma 2} \cos(\omega_2 \Delta t) \\ e^{2\Delta t \cdot \sigma 2} \sin(\omega_2 2\Delta t) & e^{2\Delta t \cdot \sigma 2} \cos(\omega_2 2\Delta t) \\ \vdots & \vdots \\ e^{N\Delta t \cdot \sigma 2} \sin(\omega_2 N\Delta t) & e^{N\Delta t \cdot \sigma 2} \cos(\omega_2 N\Delta t) \end{bmatrix} \tag{5.5}$$

$$\begin{bmatrix} A_3 \\ Nx1 \end{bmatrix} = \begin{bmatrix} e^{\Delta t \cdot \sigma 3} \\ e^{2\Delta t \cdot \sigma 3} \\ \vdots \\ e^{N\Delta t \cdot \sigma 3} \end{bmatrix} \tag{5.6}$$

In equations 5.2-5.6, the coefficients $\boldsymbol{A_0}$–$\boldsymbol{A_4}$ are constant because N, Δt, ω_0-ω_2, σ_1-σ_3 are initialized at the beginning and do not change during the least squares estimation procedure. The system of linear equations represented in Equation 5.2 is equivalent to:

$$[A][x]+[\varepsilon]=[b] \tag{5.7}$$

The least squares solution for this system, which minimizes the sum $[[\varepsilon]^T[\varepsilon]]$ over the time window, is obtained using the left pseudo-inverse of $[A]$ as follows:

$$[x]=\left[[A]^T[A]\right]^{-1}[A]^T[b] \tag{5.8}$$

From the vector of unknowns $[x]^T = [V_R\ V_I\ V_{R1}\ V_{I1}\ V_{R2}\ V_{I2}\ V_3]^T$ in Equation 5.8, only two of the unknowns are desired: V_R and V_I. Because $[A]$ in Equation 5.7 is an Nx7 matrix, its pseudo-inverse $[[A]^T[A]]^{-1}[A]^T$ in Equation 5.8 is a 7xN matrix. Therefore, to obtain the desired two unknowns only the first two rows of the pseudo-inverse are needed; the first row corresponds to the real component V_R and the second to the imaginary component V_I.

5.2.3 Selection of the Time Window Size

The proposed method requires the selection of an optimum time window. The time window is defined as $N\Delta t$. On one side, the protective operating speed requirement suggests that this time window be as short as possible. On the other side, a longer time window should provide a better accuracy of the estimation, because more data is available. Therefore, an optimum window size needs to be selected balancing both requirements: speed and accuracy. The following two sections describe the procedure for finding an optimum time window

5.2.3.1 Parameters: One of the parameters selected is the sampling period Δt. This period is the inverse of the sampling frequency, which is typically of 3840 Hz, for relays on a 60 Hz system [2]. This value of sampling frequency allows the proper representation of the frequency range from near DC up to 1920 Hz (=3840 / 2). This range was considered enough, because the focus of this work is on the fundamental frequency phasor; therefore the sampling period used was Δt =1/3840 =260.42 μs. In other words, the sampling frequency of 3840 Hz is equivalent to 64 samples per cycle (= 3840 / 60).

The other parameter to be selected is the number of samples *N* that define the data window size. The whole problem reduces to finding the optimum data window size *N*.

5.2.3.1 Selection Method: Several values of the data window size *N* were evaluated: 64, 96, 128 and 160 samples. For each value of window size, two characteristics were considered: 1) the phasor estimation error during the transition time and 2) the frequency response of the phasor estimator.

The phasor estimation error during the transition time was used as a quality indicator for the method. During this transition time the phasor estimation window contains prefault and fault data. The trajectory in the complex plane of the estimated phasor using the basic and the improved least squares method was compared. Figures 5.2 - 5.5 show these trajectories for the different window sizes.

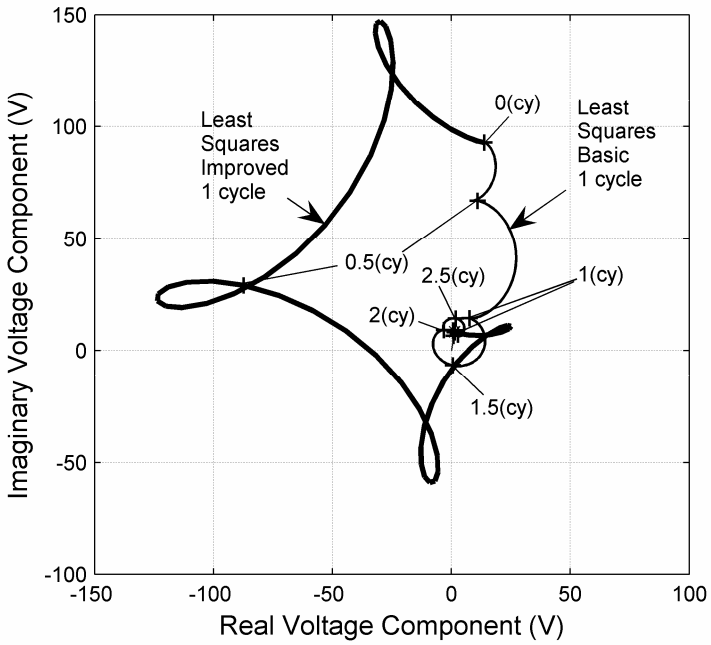

Figure 5.2 Voltage phasor estimated trajectories for N=64 samples (=1 cycle).

The trajectories for window sizes of 64 and 96 samples, in Figures 5.2 and 5.3, show a greater uncertainty compared to the basic least squares method, which is not a desired behavior.

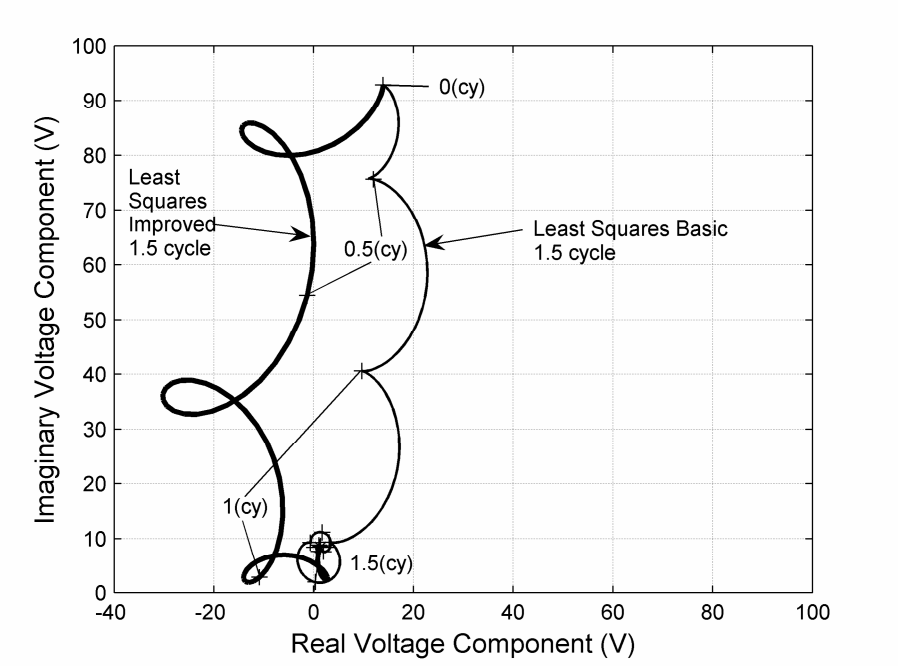

Figure 5.3 Voltage phasor estimated trajectories for *N*=96 samples (=1.5 cycles).

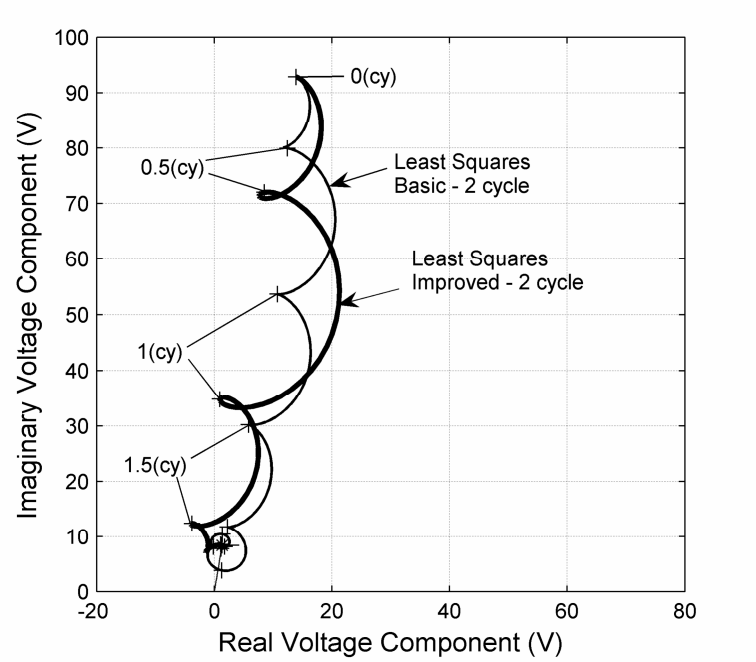

Figure 5.4 Voltage phasor estimated trajectories for N=128 samples (=2 cycles).

Relative improvement on the uncertainty in the trajectory is observed for the increases of window size from 64 to 96 and from 96 to 128 samples, as shown in Figures 5.2 - 5.4. The improvement is not significant for the window size increase from 128 to 160 samples. Based on these observations, a window size of 128 samples (= 2 cycles) was selected as the optimum.

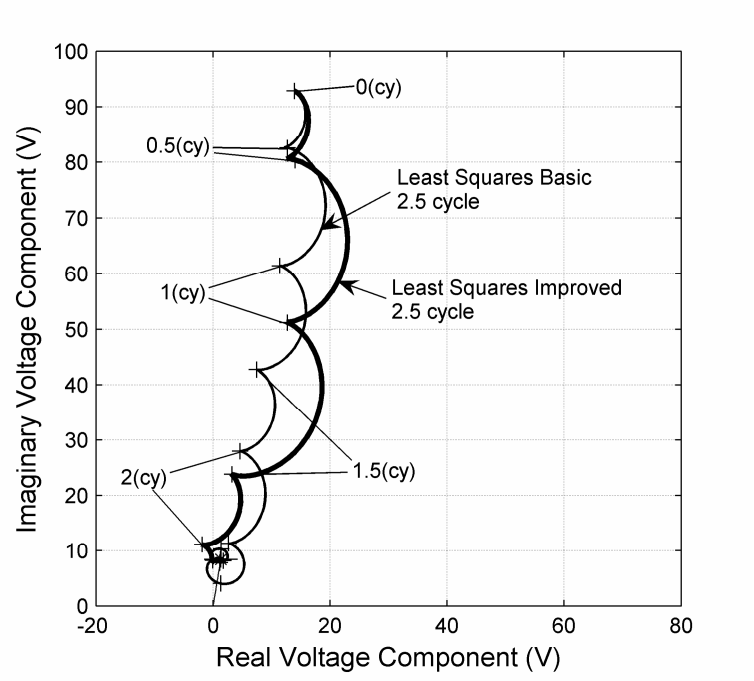

Figure 5.5 Voltage phasor estimated trajectories for *N*=160 samples (=2.5 cycles).

The frequency response of the phasor estimation was used as another quality indicator for the proposed method. The gain response against frequency was obtained using Equation 2.13 for each component of the method, the real and the imaginary. Figures 5.6 - 5.9 show these frequency responses for the window sizes previously selected.

The response for a window size of 64 samples, shown in Figure 5.6, is not desired, because it amplifies many unwanted frequencies above the fundamental, reaching a peak of +22dB of amplification at about two times the fundamental frequency.

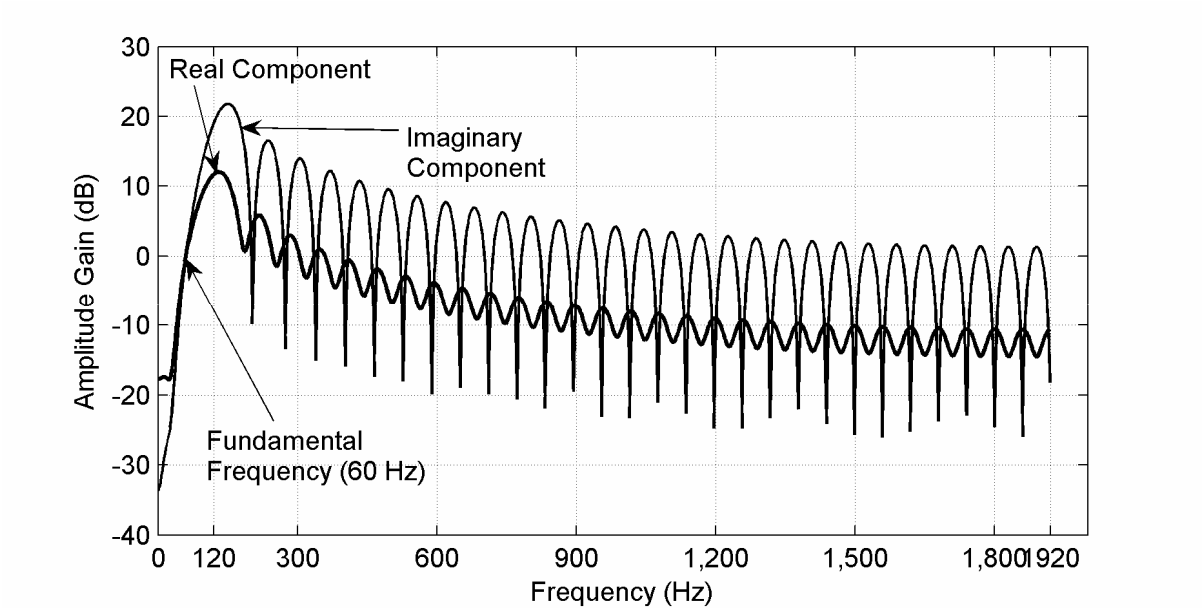

a)

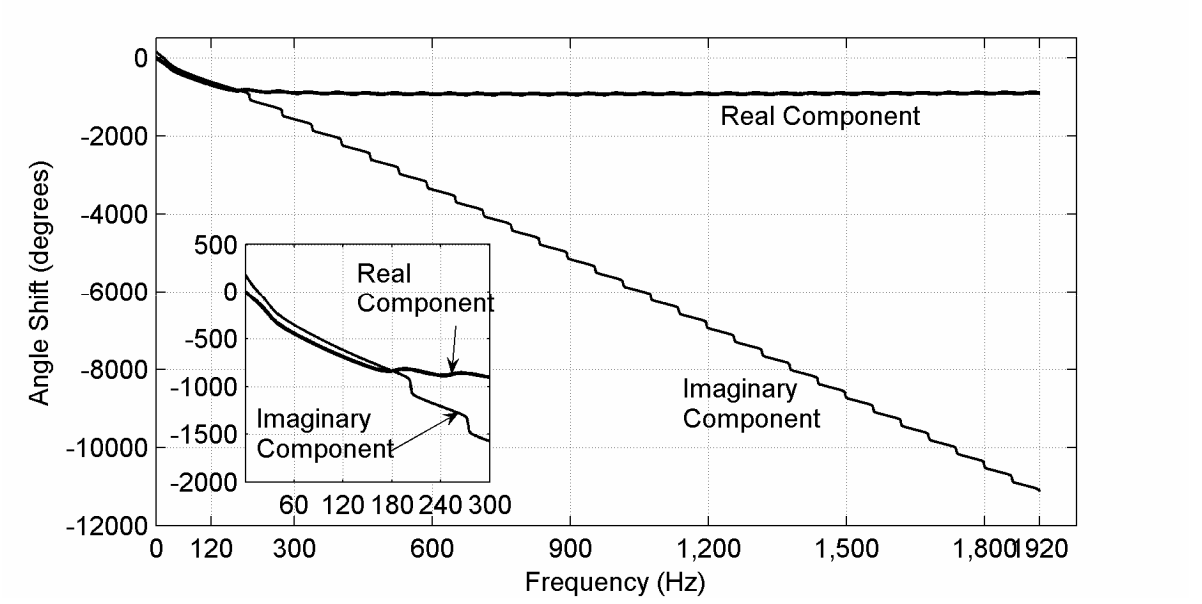

b)

Figure 5.6 Frequency response of phasor estimation method for N=64 samples(=1 cycle).

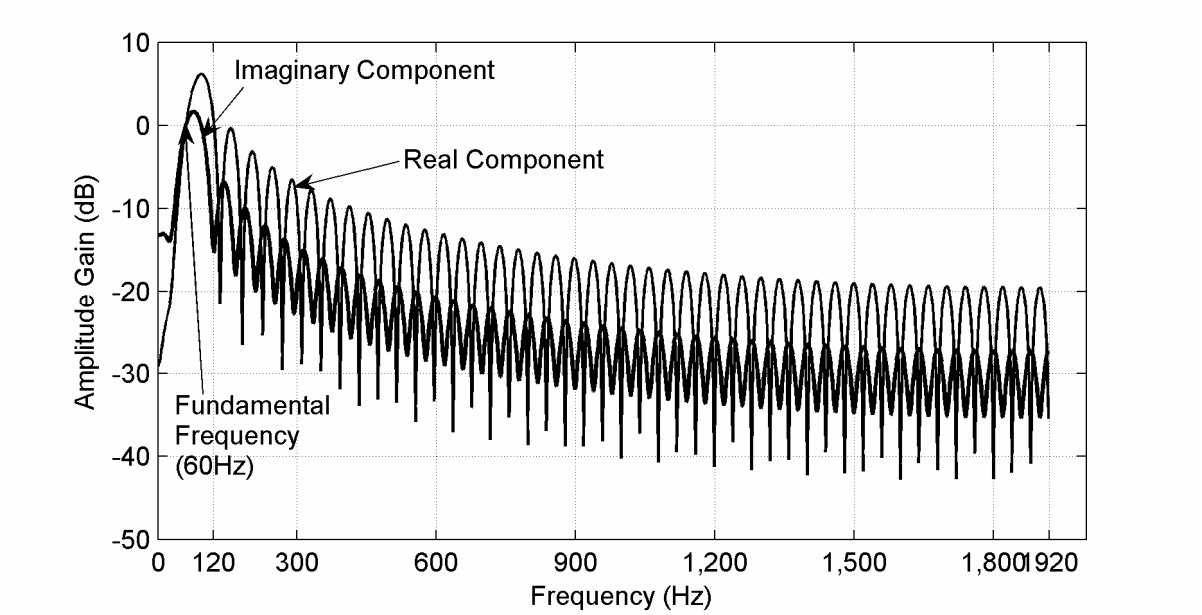

a)

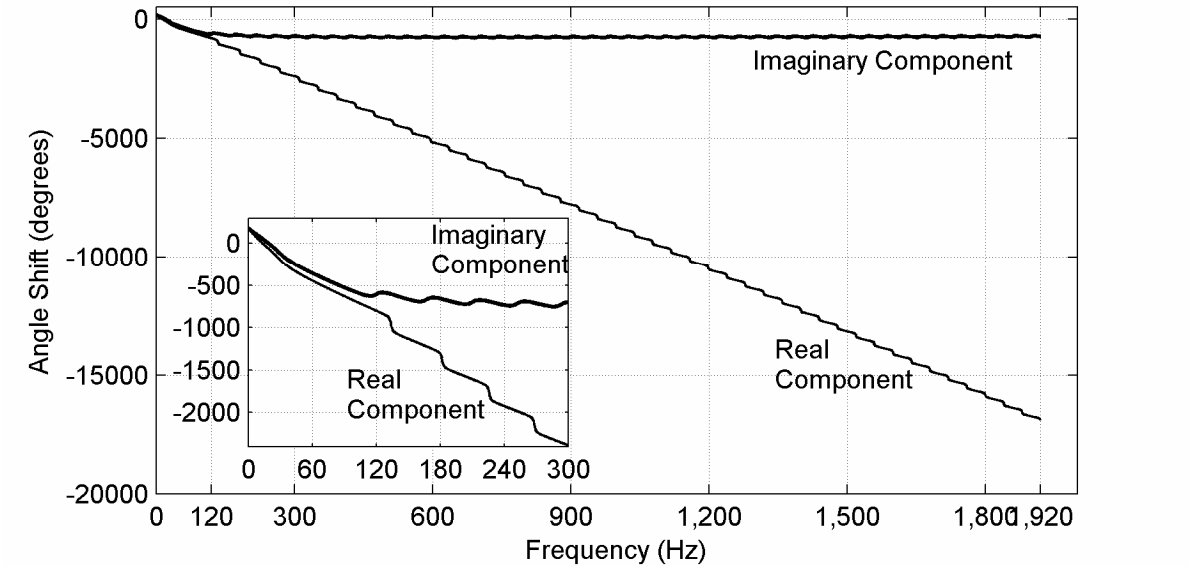

b)

Figure 5.7 Frequency response of phasor estimation method for N= 96 samples (= 1.5 cycles).

The response for a window size of 96 samples, from Figure 5.7, is not good enough, because it amplifies close frequencies above the fundamental, reaching a peak

of +6dB of amplification at slightly above the fundamental frequency. Moreover, this response does not attenuate significantly the higher frequencies.

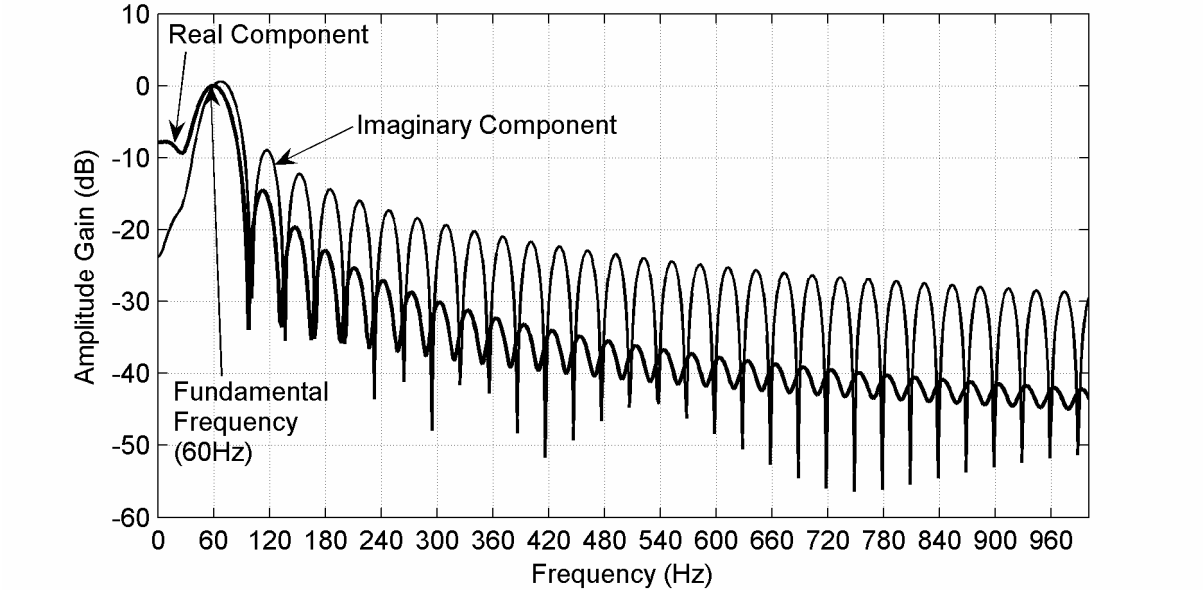

a)

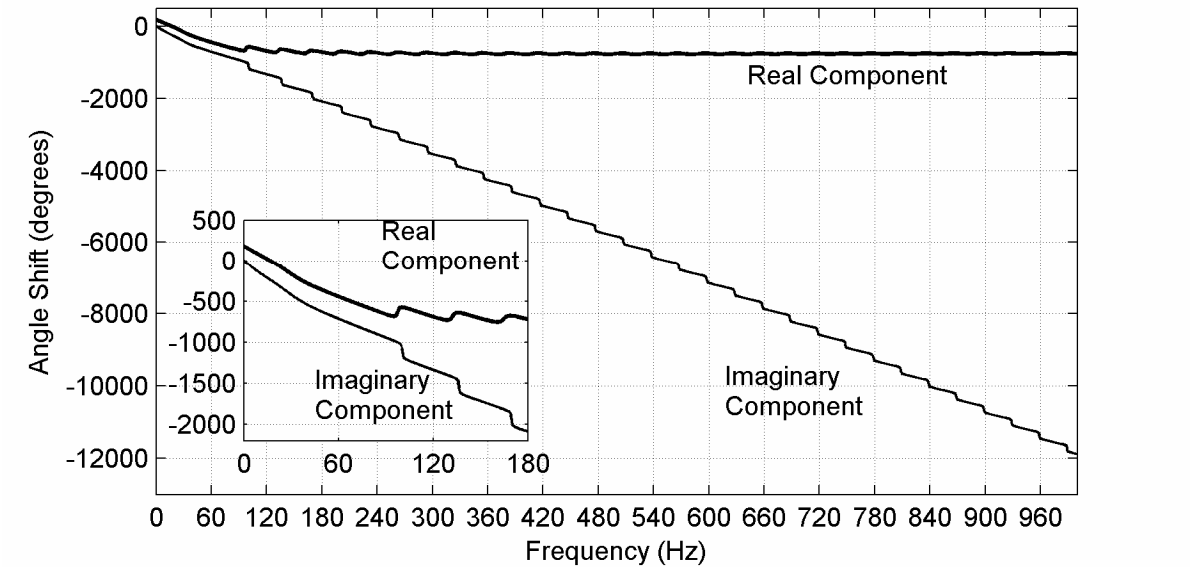

b)

Figure 5.8 Frequency response of phasor estimation method for N=128 samples (= 2 cycles).

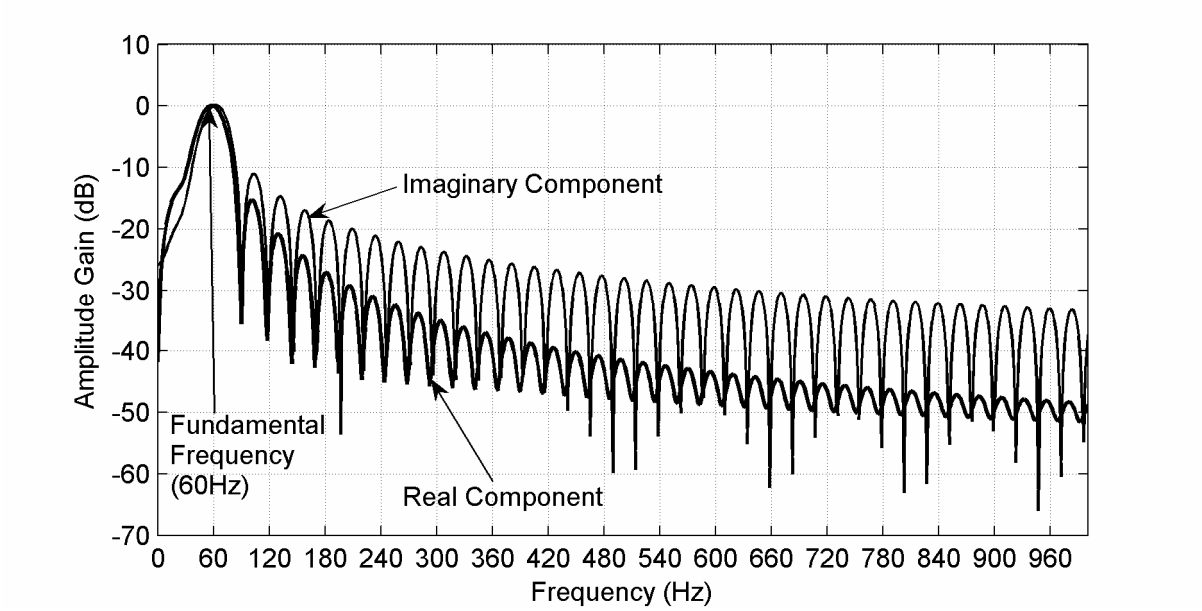

a)

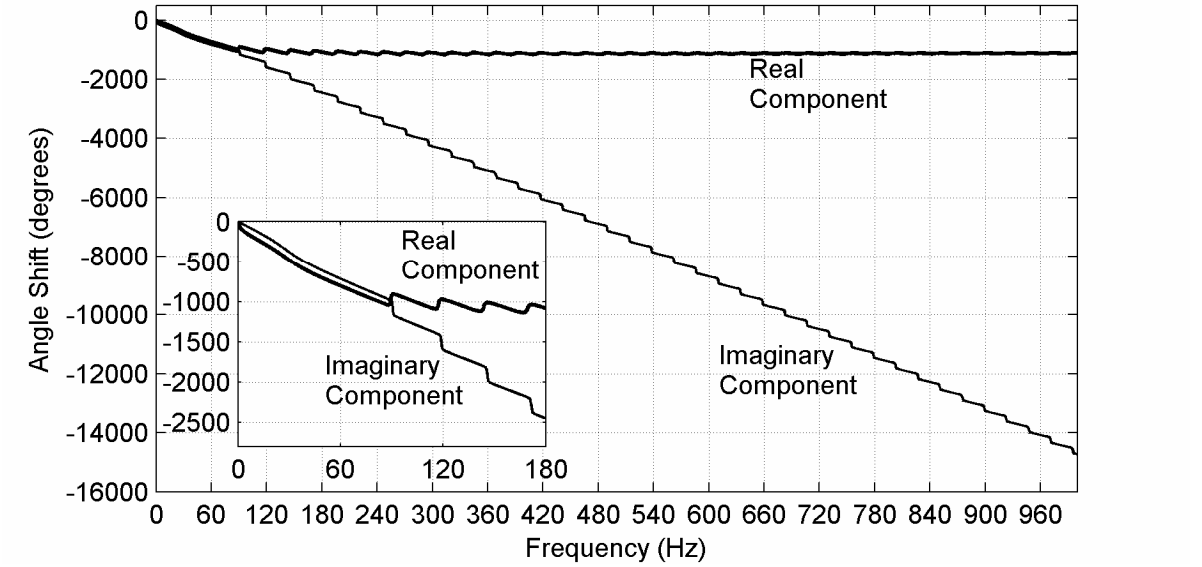

b)

Figure 5.9 Frequency response of phasor estimation method for N=160 samples (= 2.5 cycles).

Relative improvements in the response are observed for increases in the window size from 64 to 96 and from 96 to 128 samples. The peak amplification in the first lobe

of the frequency response goes down with the increase of window size: in Figure 5.6 is +22dB, in Figure 5.7 is +6dB and in Figure 5.8 is +0.5dB. At the same time, the peak of the second lobe of the frequency response also goes down: in Figure 5.6 is +16dB, in Figure 5.7 is 0dB and in Figure 5.8 is –9dB, only in the third case is an attenuation (i.e. negative decibels). However, for a window size increase from 128 to 160 samples, the improvement in the gain response is not that significant, comparing the peak responses of the first lobe and the second lobe in the same way. Based on this frequency response criteria, the optimum window size selected was also N=128 samples=2 cycles.

5.3 SUMMARY

A phasor estimation method using an improved least squares error technique is presented in this chapter. The problem with traditional least error squares methods is stated. The idea of improving the curve to be fitted using information about the CCVT behavior is presented. The phasor estimation method is developed using this concept. The optimum window size for this method is found and presented.

6. SYSTEM STUDIES

6.1 INTRODUCTION

A proposed least squares voltage phasor estimation method was described in the previous chapter. In this chapter the performance of this method is verified against realistic scenarios. These scenarios consist of faults simulated on detailed models from real power systems. Faults at different typical high voltage levels were simulated, showing the improvements over a traditional method. Moreover, some cases were identified where the proposed method is not recommended, explaining the limitations.

Additionally, the sensitivity of the proposed method against inaccuracies on the values of the CCVT parameters was studied.

6.2 REALISTIC POWER SYSTEM CASES

6.2.1 Case Selection

Several faults were simulated from which some representative cases were selected for further analysis. Only the representative cases selected are presented here.

6.2.1.1 Fault Selection: One fault type was selected that typically causes the larger magnitude of voltage changes. The use of one fault type simplifies the analysis and comparison of cases. The characteristics of the fault type selected are:

- Three phase fault, i.e. simultaneous on all three phases
- Low fault resistance, equal or less than 0.1 ohm primary
- Fault incidence angle of: 0° degree for phase A, 120° degree for phase B and 60° for phase C.

The fault selected is applied at the remote end of the line, considering the local end where the CCVT and the relay are located. In other words, the fault is located at 100% of the line, and the CCVT is located at 0% of the line. This kind of fault location is typically used when verifying distance protection performance.

6.2.1.2 Case Search and Selection Criteria: The fault just described was applied to several transmission line locations in different models of real power system networks. The purpose of simulating these faults is to obtain a voltage signal for review. The level of distortion in the voltage signal compared to the final steady state value was observed.

Two criteria were used in the selection of the cases for further analysis: high voltage level and distortion level. The high voltage level is a measure of the importance of the line; higher voltage levels are typical of more important transmission lines. The distortion level was used as a measure of the difficulty introduced to the phasor estimation algorithm, more distortion was considered more difficult and relevant. To quantify the distortion level, the high voltage input and the CCVT low voltage output were compared on a common scale, i.e. scaling down the high voltage by an ideal PT with the same ratio as the CCVT.

6.2.2 Fault Simulation

Fault simulation is used to obtain the time response of some desired power system variable to a fault condition. The following sections describe the simulation process.

6.2.2.1 Power System Model: To perform the fault simulation, it is essential to have a power system model. This overall model is based on the mathematical model of individual components. Each component model is defined by certain parameters and is valid over certain frequency range. The CCVT model is one of these individual components and is included in the overall power system model.

The individual components of the power system network need to be detailed in order to properly represent the range of frequencies desired. However, a higher level of detail makes the overall model more complex and increases the processing time required for the solution. On the other hand, a model with less detail requires the use of equivalents that represent the rest of the network concisely. Typically, these equivalents are only valid at the power system frequency and other more complete equivalent models are difficult to obtain [31].

In this work, several models of real power systems with significant level of detail were used. Each of these models included up to 50 three-phase buses with the following characteristics: voltage levels ranging from 6.9 kV up to 500 kV, distributed parameter representation of transmission lines, saturation representation of power transformers, Park's representation of synchronous machines, linear shunt reactors, capacitive series compensation including overvoltage protecting circuit, etc. The modeling details can be found in [7]. The detailed description of these models was considered beyond the scope of this work, because the proposed phasor estimation method is intended for use in any power system network. The detail of the CCVT model was described previously (section 3.3).

6.2.2.2 Time Domain Solution: The time domain solution of the power system network was performed using the Alternative Transient Program (ATP). This program implements the solution method proposed by Dommel [9,10].

Some parameters are necessary to calculate the solution: 1) the time step and 2) the duration of the simulation. The network is solved periodically, with a time period equal to the time step Δt'. Note that here Δt' represents the network simulation time period and Δt is equal to the phasor estimation algorithm sampling period.

The time step Δt' needs to be small enough to obtain a reasonable accuracy of the solution over the frequency range of interest. The corresponding sampling rate F_S' (= $1/\Delta t$') of simulation was synchronized to the desired sampling rate of the phasor estimation method proposed, i.e. a rate of simulation multiple of F_S = 3840 Hz was

chosen. This choice of sampling rate simplifies the post-processing of the signal, which is described later, in section 6.2.3. The duration of the simulation was selected to cover a minimum of 600 ms (=36 cycles at 60 Hz). This duration includes a prefault time interval of around 18 cycles, enough to obtain a good initial steady state before applying the fault. The remaining time is sufficient to observe the entire transient response.

In this simulation, the only event required is the fault being applied. The fault starting time is not a fixed number, but is actually a function of the zero crossing of the phase A voltage. This zero crossing depends on the power system and the line being simulated.

The output variables desired from the simulation are obviously the voltage signals. The high voltage input and the CCVT voltage output were both recorded for further analysis. The ATP program produces a particular file format where it records all the simulation results: the PL4 format [7].

6.2.3 Post-Processing

The voltage signals desired for analysis were obtained from the simulation results. These signals are of a sampling rate higher than the one required by the phasor estimation method. The process to reduce the sampling rate to the desired rate consists of a sequence of two operations [32]: antialias filtering and down-sampling, in that order.

The antialias filtering consists of removing the frequencies above one half of the desired bandwidth. The desired bandwidth is the sampling rate used by the phasor estimation method, i.e. F_S = 3840 Hz. Therefore, the filter needs to remove frequencies above 1920 Hz (= 3840 / 2). A low pass fifth order Butterworth filter with a cutoff (=-3 dB) frequency of 1800 Hz was used for this purpose.

The down-sampling consists of reducing the sampling rate of the signal to some desired lower rate. To facilitate this operation, the sampling rate for the simulation was

chosen as an integer multiple of the desired rate; otherwise, i.e. for a non integer multiple rate, a more complex interpolation operation would be required. If *n* is the factor that relates these two sampling rates, then down-sampling is reduced to extracting one sample of every *n* of the output signal received from the antialias filter.

6.2.4 Phasor Estimation Performance

The signals resulting from the post-processing were used to evaluate the performance of the proposed phasor estimation method. Two phasor estimation methods were used for comparison in the typical cases: the basic least squares and the improved least squares. The real and imaginary components of the phasor were calculated for the entire simulation time. The angle normalization was then applied to the resulting phasors. The magnitude and the angle of these phasors were computed based on the real and imaginary components for evaluation. An additional phasor estimation method was used in the difficult cases: single component with time shift, described in section 2.4.4, using one of the components, real or imaginary, of the improved least squares method. The component with best frequency response characteristics was selected for this purpose.

The speed and accuracy of the proposed method was compared to the basic least squares method. To illustrate the differences, the magnitude and the angle were plotted separately against time. Also, the trajectories in the complex plane of the estimated phasors were shown. For the difficult cases an additional plot was included, the magnitude of the phasor error, which was obtained subtracting the instantaneous phasor from the final stable phasor.

6.2.5 Typical Cases

6.2.5.1 Fault in a 500 kV System: A 500 kV, 169 km overhead transmission line was subjected to the pre-selected fault condition: a low resistance three phase fault at the remote end. Figure 6.1 shows the time response of the phase A voltage signal for this fault condition with a fault incidence angle of 0° degrees. A high magnitude of

voltage change of 87.9% (= 100% – 12.1%) of the prefault amplitude was observed at this location of the power system selected.

Figures 6.2 and 6.3 show the magnitude of the voltage phasor estimated using the improved least squares method. The improved least squares method stabilizes at the transition time of 2 cycles, faster than the basic least squares, as shown in Figure 6.2. The magnitude of the phasor obtained is not constant but decaying, as shown in Figure 6.3. This decay is part of the power system behavior at this location, which is confirmed by a similar behavior of the phasor magnitude estimated from the ideal PT response that was included for clarification in this figure.

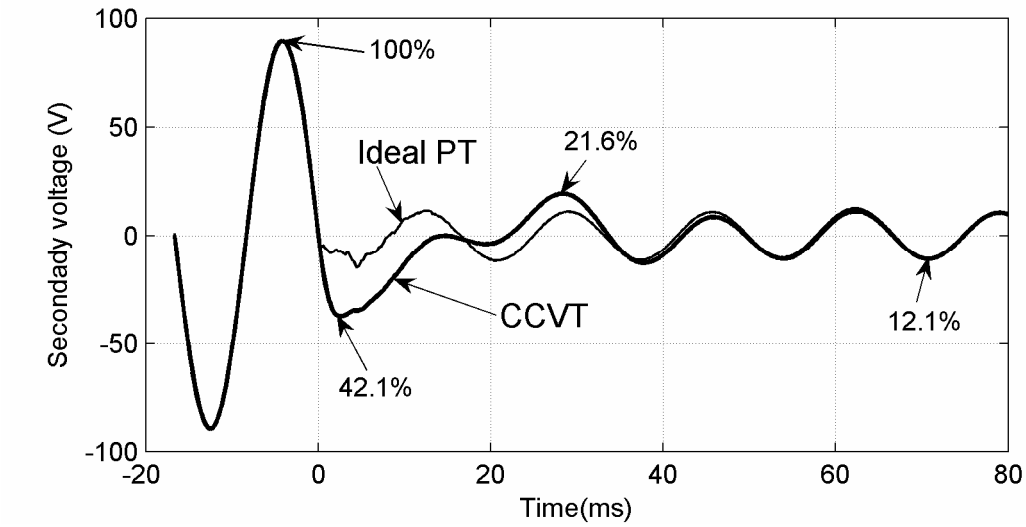

Figure 6.1 Phase A voltage time response.

Figure 6.3 also gives a measure of the improvement achieved by the improved least squares method compared to the basic least squares: the estimated magnitude accuracy is comparable to that obtained from an ideal PT, i.e. the CCVT impact is practically eliminated.

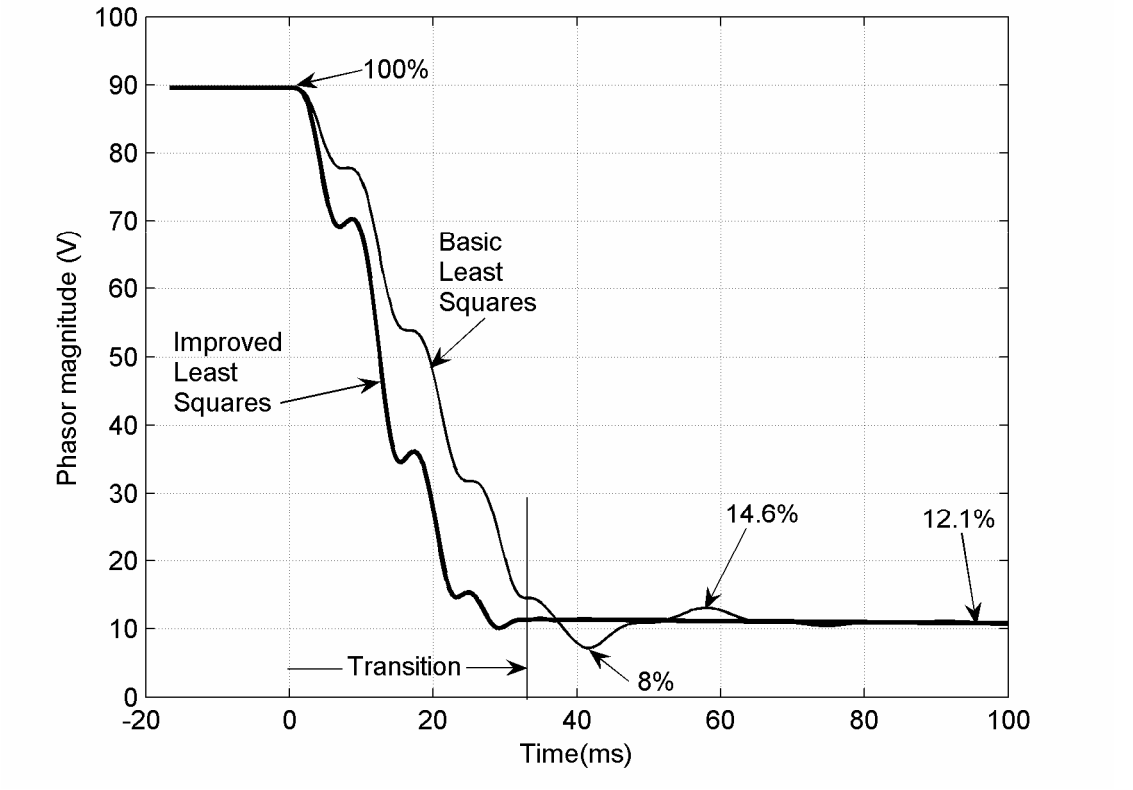

Figure 6.2 Phase A estimated voltage phasor magnitude.

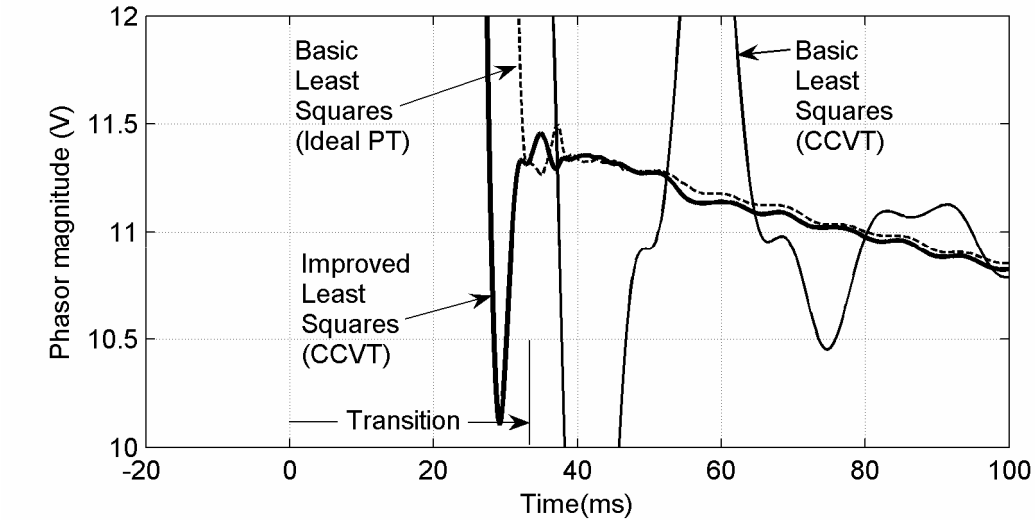

Figure 6.3 Zooming In Figure 6.2.

Figures 6.4 and 6.5 show the angle of the voltage phasor estimated using the improved least squares method. The response of the improved least squares stabilizes at the transition time of 2 cycles, as shown in Figure 6.4. The angle of the phasor is not constant but is increasing with time, as shown in Figure 6.5. This angle shifting in time

is a normal power system behavior for this location, which is confirmed by a similar behavior of the estimated angle from the ideal PT. The angle estimation accuracy with the improved least squares method is comparable to that obtained from an ideal PT. The difference observed between the improved and the ideal is due to the CCVT steady state angle error, this difference is about the same as that observed during prefault.

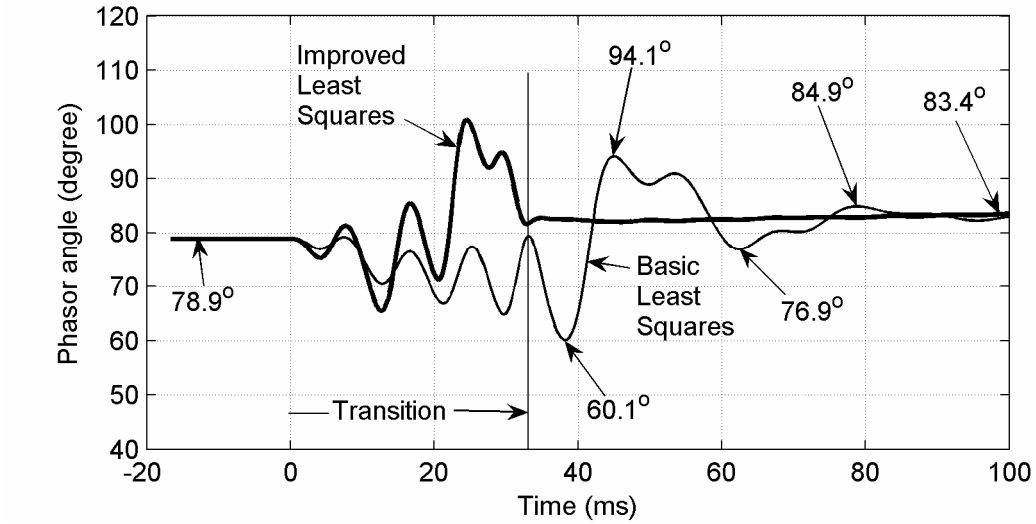

Figure 6.4 Phase A estimated voltage phasor angle.

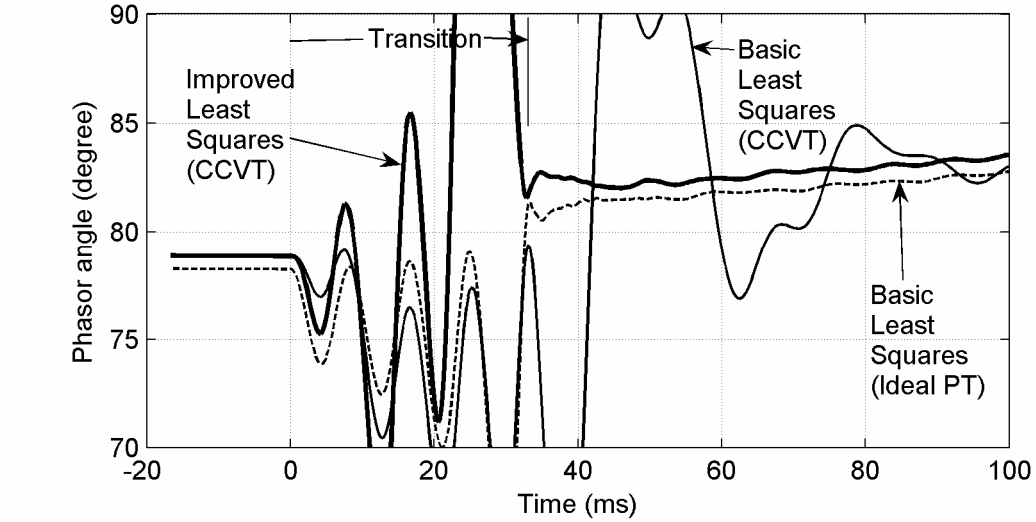

Figure 6.5 Zooming In Figure 6.4.

Figure 6.6 and 6.7 show the trajectories of the phasor estimated with the improved least squares and the basic least squares method for comparison. The improved least squares method converges at two cycles while the basic least squares method does so after four cycles.

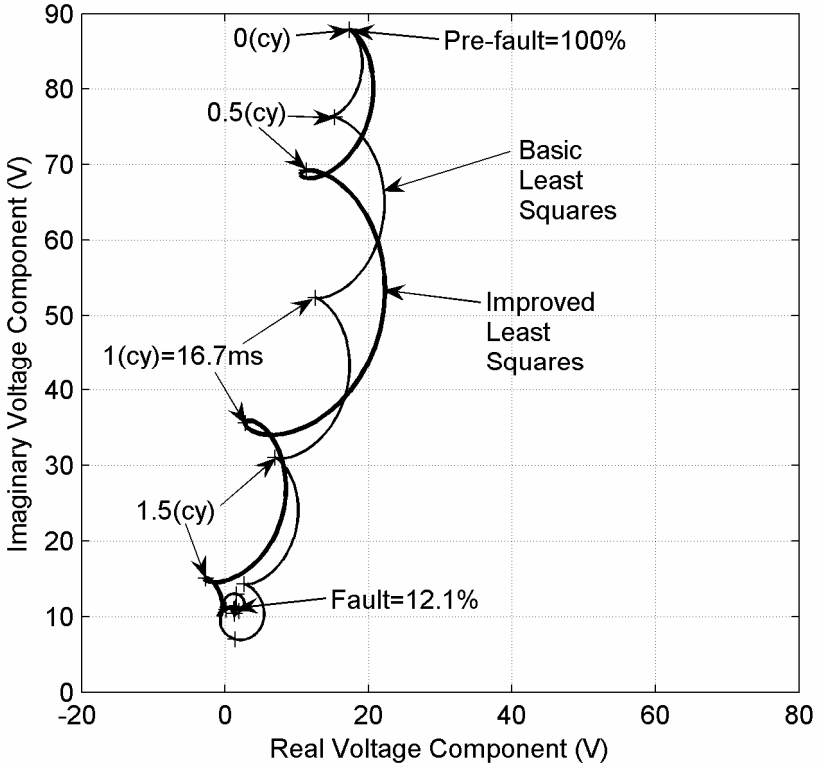

Figure 6.6 Phase A estimated voltage phasor trajectory in the complex plane.

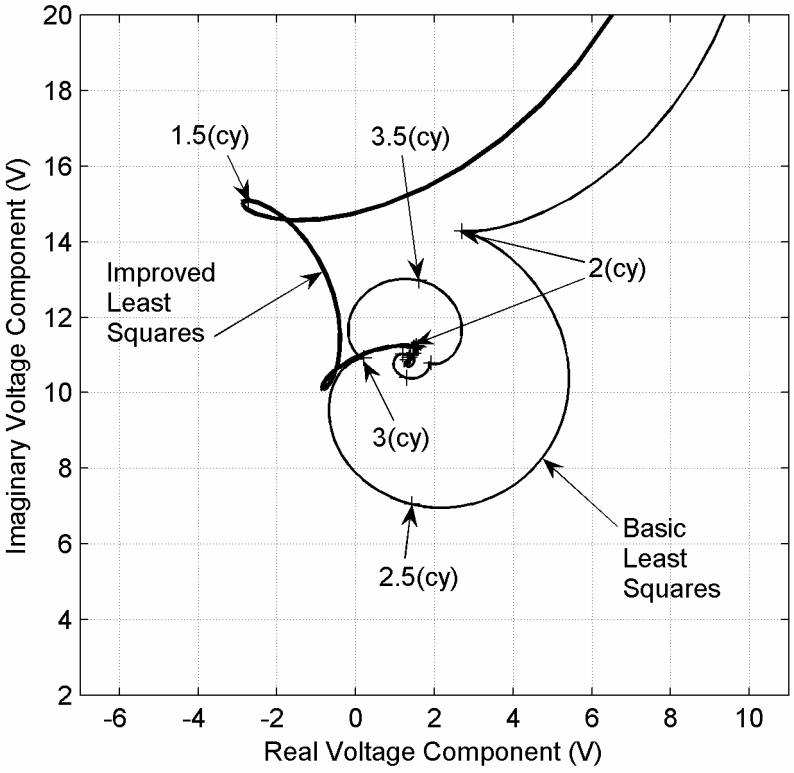

Figure 6.7 Zooming In Figure 6.6.

6.2.5.2 Fault in a 138 kV System: A 138 kV, 206 km overhead transmission line is subjected to the remote end three phase fault condition, previously selected. Figure 6.8 shows the phase C voltage signal for this fault condition. The fault incidence angle of this fault is 120° and the magnitude of voltage change is 78.6% (= 100% – 21.4%). This power system location presents a natural frequency of approximately five times the fundamental frequency, which produces a decaying transient of that frequency for certain fault incidence angles, shown as the ideal PT plot in Figure 6.8.

Figures 6.9 and 6.10 show the magnitude of the phasor estimated using the improved least squares method. The magnitude of the phasor estimated with the improved least squares method stabilizes within 1.3 V of the final value at the transition time of 2 cycles. The uncertainty in the estimated magnitude is smaller compared to the basic least squares method, as shown in Figure 6.10. The impact of the power system noise in the accuracy of the method is small. The power system noise is attenuated by the CCVT in the first place, as seen in Figure 6.8. The filtering capability of the improved least squares phasor estimation method attenuates the remaining part of the noise and obtains the fundamental frequency phasor with improved accuracy.

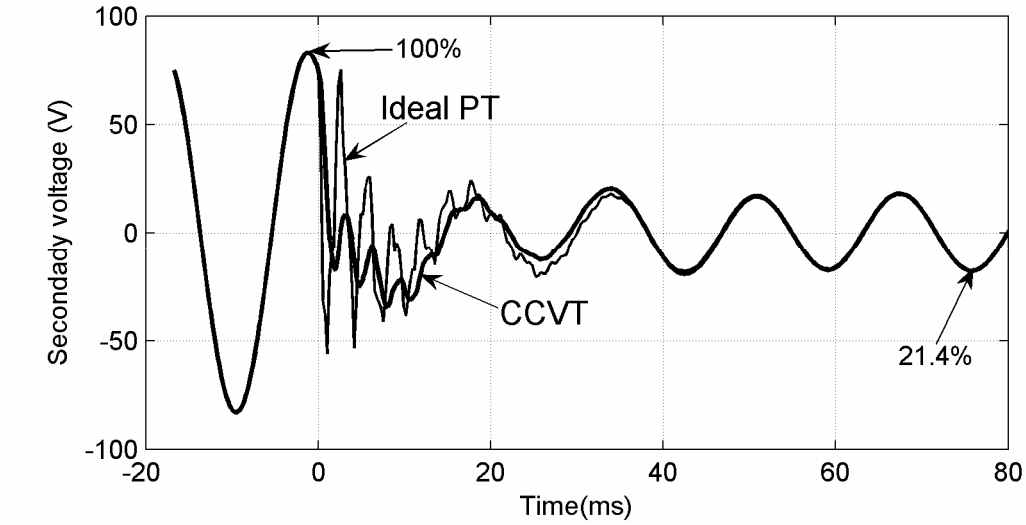

Figure 6.8 Phase C voltage time response.

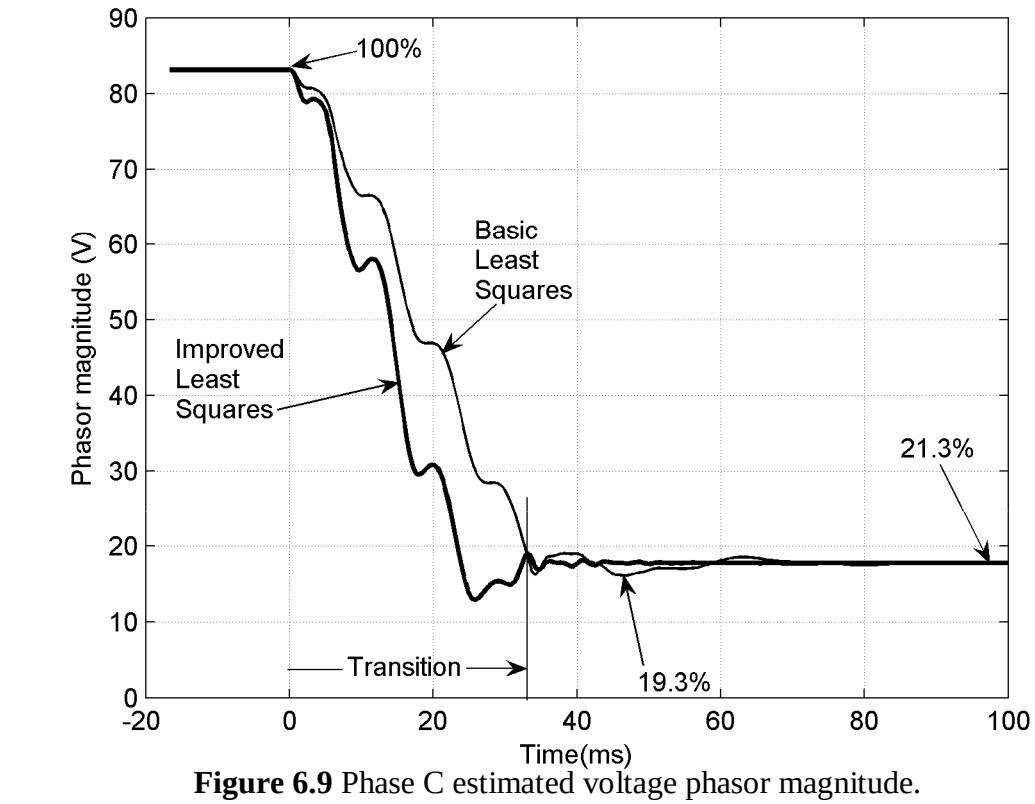

Figure 6.9 Phase C estimated voltage phasor magnitude.

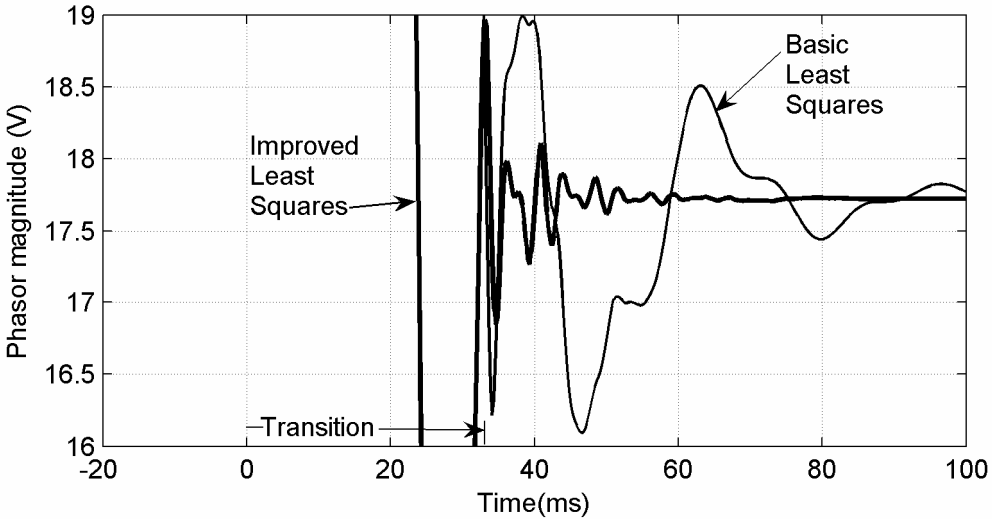

Figure 6.10 Zooming In Figure 6.9.

Figures 6.11 and 6.12 show the angle of the phasor estimated with the improved least squares method. The angle stabilizes within 2.5° of the final value at the transition

time of 2 cycles, as shown in Figure 6.12. The uncertainty on the angle is smaller and decays faster than in the basic least squares method.

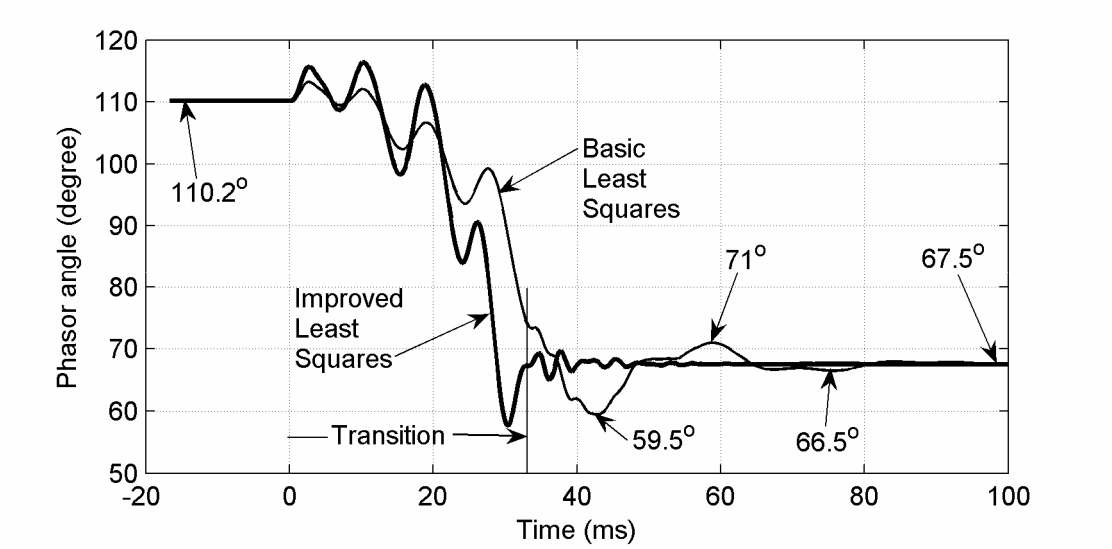

Figure 6.11 Phase C estimated voltage phasor angle.

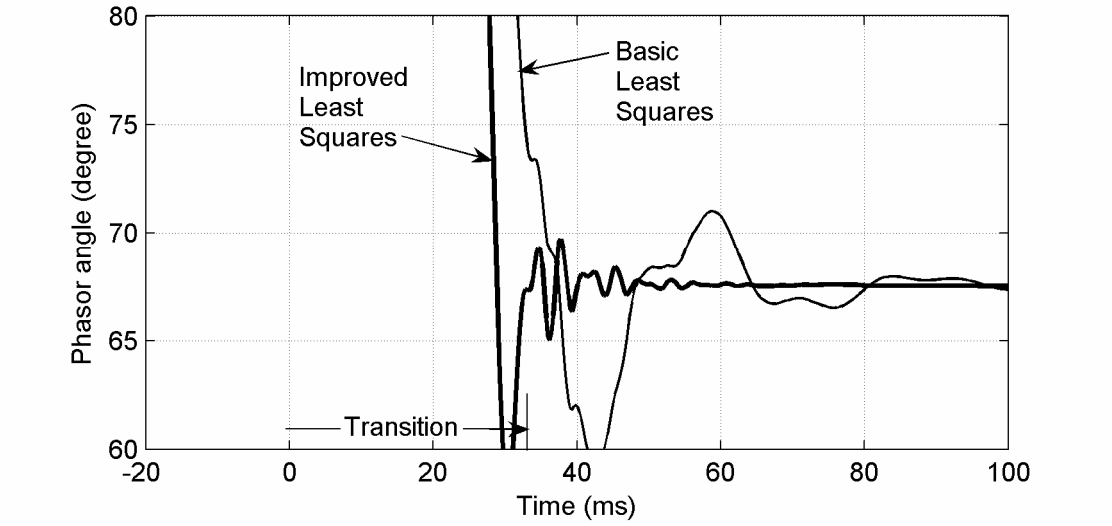

Figure 6.12 Zooming In Figure 6.11.

Figure 6.13 and 6.14 show the trajectories of the phasor estimated with the improved least squares and the basic least squares for comparison. The improved least squares method converges at two cycles while the basic least squares does so after four cycles.

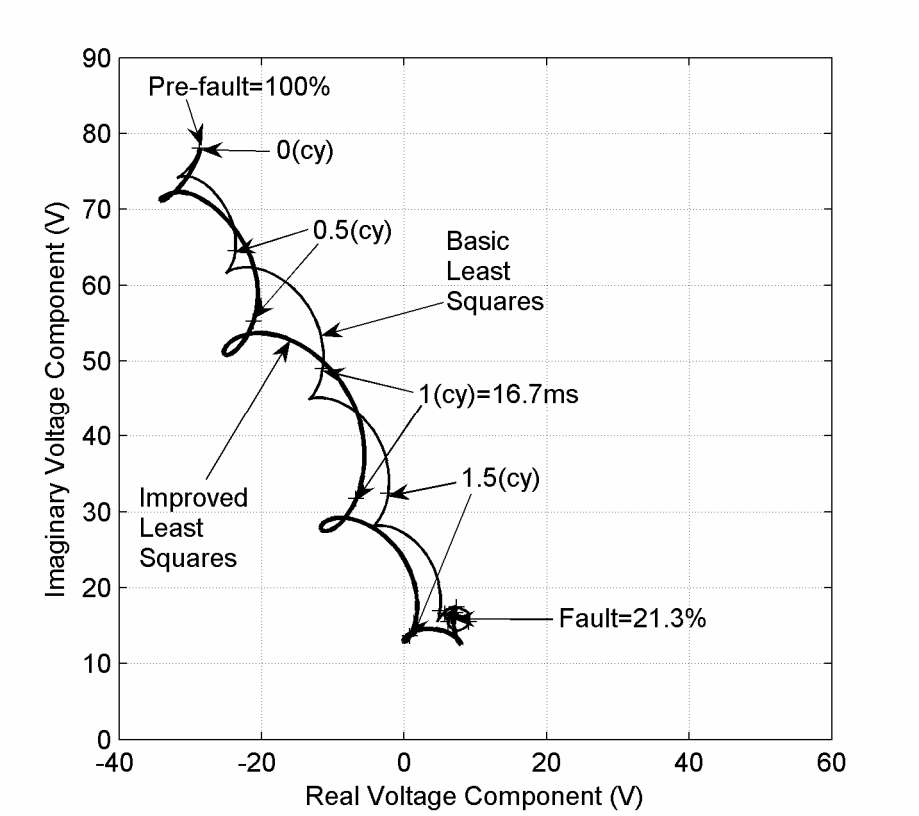

Figure 6.13 Phase C estimated voltage phasor trajectory in the complex plane.

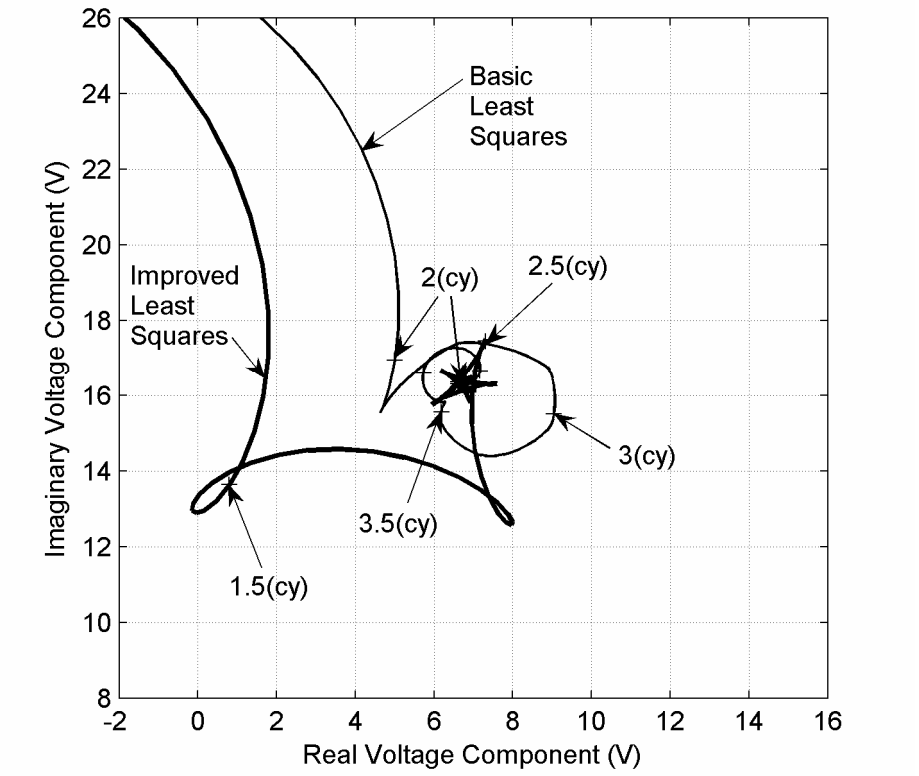

Figure 6.14 Zooming In Figure 6.13.

6.2.6 Difficult Scenarios

The improved least squares method has difficulty to obtain a good estimate of the fundamental frequency phasor in some conditions. The presence of transients in the power system with frequencies close to that of the CCVT but longer time constants of decay characteristic seem to be the main reason for this difficulty. Two cases were selected that did not produce any improvement in the estimated phasor: 1) a significantly long transmission line system and 2) a line adjacent to a series capacitor.

6.2.6.1 Fault in a 230 kV Long Transmission System: A 230kV, 325 km transmission line is subjected to the fault condition used in previous cases: the low resistance, three phase fault at the remote end. This line is part of a series of adjacent lines extending approximately 930 km, of which 655 km is at 230 kV and the remaining 275 km is at 138 kV. Shunt reactors are used at several points in the 230 kV portion to compensate the shunt capacitance of the transmission lines. Figure 6.15 show the phase B voltage signal for this fault condition. The fault incidence angle is 60° and the magnitude of voltage change is 88.3% (= 100% – 11.7%). This power system location presents a natural frequency of approximately two times the fundamental frequency, which results in a decaying transient of that frequency for certain fault incidence angles, shown as the ideal PT plot in Figure 6.15.

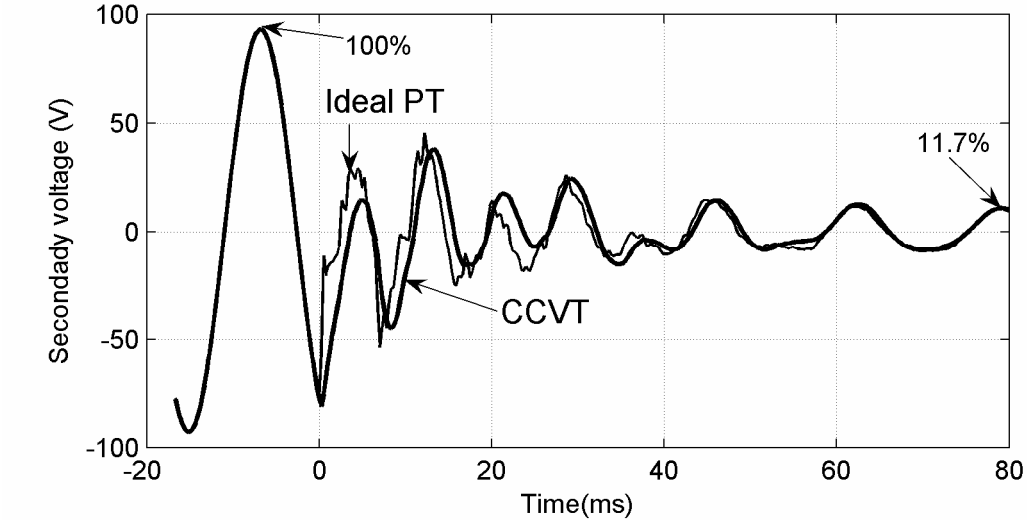

Figure 6.15 Phase B voltage time response.

Figure 6.16 shows the magnitude of the phasor estimated using the improved least squares method. The magnitude of the phasor estimated with this method stabilizes slower than the basic least squares method. Figure 6.16 shows that there is no improvement compared to the basic least squares. The single component method with time shift of 90^o was combined with the real component of the improved least squares method. The results are plotted in Figure 6.16 as well. The real component of the improved least squares method shows an improvement compared to the improved least squares method, but is not better than the basic least squares.

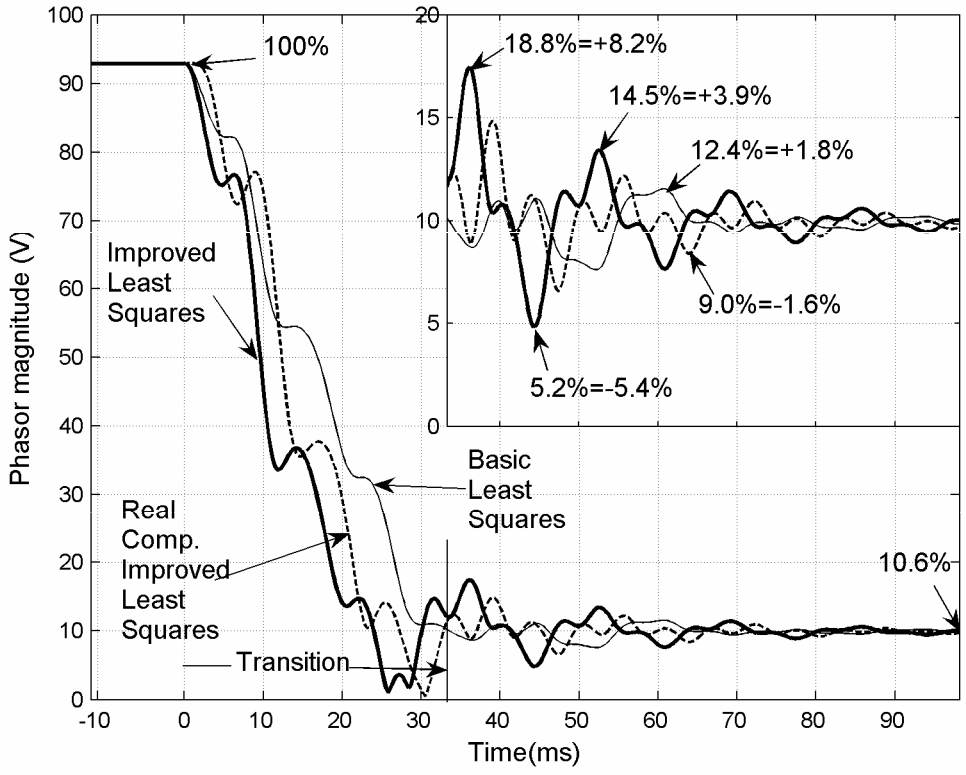

Figure 6.16 Phase B estimated voltage phasor magnitude.

Figure 6.17 show the angle of the phasor estimated using the improved least squares method. The angle of the phasor estimated with this method stabilizes slower than the basic least squares method. Figure 6.17 shows no improvement using the improved least squares method compared to the basic least squares. The real component of the improved least squares method shows again an improvement

compared to the improved least squares method, but is not better than the basic least squares.

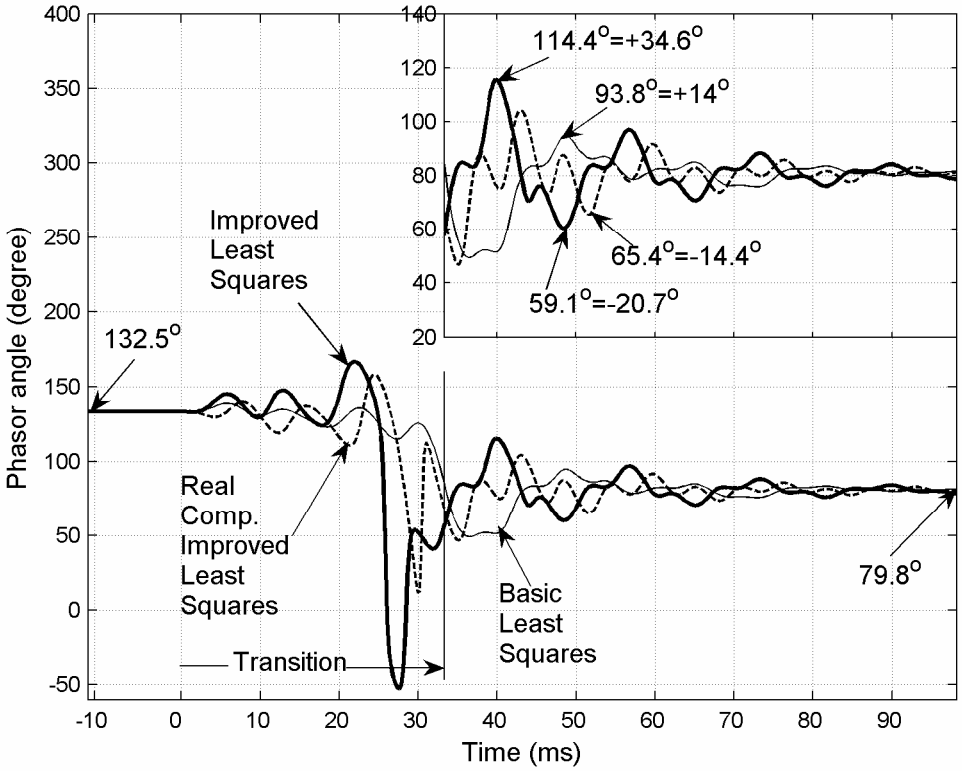

Figure 6.17 Phase B estimated voltage phasor angle.

Figures 6.18 to 6.21 show the trajectories of the phasor estimated with the improved least squares, the basic least squares and the real component of the improved least squares for comparison. The basic least squares method converges faster than the improved least squares method to the final voltage phasor value. Also, the basic least squares method converges faster than the real component of the improved least squares.

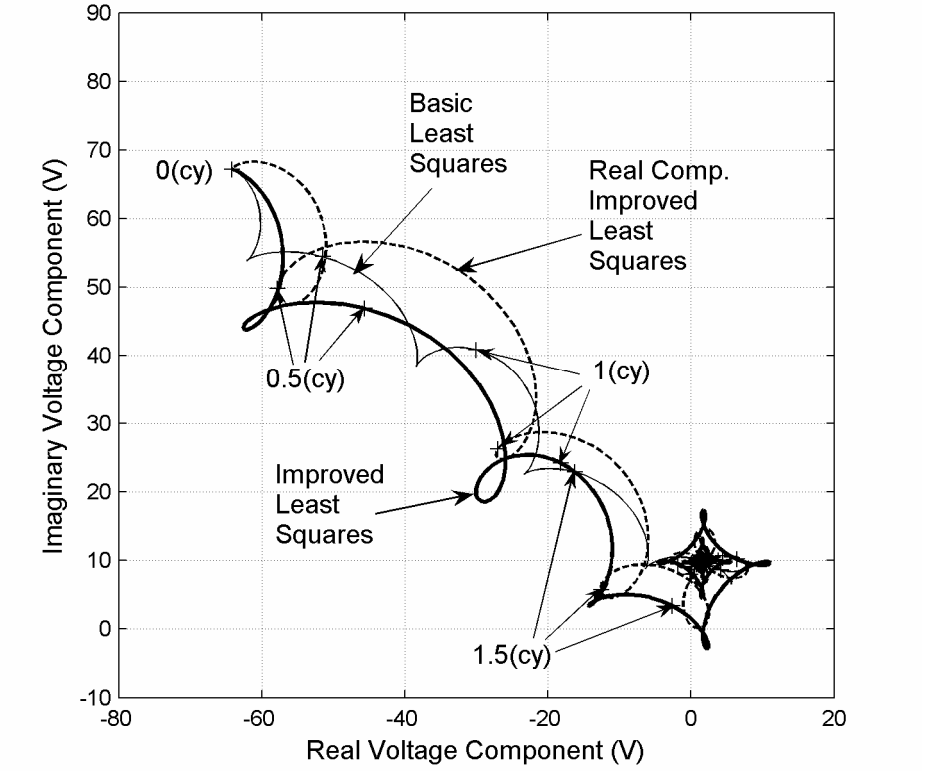

Figure 6.18 Phase B estimated voltage phasor trajectory in the complex plane.

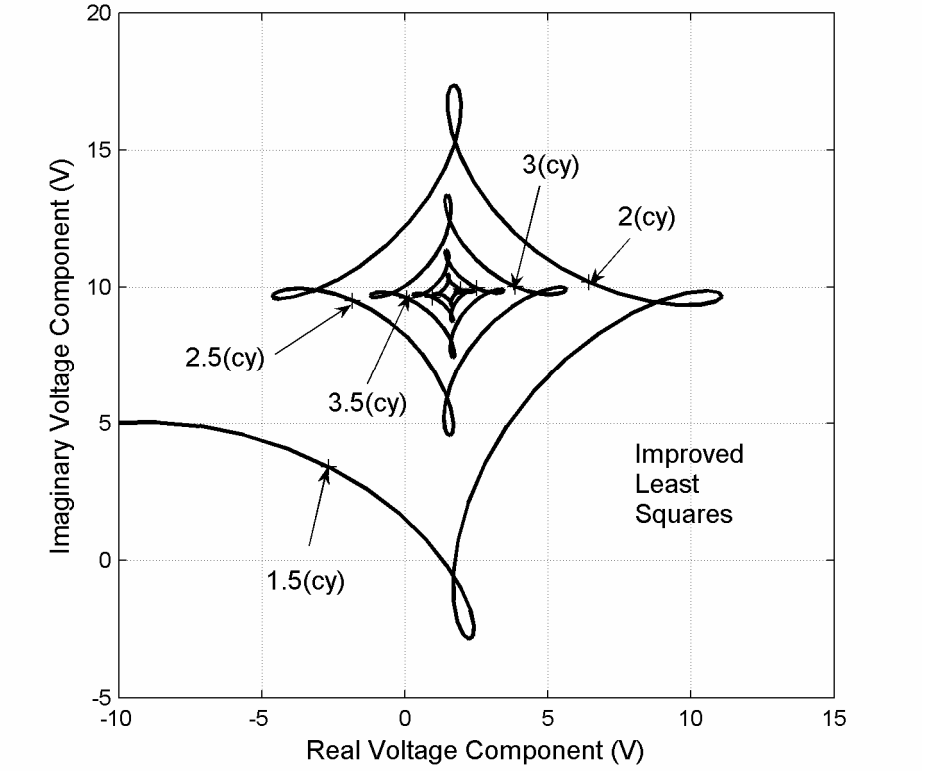

Figure 6.19 Zooming In Figure 6.18. Improved Least Squares

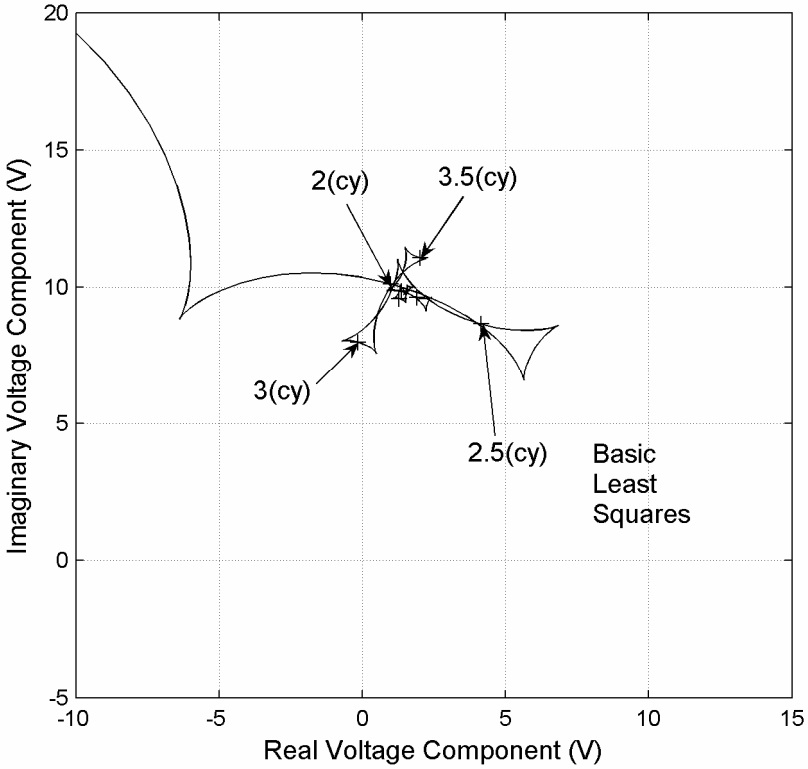

Figure 6.20 Zooming In Figure 6.18. Basic Least Squares

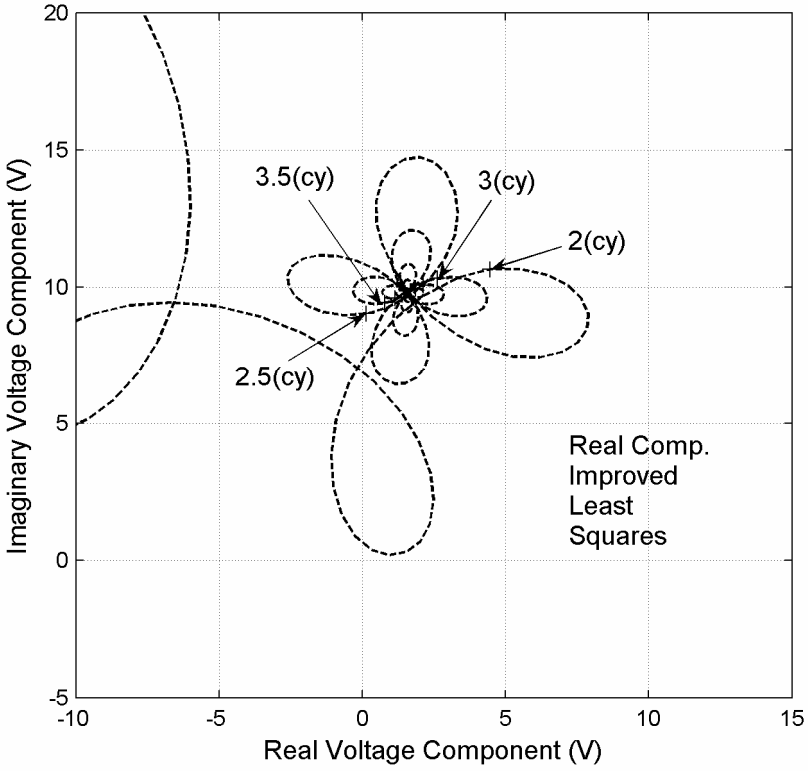

Figure 6.21 Zooming In Figure 6.18. Real Component Improved Least Squares

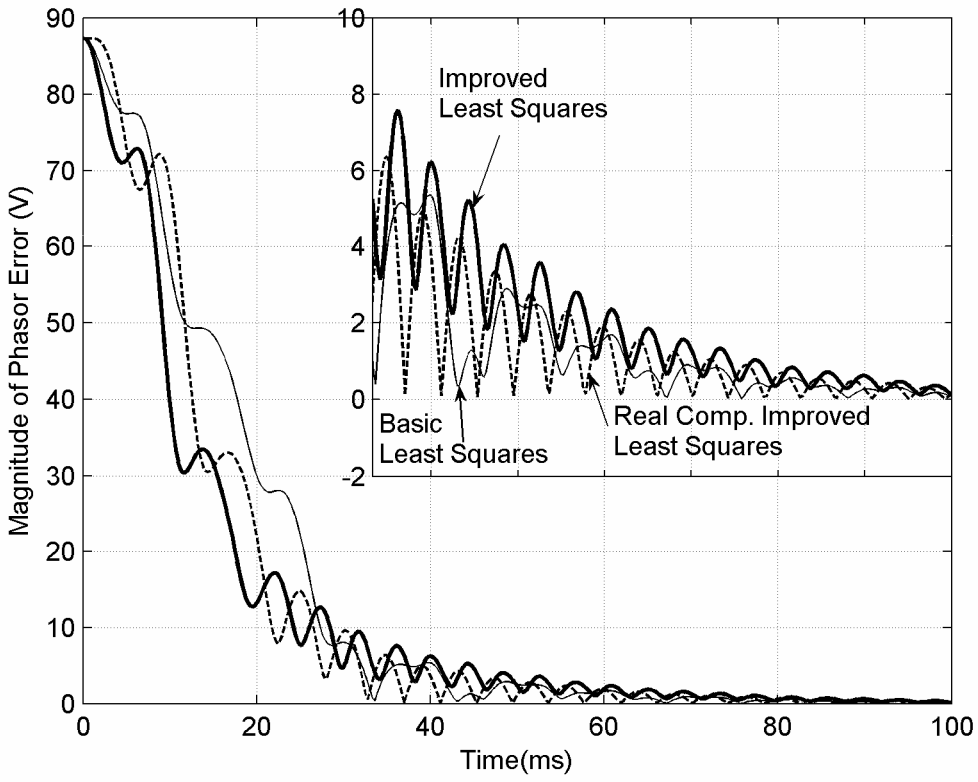

Figure 6.22 Magnitude of phasor error as a function of time

Figure 6.22 shows the magnitude of the phasor error, i.e. the amount of deviation from the final stable value. This plot shows clearly that the real component of the improved least squares method alone performs better than the improved least squares, for this case. This method also confirms that none of the new methods (Improved Least Squares and Real Component of Improved Least Squares) proposed here improve the results obtained by the basic least squares.

6.2.6.2 Fault in a 500 kV Line Adjacent to Series Capacitor: A 500 kV, 212 km overhead transmission line is subjected to the same fault used in previous cases: a low resistance, three phase fault at the remote end. This line is adjacent to a system of three parallel lines, 500 kV and 388 km, with series capacitors compensation of approximately 55% of the reactance of the line. Figure 6.23 shows the phase C voltage signal for this fault condition. The fault incidence angle is 120° but the magnitude of voltage change could not be calculated directly from the graphic, this value was calculated better after the phasor is estimated. The power system presents natural

frequency components below and above the fundamental frequency (i.e. high and low frequencies), which results in decaying transients of those frequencies for certain fault incidence angles, as shown in the ideal PT plot in Figure 6.23. In this case it was verified that the series capacitors were operating in their linear region, with no influence of their associated protective equipments.

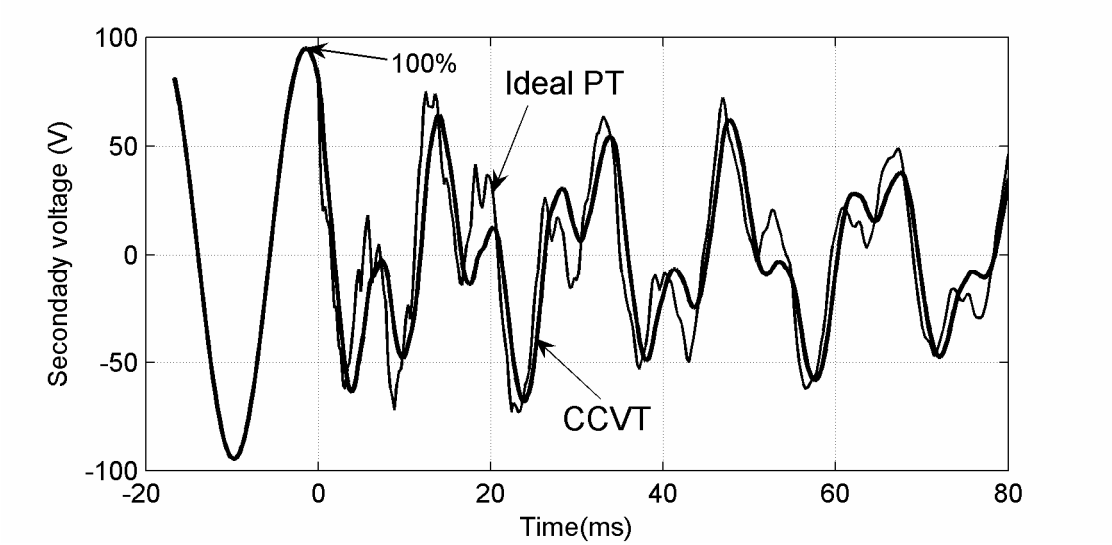

Figure 6.23 Phase C voltage time response.

Figures 6.24 and 6.25 show the magnitude and the angle, respectively, of the phasor estimated using the improved least squares method. The magnitude and the angle of the phasor estimated with this method stabilize slower than the basic least squares method; i.e. no improvement is observed. The magnitude of voltage change calculated is 59.7% (= 100% – 40.3%). The single component method is also plotted in Figures 6.24 and 6.25. The real component and the imaginary component show slower convergence compared to the basic least squares method. In this case, the presence of frequencies above and below the fundamental makes difficult the selection of a single component method.

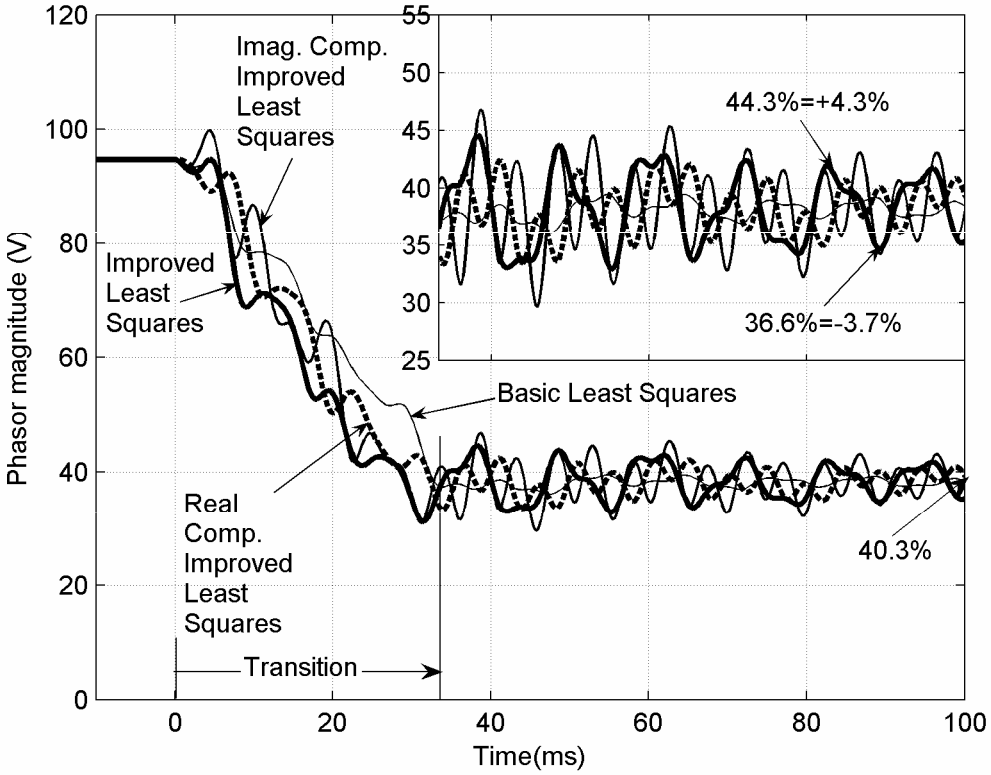

Figure 6.24 Phase C estimated voltage phasor magnitude.

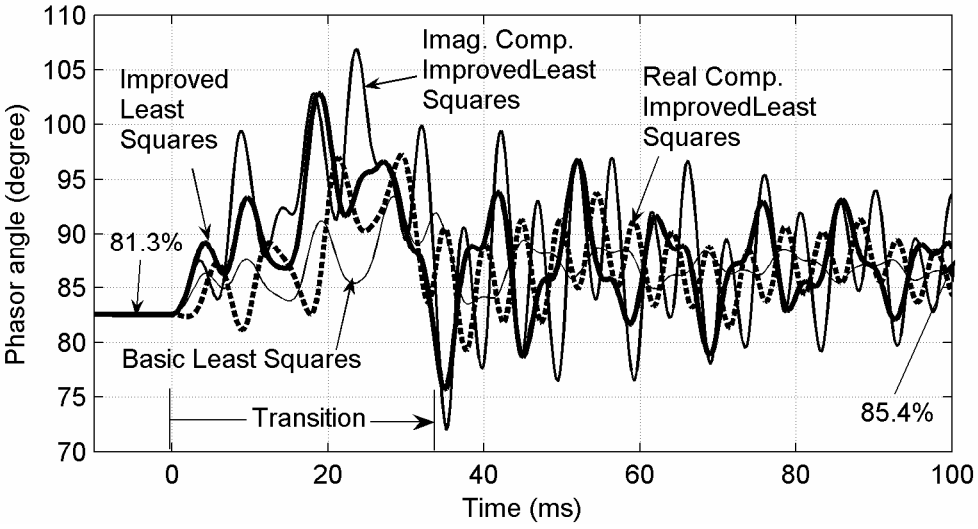

Figure 6.25 Phase C estimated voltage phasor angle.

Figure 6.26 shows the trajectories of the phasor estimated with the improved least squares, the basic least squares, the real component of the improved least squares and the imaginary component of the improved least squares for comparison.

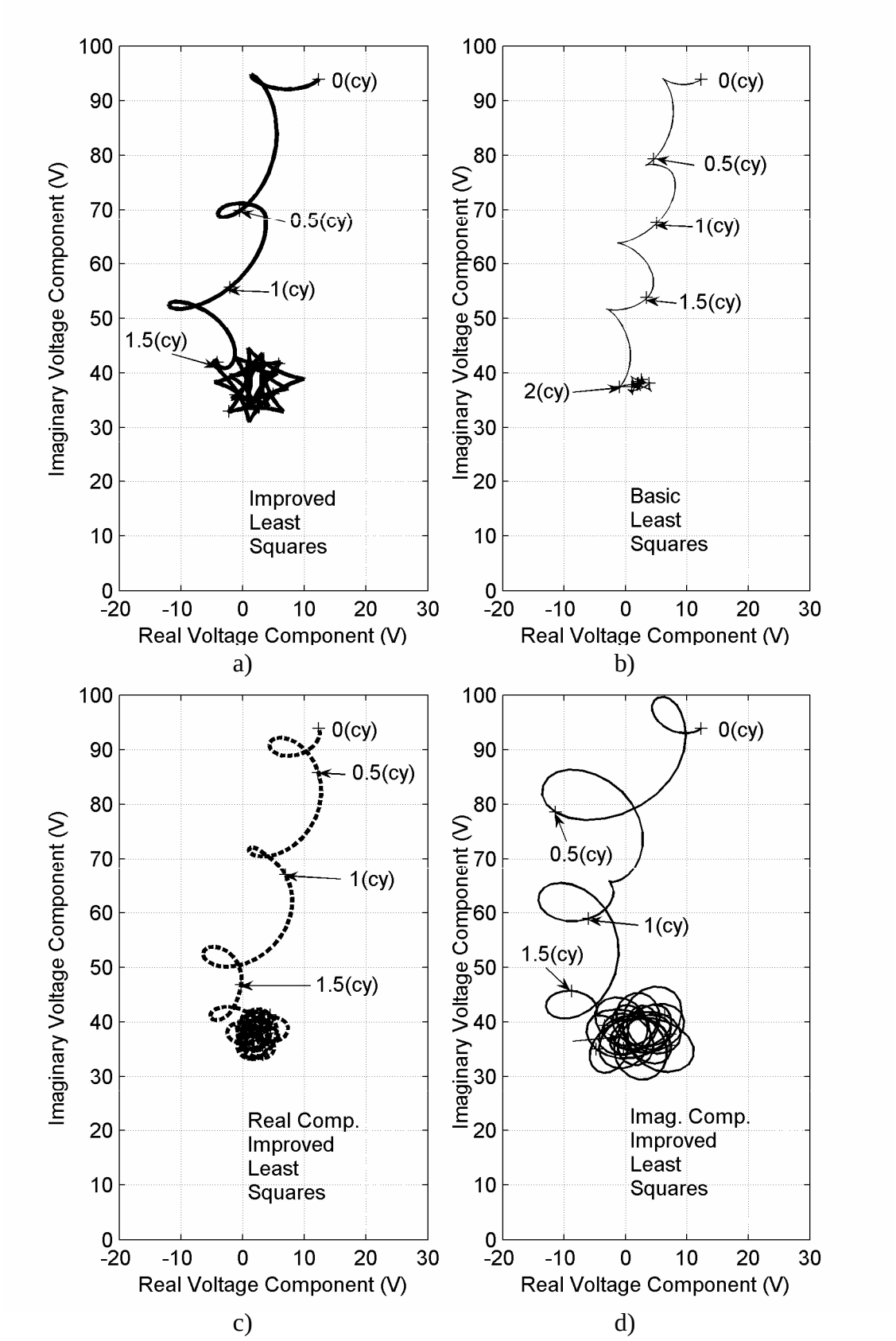

Figure 6.26 Phase C estimated voltage phasor trajectory in the complex plane.

Figure 6.26 shows that the basic least squares method is faster than all the other methods (Improved Least Squares, Real Component of Improved Least Squares and Imaginary Component of Improved Least Squares) in converging to the final voltage phasor value. At the same time the real component of the improved least squares is slightly better than the improved least squares. The response of the imaginary component of the improved least squares method is worse than the improved least squares.

Figure 6.27 shows more clearly that all the improved methods converge very slowly compared to the basic least squares method, for this difficult case.

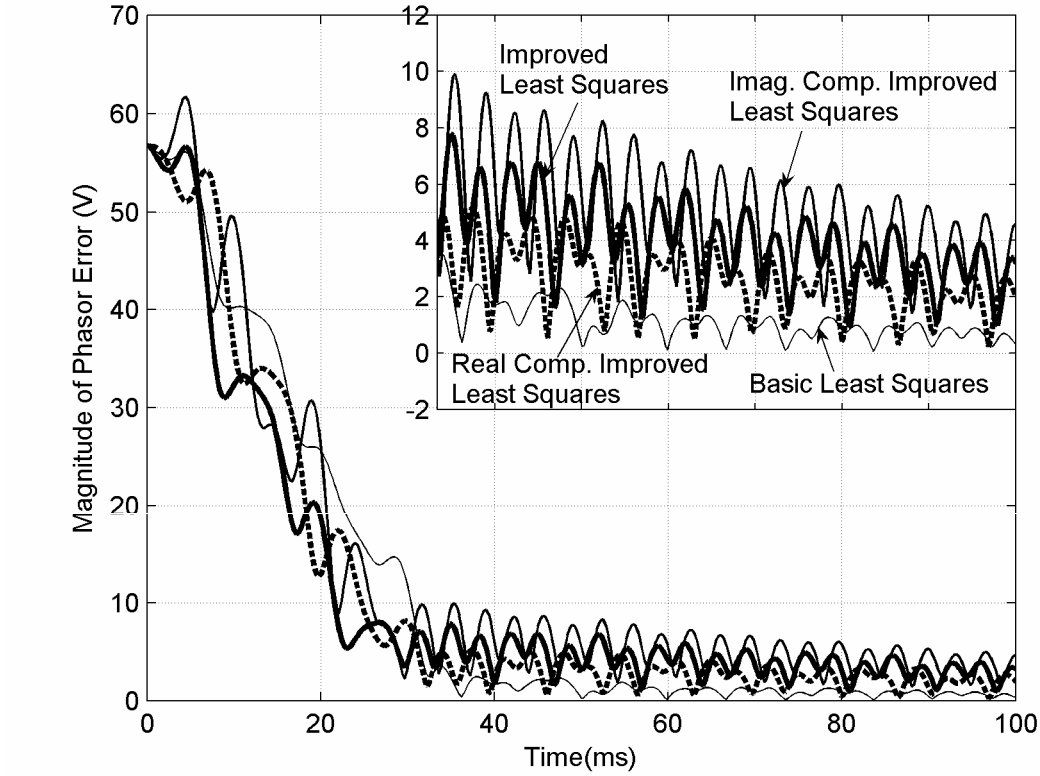

Figure 6.27 Magnitude of phasor error as a function of time

6.3 ALGORITHM SENSITIVITY TO CCVT PARAMETERS

The results previously presented assume a very good accuracy of the CCVT parameters. In a real scenario, these parameters are known, but with some percentage of

error. To evaluate the impact of these errors on the response of the improved least squares algorithm, a parameter sensitivity study was performed.

6.3.1 Definition of the Reference Condition

A reference condition is defined to compare the effect of CCVT parameter variations in the response of the improved least squares algorithm. The CCVT and burden parameters, without any variation, are used to produce a linear transfer function, as explained in section 3.3.2.1. From this transfer function, the characteristic frequencies and time constants obtained are used to build the improved least squares algorithm. This would be the ideal case where the CCVT parameters are known with very good accuracy.

For this reference condition, a fault is simulated where the effect of the error introduced by the CCVT is more noticeable. This same fault would be used for all parameter variations. A system with an SIR = 30 is selected, which would result in a very low fault voltage, and at the same time significant change on the voltage magnitude. This condition is representative of a weak system where the source impedance is large, but also can be the case of a very short line. A fault incidence angle of zero degrees would introduce the biggest distortion of all possible incidence angles. A very low fault resistance of R_F = 0.01 ohm is selected, as the lower resistance faults would produce more damage. The fault is located at the remote end of the line. This location has been used typically to evaluate transient overreach and underreach in distance protection applications.

The voltage fault signal received from the CCVT is processed by the improved least squares algorithm. The magnitude and angle of the voltage phasor estimated would be the reference conditions for the comparison. This reference condition is shown in Figures 6.28 and 6.29. The improved least squares algorithm converges to a very stable phasor value after the two cycle window is inside the fault. This is because a very simple power system was chosen and therefore any deviation observed would be caused exclusively by the parameter variation applied. For comparison, the output of the basic least squares algorithm with a two cycle window is also shown.

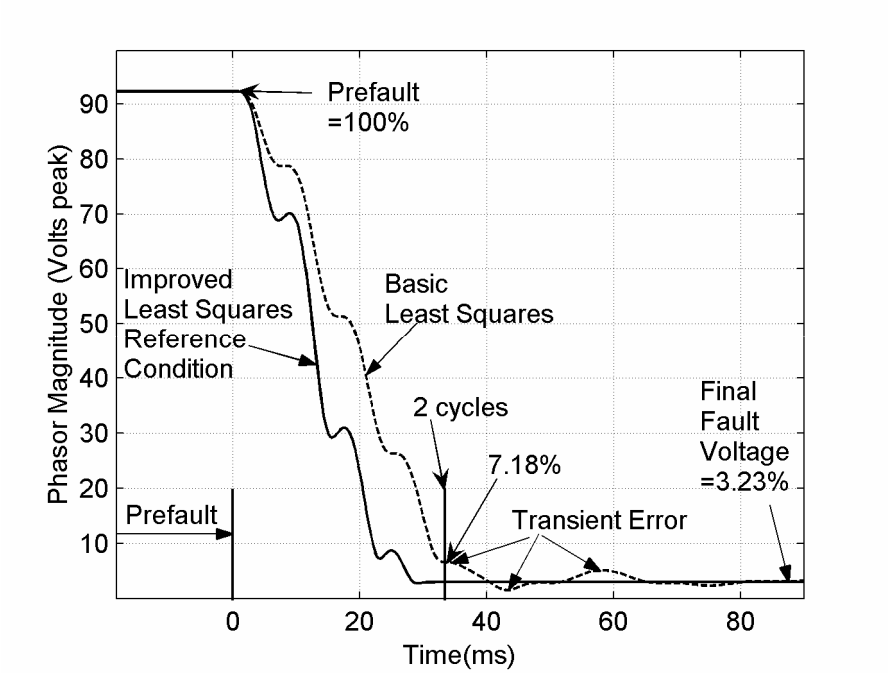

Figure 6.28 Reference Phasor Magnitude.

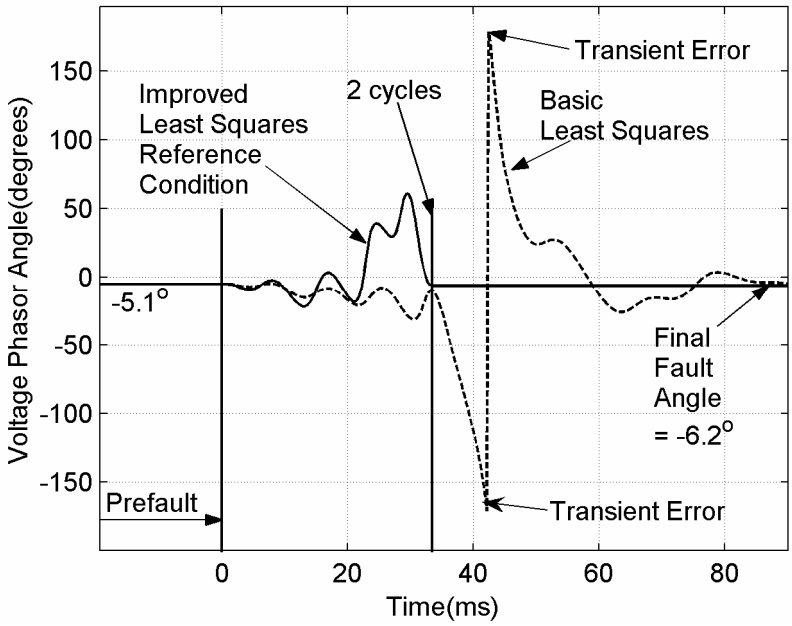

Figure 6.29 Reference Phasor Angle.

6.3.2 Parameter Variations

Two kinds of parameter variations were studied, single and combined. In the single variation, one of the CCVT parameters was modified by 5 percent in either direction. The reference fault condition was then simulated using this modified CCVT

to scale down the primary voltage. Finally the output voltage was processed using the improved least squares algorithm that was based on the original unmodified CCVT parameters. In the combined variation, several parameters were modified simultaneously, all of them in the same direction and by the same percentage.

Also, two kinds of deviations were measured, steady state and transient. The steady state deviation is the difference, considering the sign, on the prefault voltage magnitude and angle compared to the prefault reference condition. This steady state deviation is representative of the impact of the specific parameter on the accuracy of the CCVT. The transient deviation is the maximum absolute difference in magnitude and angle compared to the corresponding final stable value. The first two cycles after the fault inception were ignored for this transient deviation, because the improved least squares window is not fully inside the fault. This transient deviation is a measure of the uncertainty in the estimation of the fault voltage, introduced by the parameter varied.

6.3.3 Observations

The results of the parameter sensitivity study are summarized in Tables 6.1 and 6.2. Refer to Figure 3.10 for the names of parameters. The steady state deviation shows the direct impact on the accuracy of the CCVT that the capacitors C_1 and C_2 have, when they are varied individually. At the same time it is shown that a combined variation of these capacitors does not affect the accuracy that much, although it is still significant compared to the others. Another parameter that significantly affects this steady state deviation is the series inductance L_{LE} .

CCVT Parameter	Magnitude Deviation (%)	Angle Deviation (degrees)
C_1	+ 5.	- 0.015
C_2	- 5.	- 0.511
R_{LE}	- 0.030	+ 0.007
L_{LE}	- 0.310	- 0.489
R_{PE}	- 0.030	+ 0.006
L_{PE}	- 0.020	- 0.032
R_{SE}	- 0.050	+ 0.010
L_{SE}	- 0.020	- 0.027
R_F	- 0.004	+ 0.003
C_F	- 0.068	- 0.079
L_F	- 0.027	- 0.063
C_1,C_2	- 0.340	- 0.525

Table 6.1 Steady state deviation in prefault voltage measurement for a five percent increase in the parameter (s).

CCVT Parameter	Magnitude Deviation (|%|)	Angle Deviation (|degrees|)
C_1	0.012	0.14
C_2	0.545	7.35
R_{LE}	0.004	0.10
L_{LE}	0.105	1.38
R_{PE}	0.007	0.10
L_{PE}	0.009	0.13
R_{SE}	0.006	0.14
L_{SE}	0.008	0.12
R_F	0.120	1.58
R_{CF}	0.005	0.05
C_F	0.107	2.78
R_{LF}	0.020	0.48
L_F	0.242	2.81
C_1,C_2	0.555	7.49
R_O,R_{LO},L_O	0.176	3.20

Table 6.2 Absolute transient deviation in fault voltage after 2 cycles for an absolute variation of five percent in the parameter (s).

The results of the transient deviation shown in Table 6.2 are of significant importance, because these results show that the uncertainty in the phasor estimation is what causes the transient overreach or underreach. The maximum transient error is observed for a combined variation of C_1 and C_2 of 5%. This maximum transient error is illustrated in Figures 6.30 and 6.31.

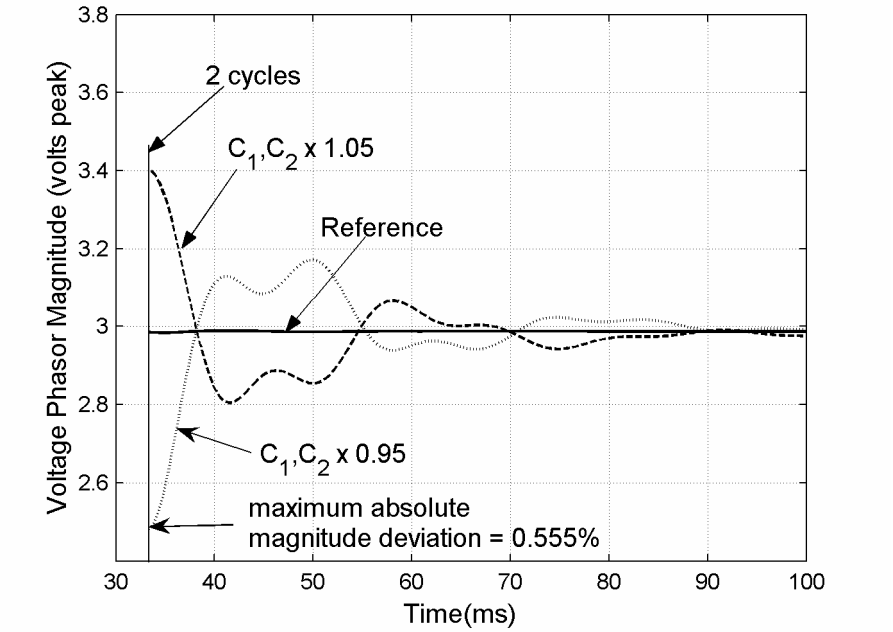

Figure 6.30 Transient magnitude deviation for a combined variation of C1 and C2.

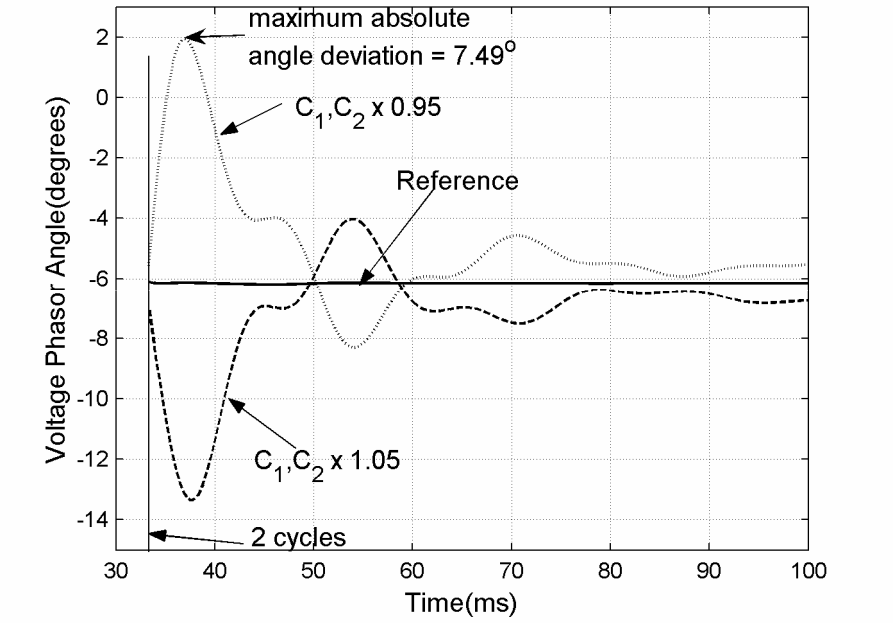

Figure 6.31 Transient angle deviation for a combined variation of C1 and C2.

Comparing this with the basic least squares method with a two cycle window (Figures 6.28 and 6.29), which has a transient deviation of 3.95% (=7.18% - 3.23%) in magnitude and +/-180^{o} degrees in angle, the improvement in the results using the Improved Least Squares can be seen.

6.4 SUMMARY

The performance of the improved least squares phasor estimation method in Chapter 5 is evaluated in this chapter. Several faults are simulated on different power system models, obtaining a voltage signal output from the CCVT to these faults. The results of these simulations are processed and the phasor estimation method is applied to obtain the desired voltage phasors. Typical cases that show the improvements of the method are illustrated. Also, difficult cases are found where the method has limitations. The reasons describing these limitations are also explained.

The improved least squares method for phasor estimation uses the CCVT parameters to develop the appropriate equations. Therefore, it is important to evaluate the sensitivity of this method to inaccuracies in the knowledge of these parameters. The results of the sensitivity study are also presented in this chapter.

7. SUMMARY AND CONCLUSIONS

The power systems normal operation depends on several of its components performing different functions. This normal operation can be disrupted by the presence of faults. Many of these faults are avoided by preventive measures, but not all can be prevented for economical reasons. The fault protection is an important function that minimizes the consequences of these faults, contributing to the normal operation of the power system. In Chapter 1, the basic concepts associated with protection of power systems were reviewed.

The numerical relays are one of the most important elements involved in the process of isolating a fault. They receive currents and voltage information from the CTs and PTs, and command the breaker to interrupt the high voltage circuit whenever a fault is detected. The microprocessor architecture used in numerical relays provides with additional useful functions, such as recording, communication and auto-diagnostics. The process of detecting a fault requires two components: the phasor estimation and the protective function. The two most commonly used phasor estimation techniques: DFT and least squares error methods were described in Chapter 2. The basic protection functions and the protective problems they can solve were also presented in Chapter 2.

In many cases CCVTs are used instead of PTs, for economical reasons. The CCVTs perform the same functions as the PTs, but they are more complex in design and performance. The CCVTs actually introduce a problem in protection functions that need voltage measurements. This problem is a consequence of the distortion introduced by the CCVT during the initial few cycles after a sudden voltage change which is typical for many kinds of faults. The characteristics of the CCVT response were studied in Chapter 3. The modeling methods were also presented in this chapter.

The impact of CCVT distortions was analyzed in Chapter 4. The impact was analyzed using magnitude and angle errors in the voltage phasors estimated. Several relays were studied to understand the risk of incorrect operation introduced by these errors. The relays that were not affected were also listed as a reference for the reader. Various techniques currently available to minimize the impact of the CCVT in protective functions were also described.

The objective of this thesis was realized by the new design methodology proposed in Chapter 5. A method for phasor estimation that improves the accuracy and speed of convergence of the voltage phasor obtained in CCVT applications was developed. The method uses the least error squares technique for curve fitting applied to phasor estimation. The idea proposed was to improve the description of the curve to be fitted, knowing that the CCVT output signal contains oscillatory decaying transient components of frequencies and time constant of the decay that correspond to the CCVT transfer function. The data window size for this method was found comparing the phasor trajectories and frequency responses of the method for different sizes of data window.

The proposed method was verified by performing test studies in Chapter 6. Several faults were simulated using real power system models to ascertain the benefits and also find the limitations of the method proposed. A test method was described to perform the simulations. This test method described the cases to be tested, the fault simulation, the post-processing of the results and the criteria for phasor estimation performance evaluation. Several cases were found that show significant improvements using the proposed methodology. Scenarios where the proposed method did not show any improvement were also described. This is due to the following reason: since the basic assumption made for curve fitting in the proposed methodology was that all transients of a particular frequency had an associated time constant of decay. In these particular cases, the natural frequencies of the power system were close to the natural frequencies of the CCVT described above. However, the time constants of decay of the

power system natural frequencies were quite different from those of the CCVT. So the curve fitting did not happen correctly.

Additionally, in Chapter 6 a parameter sensitivity study was presented. The least squares method proposed was based on using a curve description dependent on the CCVT parameters. Therefore, studying the effect of inaccuracies on these parameters was also an important consideration. It was found, that the improvements achievable were more significant than the errors introduced due to the parameter variations; a maximum variation of 5% was used in this study. In other words, it means that the method has low sensitivity to CCVT parameter error.

The following conclusions can be drawn from this thesis:

1) The distortion introduced by the CCVT during fault conditions produces errors in the voltage phasor estimated that may locate the resulting phasor in the incorrect operating region and therefore increases the risk of mal-operation of protective relays.

2) The use of CCVT design parameters, obtained within reasonable accuracy, can reduce the error and accelerate the convergence of the voltage phasor estimation, using a least squares approach, and consequently can reduce the impact of CCVT distortions in protective relaying.

3) CCVT design parameters can not be used in all cases in the way it was proposed here, because this method may increase the resulting phasor estimation error in presence of power system transients with frequencies and/or time constants of decay similar to those of the CCVT response.

7.1 FUTURE WORK

The following is a list of some suggestions received, as well as ideas collected that may improve the studies presented in this thesis:

1) The performance of the proposed method during overvoltage conditions was not studied here. There is no evidence to say that this condition will affect significantly the results of the method proposed, but it has to be properly verified.

2) The implementation issues were not completely evaluated, since the proposed method was not implemented on a physical device, but only on a software simulator in a computer. Considerations such as processing power required, number of significant bits required, the kind of arithmetic operations required, floating point or fixed point, are questions to be answered.

3) The use of oscillography data pre-recorded by some Electric Utilities during fault conditions is an even more realistic way of verifying the performance of the proposed method.

4) Simulation of fault conditions using other tools, such as the Real Time Digital Simuator (RTDS), is useful in evaluating a possible implementation of this method.

REFERENCES

[1] Adamiak, M.G., Alexander G.E. and Premerlani, W., "Advancements in Adaptive Algorithms for Secure High Speed Distance Protection", General Electric Company, GER-3962, 1996.

[2] ALPS Advanced Line Protection System, General Electric Company, GE Multilin, Ontario, Canada, 2005. [Online]. Available at http://www.geindustrial.com/ products/brochures/alps.pdf.

[3] *American National Standard Requirements for Power-Line Coupling Capacitor Voltage Transformers,* ANSI C93.2-1976, September 1976.

[4] Anderson, P.M., *Power System Protection*, McGraw-Hill, 1999.

[5] Benmouyal, G., "An Adaptive Sampling-Interval Generator for Digital Relaying", *IEEE Transactions on Power Delivery*, Vol. 4, No. 3, May 1989, pp. 1602-1609.

[6] Berdy, J., "The Protection of EHV Systems 345kV – 800kV", General Electric Company, GET-7207A, 1983.

[7] Canadian / American EMTP User Group, *Alternative Transients Program Rule Book*, 1999.

[8] *Capacitor Voltage Transformer*, Trench Limited, Instrument Transformer Division, Ontario, Canada, 2004. [Online]. File E214.12.pdf available at http://www. trenchgroup.com/_FramesPages/Brochures_articles_overview.htm.

[9] Dommel, H.W., *Electromagnetic Transients Program Reference Manual (EMTP Theory Book)*, Bonneville Power Administration, 1986.

[10] Dommel, H.W., "Digital Computer Solution of Electromagnetic Transients in Single and Multiphase Networks", *IEEE Transactions on Power Apparatus and Systems*, Vol. PAS-88, No. 4, May 1969, pp. 388-399.

[11] Elmore, W.A., *Protective Relaying Theory and Applications*, Marcel Dekker Inc., 2004.

[12] Fernandes, D., Neves, W.L.A. and Vasconcelos, J.C.A., "Identification of Parameters for Coupling Capacitor Voltage Transformers", IPST Conference, 2001.

[13] Fernandes, D., Neves, W.L.A. Vasconcelos, J.C.A. and Godoy, M.V., "Capacitor Voltage Transformer: Laboratory Tests and Digital Simulations", IPST Conference, 2005.

[14] G.E. Alexander, J.G. Andrichack and W.Z. Tyska, "Relaying Short Lines", General Electric Company, GER-3735, February 1992.

[15] Gertsch, G.A., Antolic, F. and Gygax, F., "Capacitor Voltage Transformers and Protective Relays", CIGRE Report 31-14, 1968.

[16] Horowitz, S.H. and Phadke, A.G., "Boosting Immunity to Blackouts", *IEEE Power and Energy Magazine*, vol. 2, No. 5, September/October 2003, pp. 47-53.

[17] Hou, D. and Roberts, J., "Capacitive Voltage Transformer: Transient Overreach Concerns and Solutions for Distance Relaying", *Canadian Conference on Electrical and Computer Engineering*, IEEE, 1996, pp. 119-125.

[18] Hughes, M.A., "Distance relay performance as affected by capacitor voltage transformers", *IEE Proc.*, vol. 121, No. 12, December 1974.

[19] *IEEE Guide for Power-Line Carrier Applications*, ANSI/IEEE Std 643-1980, July 1982.

[20] IEEE Tutorial Course, *Computer Relaying*, The Institute of Electrical and Electronic Engineers, 1979.

[21] IEEE Tutorial Course, *Microprocessor Relays and Protection Systems*, The Institute of Electrical and Electronic Engineers, 1988.

[22] Iravani, M.R., Wang, X., Polishchuk, I., Ribeiro, J. and Sarshar, A., "Digital Time-Domain Investigation of Transient Behaviour of Coupling Capacitor Voltage Transformer", *IEEE Transactions on Power Delivery*, Vol. 13, No. 2, April 1998, pp. 622-629.

[23] Izykowski, J., Kasztenny, B., Rosolowski, E., Saha, M.M. and Hillstrom, B., "Dynamic Compensation of Capacitive Voltage Transformers", *IEEE Transactions on Power Delivery*, Vol. 13, No. 1, January 1998, pp. 116-122.

[24] Kasztenny, B., Sharples, D., Asaro, V. and Pozzuoli, M., "Distance Relays and Capacitive Voltage Transformers – Balancing Speed and Transient Overreach", General Electric Company, GER-3986, 2000.

[25] Kezunovic, M., Abur, A., Edris, A. and Sobajic D., "Data Integration / Exchange", *IEEE Power and Energy Magazine*, vol. 2, No. 2, March/April 2004, pp. 14-19, vol. 2, No. 3, May/June 2004, pp. 24-29.

[26] Kezunovic, M., Fromen, C.W. and Nilsson, S.L., "Digital Models of Coupling Capacitor Voltage Transformers for Protective Relay Transient Studies", *IEEE Transactions on Power Delivery*, Vol. 7, No. 4, Oct 1992, pp. 1927-1935.

[27] Kojovic, Lj., Kezunovic, M. and Fromen, C.W., "A New Method for the CCVT Performance Analysis Using Field Measurements, Signal Processing and EMTP Modeling", *IEEE Transactions on Power Delivery*, Vol. 9, No. 4, Oct 1994, pp. 1907-1915.

[28] Lucas, J.R., McLaren, P.G., Keerthipala, W.W.L. and Jayasinghe, R.P., "Improved Simulation Models for Current and Voltage Transformers in Relay Studies", *IEEE Transactions on Power Delivery*, Vol. 7, No. 1, January 1992, pp. 152-159.

[29] Martinez, J.A., Mahseredjian, J. and Walling, R.A, "Parameter Determination Procedures for Modeling System Transients", *IEEE Power and Energy Magazine*, vol. 3, No. 5, September/October 2005, pp. 16-28.

[30] Mason, C.Russell, *The Art and Science of Protective Relaying*, General Electric Company, John Wiley and Sons, 1967.

[31] Morched, A.S., Ottenvangers, J.H. and Marti, L., "Multi-Port Frequency Dependent Networks Equivalents for the EMTP", *IEEE Transactions on Power Delivery*, vol. 8, No. 3, July 1993, pp. 1402-1412.

[32] Oppenheim, A.V and Schafer, R.W, *Discrete-Time Signal Processing*, Prentice Hall, 1998.

[33] Phadke, A.G. and Thorp, J.S, *Computer Relaying for Power Systems*, John Wiley and Sons Inc, 1969, pp. 388-399.

[34] Sachdev, M.S. and Baribeau, M.A., "A New Algorithm for Digital Impedance Relays", *IEEE Transactions on Power Apparatus and Systems*, Vol. PAS-98, Nov/Dev 1979, pp. 2232-2240.

[35] Stevenson, William D., *Elements of Power System Analysis*, McGraw-Hill, 1982.

[36] Sweetana, A, Jr, and Flugum, R, W, "A New Metering Accuracy Capacitive Potential Device", *IEEE Transactions on Power Apparatus and Systems*, Vol. PAS-85, No. 5, May 1966, pp. 499-510.

[37] Sweetana, A., "Transient Response Characteristics of Capacitive Potential Devices", *IEEE Transactions on Power Apparatus and Systems*, Vol. PAS-90, September/October 1971, pp. 1989-2001.

[38] The English Electric Company, *Protective Relays Application Guide*, The Scolar Press Limited, 1973.

[39] The Institution of Electrical Engineers, *Power System Protection*, vol. 1,2,3 and 4, Short Run Press Ltd, 1995.

[40] "Transient Response of Coupling Capacitor Voltage Transformers IEEE Committee Report", *IEEE Transactions on Power Apparatus and Systems*, Vol. PAS-100, No. 12, December 1981, pp. 4811-4814.

[41] Tziouvaras, D. A., et al, "Mathematical Models for Current, Voltage, and Coupling Capacitor Voltage Transformers", *IEEE Transactions on Power Delivery*, Vol. 15, No. 1, Jan 2000, pp. 62-72.

[42] Vermeulen, H.J., Dann, L.R. and Rooijen, J. van, "Equivalent Circuit Modelling of a Capacitive Voltage Transformer for Power System Harmonic Frequencies", *IEEE Transactions on Power Delivery*, Vol. 10, No. 4, Oct 1995, pp. 1743-1749.

[43] Warrington, A.R. van C., *Protective Relays: Their Theory and Practice*, vol. I and II, Chapman and Hall, 1962, 1978.

[44] Westinghouse Electric Corporation, *Applied Protective Relaying*, 1964.

[45] Westinghouse Electric Corporation, *Electrical Transmission and Distribution Reference Book*, 1964.

[46] Wright, A. and Christopoulos, C., *Electrical Power System Protection*, Chapman and Hall, 1993.

[47] Wright, A., *Current Transformers – Their Transient and Steady State Performance*, Chapman and Hall Ltd, 1968.

[48] Ziegler, G., *Numerical Distance Protection Principles and Applications*, Siemens AG, 1999.

[49] Schweitzer, E.O. and Hou, D., "Filtering for Protective Relays" , WESCANEX 93, Conference Proceedings, IEEE, May 1993, pp. 15-23.

[50] Pajuelo, E., Ramakrishna G. and Sachdev, M.S., “An Improved Voltage Phasor Estimation Technique to Minimize the Impact of CCVT Transients in Distance Protection”, CCECE 2005, Canadian Conference on Electrical and Computer Engineering, Conference Proceedings, IEEE, May 2005, pp. 454-457.

[51] Pajuelo, E., Ramakrishna, G. and Sachdev, M.S., “Least Squares Algorithm to Overcome the Effect of CCVT Transients and the Algorithm Sensitivity to CCVT Parameter Variations”, NPSC 2006, National Power System Conference - India, Submitted: May 2006.

[52] Pajuelo, E., Ramakrishna, G. and Sachdev, M.S., “An Improved Least Squares Voltage Phasor Estimation Technique to Minimize the Impact of CCVT Transients in Distance Protection” , *IEEE Transactions on Power Delivery*, IEEE, Submitted.